N O T I C E

THIS DOCUMENT HAS BEEN REPRODUCED FROM MICROFICHE. ALTHOUGH IT IS RECOGNIZED THAT CERTAIN PORTIONS ARE ILLEGIBLE, IT IS BEING RELEASED IN THE INTEREST OF MAKING AVAILABLE AS MUCH INFORMATION AS POSSIBLE

CR-166196
(D. Kanakia)

FIRE TEST METHODOLOGY FOR AEROSPACE MATERIALS

I. Thermal and Smoke Toxicological Assessments of Graphite/Bismaleimide and Graphite/Epoxy Systems

By
M. D. Kanakia
W. G. Switzer
G. E. Hartzell
H. L. Kaplan

FINAL REPORT

October 1980

Distribution of this report is provided in the interest of information exchange. Responsibility of the contents resides in the author or organization that prepared it.

Prepared under Contract No. NAS2-10140
by SwRI Project No. 03-5565-001

For

NATIONAL AERONAUTICS AND SPACE ADMINISTRATION
AMES Research Center
Chemical Research
Moffett Field, California 94035

(NASA-CR-166196) FIRE TEST METHODOLOGY FOR AEROSPACE MATERIALS. 1: THERMAL AND SMOKE TOXICOLOGICAL ASSESSMENTS OF GRAPHITE/BISMALEIMIDE AND GRAPHITE/EPOXY SYSTEMS Final Report (Southwest Research
N81-26185
Unclas
G3/24 28570

JUL 1981
RECEIVED
NASA STI FACILITY
ACCESS DEPT.

SOUTHWEST RESEARCH INSTITUTE
SAN ANTONIO HOUSTON

SOUTHWEST RESEARCH INSTITUTE
Post Office Drawer 28510, 6220 Culebra Road
San Antonio, Texas 78284

DEPARTMENT OF FIRE TECHNOLOGY

FIRE TEST METHODOLOGY FOR AEROSPACE MATERIALS

I. Thermal and Smoke Toxicological Assessments of Graphite/ Bismaleimide and Graphite/Epoxy Systems

By
M. D. Kanakia
W. G. Switzer
G. E. Hartzell
H. L. Kaplan

FINAL REPORT

October 1980

Distribution of this report is provided in the interest of information exchange. Responsibility of the contents resides in the author or organization that prepared it.

Prepared under Contract No. NAS2-10140
by SwRI Project No. 03-5565-001

For

NATIONAL AERONAUTICS AND SPACE ADMINISTRATION
AMES Research Center
Chemical Research
Moffett Field, California 94035

Approved by:

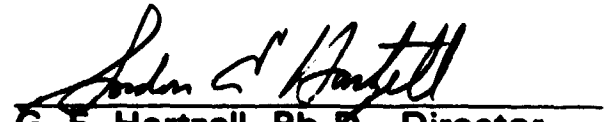

G. E. Hartzell, Ph.D., Director
Department of Fire Technology

TABLE OF CONTENTS

I. ABSTRACT

Two composite materials, a graphite/epoxy and a graphite/bismaleimide, were subjected to laboratory performance evaluations for assessment of thermal and smoke toxicological properties.

Both materials possess a high degree of thermal stability, with total heat release values being essentially identical under piloted ignition conditions over a range of 5 to 10 W/cm^2 incident heat flux. The graphite/epoxy material had a tendency to auto-ignite at a lower heat flux (about 7 W/cm^2) and produced about 23 percent higher peak heat release rates, approximately 42 percent more carbon monoxide and considerably more smoke than the graphite/bismaleimide under conditions of piloted ignition.

Toxicological potencies of smoke produced from the two composites were equivalent for 30-minute exposures. Potencies were also comparable to many common materials, such as wood. There was no evidence for the formation of an "unusual toxicant" nor for any short-term post-exposure toxicological effects. Carbon monoxide was the sole toxicant of significance for both materials except for an observable contribution suggested for hydrogen cyanide arising from the graphite/epoxy material which underwent intermittent flaming combustion at 10 W/cm^2. At high smoke concentrations in intense fires, it is suggested that hydrogen cyanide produced from the graphite/epoxy material may have a detrimental effect on time-to-incapacitation.

Methodology giving rise to relative time-to-incapacitation assessment would appear to be more relevant to potential aircraft fire scenarios than classical toxicological potencies. It is recommended that future studies place greater emphasis on time related biological observations.

II. GENERAL INTRODUCTION

There is a critical need for assessment of both the combustion properties and resulting toxicological characteristics of materials for aerospace applications. Conventional testing methodologies do not necessarily reflect the specialized aerospace environmental conditions and fire scenarios to which materials may be subjected. Accordingly, examination and assessment of testing techniques used for materials are required and well-justified. The purpose of this program was to assess the flammability and smoke toxicity characteristics of two polymeric materials when exposed to high radiant heat fluxes selected to represent potential post-crash aircraft fire scenarios. Since jet fuel pool fires can very rapidly impinge thermal radiations of 5 to 10 W/cm^2, both on the aircraft fuselage and to the interior through door-size openings, heat flux values within this range were chosen for this study.

Characteristics of a fire which affect the occupants of a given space are the rapidity of temperature rise, the rate of development of a toxic environment, and the potency of that environment. Together these determine the survival possibilities of exposed humans.

In a fire, these properties are controlled by the release rates of heat, smoke and toxic gases from the material. A small-scale calorimeter such as the Ohio State University (OSU) Release Rate Apparatus[1,2] can satisfactorily measure heat, smoke evolution, and the release rates of combustion products. Analytical determination of release rates of major combustion gases, such as CO, CO_2, and total hydrocarbons are indicative of the rate of development of a toxic atmosphere. However, other factors are often operational and not readily measurable in quantifying toxic impact. Therefore, experimental animals are often exposed

in scaled-down real fire tests. An animal, usually a rodent, is used as an integrative model reflecting insults due to common toxicants, synergistic effects, irritant gases, particulate matter and dosage rates. Observations are made for behavioral incapacitation, mortality and morbidity as functions of smoke concentration and time.

Toxicological insults may then be expressed in conventional concentration units statistically associated with 50-percent effect (e.g., LC_{50}) or in comparative times-to-effect as a function of smoke concentration.

Excessive air flow in the OSU calorimeter is required for accurate heat release measurement. Since toxicity is dependent upon the concentration of combustion of gases, dilution resulting from high air flows normally prevents the simultaneous assessment of heat release rate and combustion products toxicity. Therefore, these properties are normally measured and evaluated separately.

III. THERMAL PROPERTIES OF MATERIALS

A. INTRODUCTION

Although the rate of heat release from a pure homogenous material burning uniformly in free air can be estimated from the energetics of the combustion reaction, heterogeneous materials under unsteady-state conditions with formation of char present a complex problem. For practical purposes, feasible determinations of burning properties utilize a release rate calorimeter.

Accurate calorimetry is essential for realistic comparisons between the burning properties of materials. No great difficulties are normally encountered when measuring the total heat of combustion, but when the critical factor is rate of heat release, the thermal inertia of the system may limit the results that are obtained. The problems, however, are not insurmountable. Release rate calorimeters utilize some element within the fire environment as a heat sink. The heat sink may be static (walls of the calorimeter) or flowing (moving air stream).

In the case of static heat sink, the total heat released (Q) is proportional to the temperature rise (ΔT) of the heat sink. The rate of heat release, $\dot{Q}$, is proportional to the rate of temperature changes:

$$\dot{Q} = dQ/dt = k_s dT/dt = k_s \dot{T}$$

The proportionality constant k_s contains the heat capacity Cp (assumed to be a constant) and the mass of the heat sink. In practice, materials of known heating value are burned in the calorimeter to determine an effective k_s which compensates for systematic heat losses of the system.

For flowing heat sinks, the rate of heat release, $\dot{Q}$, is proportional to the temperature rise of the heat sink.

$$\dot{Q} = k_s \Delta T$$

The proportionality constant k_s contains the heat capacity and mass flow rate of the heat sink materials and systematic heat losses of the system. The total heat released by the fire can be obtained by integrating the heat release rate over the time of the experiment.

$$Q = \int_0^t \dot{Q} dt$$

There are currently a number of calorimeters being used which utilize moving air streams as heat sinks. The OSU Release Rate Apparatus is probably the most common. The National Bureau of Standards (NBS) type calorimeter maintains a constant ΔT by burning metered fuel and the heat release is calculated by difference.

The rate of air flow (heat sink) is normally high enough to maintain a moderate air temperature rise, but more importantly minimizes the temperature rise of the walls of the burn chamber. These systems are considered dynamic, but the response time to fast thermal changes is limited by the thermal inertia of the system (primarily the walls of the burn chamber). The more massive the walls, the slower the response time. This is partially compensated for by more massive air flows to reduce the temperature of the walls.

Heat release rate calorimeters are primarily designed for a specific purpose and as a consequence have a very high air flow rate. The basic useful measurable data are heat release rate, flame travel rate, smoke obscuration rate, and rates of combustion product release. Derived data such as ignitability (slope of the heat release rise rate) and maximum heat release rate depend strongly on the response time of the calorimeter.

In theory, any calorimeter results could be extrapolated to actual-use conditions by use of mathematical system modeling. However, with

composite materials and varying enclosure geometries, the preferable approach would be full-scale calorimetry in the most critical usage environment.

B. EXPERIMENTAL METHODS

Materials supplied by NASA-Ames Research Center and evaluated under this program were the graphite/epoxy and graphite/bismaleimide materials listed in Table I.

1. Limiting Oxygen Index

The limiting oxygen index (LOI) of each laminated composite was determined according to ASTM D2863. The LOI is used to rank the relative flammability of materials by measuring the minimum concentration of oxygen (volume %) in a mixture of oxygen and nitrogen that will just support the combustion. The test specimens, 0.64 x 15.34 cm (0.25 x 6 in.), for the LOI test were obtained from NASA Sample No. 1012, Panel No. 9 graphite/epoxy and NASA Sample No. 1017, graphite/bismaleimide A.

2. Thermal Analysis

A duPont Thermal Analyzer Model No. 990 with a Model No. 951 Thermogravimetric Module was used to measure sample weight as a function of temperature in both air and nitrogen environments. The instrument recorded the thermogravimetric analysis (TGA) weight loss curve and its continuous derivative (DTG). The gas flow rate (air or nitrogen) was maintained at 50 cc/min in a quartz chamber containing the powdered sample. The chamber was heated to a maximum of 1000°C at a specified temperature rise rate of either 5°, 20°, or 50°C/min.

TABLE I. LIST OF MATERIALS

Graphite/Epoxy	
NASA Panel No. 1002	One 12 x 12 x 1/8-in. panel. Material: 10 plies, HMF 133/34. Orientation: Parallel warp. Cured Resin Content: 28.2%. Cured Specific Gravity: 1.590.
NASA Sample No. 1007	Panel No. 4. One 6 x 12 x 1/8-in. panel. Material: 10 plies, HMF 133/34. Orientation: Parallel warp. Cured Specific Gravity: 1.596.
NASA Sample No. 1008A	Size: 12 x 12 x 1/8-in. panel. Material: 18 plies, HMF 133/34. Orientation: 0° to 90°.
NASA Sample No. 1012	Nine 3 x 3 x 1/8-in. pieces. Graphite 133/ Epoxy 134.
NASA Sample No. 1008J	One 12 x 12 x 1/8-in. panel. Material: 18 plies, HMF 133/34 Graphite/Epoxy. Orientation: 0° to 90°.
NASA Sample No. 1012	Panel No. 9. Four 6 x 12 x 1/8-in. panels, Graphite/Epoxy.
Graphite/Bismaleimide	
NASA Panel No. 1003	One 12 x 12 x 1/8-in. panel. Material: 10 plies, HMF 133/M751. Orientation: Parallel warp.
NASA Sample No. 1003C	Panel No. 6. One 12 x 12 x 1/8-in. panel. Material: HMF 133/NASA M-751.
NASA Sample No. 1013	Sixteen 3 x 3 x 1/8-in. pieces. Graphite W134/ Bismaleimide M751.
NASA Sample No. 1017	Seven 6 x 6 x 1/8-in. pieces, Bismaleimide A, Resin M751. Fabric: Fibretite W-134.
M751 Bismaleimide/133	Seven 6 x 6 x 1/8-in. pieces. Graphite
NASA Sample No. 1001	Five 4 x 1/4-in. pieces. Material: Bismaleimide M751 Neat Resin.

3. Release Rate Calorimetry

The Ohio State University (OSU) Heat Release Apparatus was used to obtain the following data as a function of heat flux:

1. Heat Release Rate
2. Ignitability (slope of the heat release rise curve)
3. Maximum Heat Release Rate
4. Flame Travel Rate
5. Smoke (Obscuration) Evolution Rate
6. Common Combustion Products Release Rate
7. Temperature development at the back surface of the sample

The basic OSU calorimeter (Appendix Figure 11) consisted of a sample holding chamber, exposure chamber with radiant panels, pilot flame and smoke opacity detector. The apparatus had a total air supply of 0.04 m^3/sec (84 cfm). One-third of this air supply was fed to the exposure chamber through distribution plates and the remainder was used to cool the conical section. The two streams of air were combined and exhausted through the rectangular stack. The apparatus was modified for fast response by incorporating a thermal inertia compensator in the exhaust stack such that 90-percent full-scale response was obtained in 8 to 10 seconds. A continuous gas sampling probe was installed in the exhaust stack to determine the release rates of CO, CO_2, CH_x and oxygen depletion. Gas samples were transferred to Beckman continuous analyzers via a heated (250°F) teflon line. The sample flow rate to the analyzers was sufficiently high as to provide a response time of 15 seconds. The

gas sampling probe was located above the smoke detector path in an extension of the stack so that smoke obscuration measurements were not affected.

The 150 x 150-mm (6 x 6-in.) specimens were tested in a vertical orientation. Piloted ignition consisted of an impinging flame (methane-air) in the center of the lower edge of the specimen. The unexposed surfaces of the specimen were covered with two thicknesses of 0.025-mm aluminum foil pressed tightly to the sides and back. The specimen holder was provided with a V-shaped spring pressure plate and a 12.7-mm (1/2-in.) thick backing plate of rigid insulation board having a density of 720 ± 80 kg/m^3 (45 ± 5 lb/ft^3) and a thermal conductivity of 0.012 ± 0.1 W/m,°K (0.8 ± 0.1 Btu·in./°F·ft^2·hr). A Chromel-Alumel (28-gauge) thermocouple, placed in the center of the interface between the specimen and insulation board, was used to monitor temperature development at the back surface of the specimen.

C. RESULTS AND DISCUSSION

1. Limiting Oxygen Index

The limiting oxygen index (LOI) for the graphite/epoxy material was determined to be 39.5; that for the graphite/bismaleimide material was 39.0.

2. Thermal Analysis

Results of thermal analysis tests performed on bismaleimide resin (Sample No. 1001), graphite/bismaleimide composite (Sample No. 1013), and graphite/epoxy composite (Sample No. 1012) are summarized in Tables II, III, and IV.

TABLE II. SUMMARY OF THERMOGRAVIMETRIC ANALYSIS OF BISMALEIMIDE RESIN (SAMPLE NO. 1001)

	AIR 50 cc/min			NITROGEN 50 cc/min		
HEATING RATE →	5°C/min	20°C/min	50°C/min	5°C/min	20°C/min	50°C/min
Stage I Degradation						
Temperature Range (°C)	300-430	340-450	350-500	310-450	320-490	330-520
Temp. of Maximum Rate (°C)	400	430	450	400	440	450
Percent Weight Remaining at Maximum Rate	83.8	87.8	86.9	89.3	82.3	83.5
Maximum Rate (Percent Weight Loss/min)	1.05	3.4	7.4	1.2	5.1	11.4
Stage II Degradation						
Temperature Range (°C)	440-580	460-650	500-700	450-1000	500-800	530-850
Temp. of Maximum Rate (°C)	530	560	580	500	550	570
Percent Weight Remaining at Maximum Rate	24.7	46.0	52.6	74	63	65.2
Maximum Rate (Percent Weight Loss/min)	5.8	19.5	35.2	1.0	3.2	6.8
Percent Char Yield						
At 800°C	1.8	5.6	0.8	40.0	46.5	56.8
At 1000°C	--	--	--	16.0	40.0	51.0

TABLE III. SUMMARY OF THERMOGRAVIMETRIC ANALYSIS OF GRAPHITE/BISMALEIMIDE (SAMPLE NO. 1013)

	AIR 50 cc/min		
HEATING RATE →	5°C/min	20°C/min	50°C/min
Stage I Degradation			
Temperature Range (°C)	300-430	340-460	370-4.0
Temp. of Maximum Rate (°C)	390	410	435
Percent Weight Remaining at Maximum Rate	89.6	92.0	90.2
Maximum Rate (Percent Weight Loss/min)	0.5	1.4	3.8
Stage II Degradation			
Temperature Range (°C)	430-570	480-630	490-690
Temp. of Maximum Rate (°C)	550	610	640
Percent Weight Remaining at Maximum Rate	30.5	45.3	41.5
Maximum Rate (Percent Weight Loss/min)	7.85	27.7	36.9
Percent Char Yield			
At 800°C	1.5	1.8	1.5
At 1000°C	1.5	1.8	1.5

TABLE IV. SUMMARY OF THERMOGRAVIMETRIC ANALYSIS OF GRAPHITE/EPOXY (SAMPLE NO. 1012)

	AIR 50 cc/min		NITROGEN 50 cc/min
HEATING RATE →	20°C/min	50°C/min	20°C/min
Stage I Degradation			
Temperature Range (°C)	250-330	250-350	250-400
Temp. of Maximum Rate (°C)	280	320	350
Percent Weight Remaining at Maximum Rate	95.8	94.0	95.5
Maximum Rate (Percent Weight Loss/min)	2.1	6.9	2.6
Stage II Degradation			
Temperature Range (°C)	450-580	450-610	400-1000
Temp. of Maximum Rate (°C)	530	560	--
Percent Weight Remaining at Maximum Rate	77.3	78.7	--
Maximum Rate (Percent Weight Loss/min)	4.5	11.3	1.9
Stage III Degradation			
Temperature Range (°C)	590-660	610-780	--
Temp. of Maximum Rate (°C)	650	690	--
Percent Weight Remaining at Maximum Rate	37	46.2	--
Maximum Rate (Percent Weight Loss/min)	32	27	--
Percent Char Yield			
At 800°C	3.0	3.1	56
At 1000°C	3.0	3.1	39

Examination of data in Table II shows that the bismaleimide resin degradation occurs in two stages, both in nitrogen and in air. The peak degradation temperatures for both stages increased with an increase in the heating rate. This is shown graphically by the TGA thermograms of the bismaleimide resin in air and in nitrogen (Appendix Figures 1 and 2). The first-stage degradation in both environments occurs in the temperature range of 300 - 450°C with the maximum degradation at 15-percent weight loss and 430 ± 25°C. Appendix Figure 3 compares the effect of environment on the thermal degradation of the bismaleimide resin. The second stage of degradation in both environments commences at ~450°C with the maximum occurring at 555 ± 25°C. This is a major degradation in air environment and almost all of the sample is consumed in the 600 to 700°C range. However, in the nitrogen atmosphere, it is a secondary degradation, and slow weight loss is continued up to 1000°C, yielding 16- to 50-percent char, depending on the heating rate.

Table III and Appendix Figure 4 present the thermal analysis of the graphite/bismaleimide composite in air. The composite degrades in the same manner as the pure resin; however, the first-stage peak is suppressed and the second-stage peak is enhanced for the composite. The second-stage degradation temperature range is also slightly higher as shown in Appendix Figure 5.

The thermal degradation characteristics of the graphite/epoxy composite are summarized in Table IV. The graphite/epoxy composite degrades in three stages in air. The first degradation (minor) occurs in the 250 to 350°C range with a maximum at 300 ± 20°C. The second-stage degradation is in the 450 to 600°C range with a maximum at

545 ± 15°C. The third-stage degradation (major) is in the 600 to 800°C range with a maximum at 670 ± 20°C. The graphite/epoxy degradation in the nitrogen atmosphere takes place in two stages. The first stage was the same as in air at the 250 to 400°C range. The main degradation was gradual in the 400 to 1000°C range with a char yield of 39 percent at 1000°C. Figure 6 shows the effect of environment on the thermal degradation of this composite.

The two materials are compared for their thermal decomposition characteristics in Appendix Figures 7 and 8. Examination of these figures shows that in both environments, the graphite/epoxy system would appear to possess slightly higher thermal stability than the graphite/bismaleimide composite under the conditions of the TGA determinations.

Differential scanning calorimeter (DSC) data on both composites were obtained on a duPont DSC910 Cell Base. The DSC cell had a maximum temperature limit of 600°C; therefore, these experiments were conducted in air using an isothermal mode at 600°C. Appendix Figure 9 shows the DSC thermogram of the graphite/bismaleimide (Sample No. 1013, initial weight 1 mg) in air. The thermogram shows a two-stage exothermic degradation with the second stage being a major exotherm. The total energy of the exotherms for the graphite/bismaleimide sample was 2611.43 cal/g. An isothermal DSC thermogram in air at 600°C for the graphite/epoxy composite, (Sample No. 1012, initial weight 1 mg) is presented in Appendix Figure 10. The thermogram shows three-stage exothermic degradation. Energy associated with the first two exotherms was 927.62 mcal while the third exotherm contributed 1598.1 mcal. Thus, the total exothermic energy due to complete degradation of the graphite/epoxy was 2525.72 cal/g. It is unlikely that a significant

difference exists between the two composite materials in total exothermic energy as determined from differential scanning calorimetry.

The DSC method was also used to determine the heat capacity of the two materials by using the difference in the energy between the sample and the reference material. The heat capacity of bismaleimide was calculated to be 1.7 cal/g·°C at 100°C, 1.53 cal/g·°C at 200°C, and 1.4 cal/g·°C at 300°C. The heat capacity values for graphite/epoxy were 1.55 cal/g·°C at 100°C, 1.21 cal/g·°C at 200°C and 0.64 cal/g·°C at 300°C.

3. Release Rate Calorimetry

Eight release rate tests were conducted on each material. These consisted of six tests (at 5, 6, 7, 8, 9 and 10 W/cm^2) with piloted ignition and two tests (at 7 and 10 W/cm^2) with non-piloted ignition. Data gathered in the release rate experiments are summarized in Tables V and VI. Individual curves for each experiment are presented in Appendix Figures 12 through 74.

Maximum heat release rate (MHRR) data for piloted ignition tests shown in Table V suggest that the two composite materials have comparable values, with the graphite/epoxy exhibiting an average of 23 percent greater peak release rates over the range of heat fluxes studied. (Replicatibility of the determination is approximately ± 10 percent). Both materials also show a trend of increasing MHRR values up to 6-8 W/cm^2, followed by decreasing MHRR upon further increase of heat flux.

TABLE V. HEAT RELEASE AND FLAME TRAVEL RATES

Sample No.	Heat Flux W/cm^2	Ignition Piloted or Non-Piloted	Max. Heat Release Rate (HRR) kW/m^2	Time to Max. HRR, s	Total Heat Release at 5 min MJ/m^2	Ignitability $kW/s \cdot m^2$	Flame Travel Rate mm/s	Specimen Back Surface Temp. °C Temp. °C at 5 min
				GRAPHITE/BISMALEIMIDE				
1017	5.0	Piloted	68.1	82	14.1	0.952	5.22	314
H751	6.0	Piloted	83.2	36	15.78	1.149	6.8	327
H751	7.0	Piloted	77.2	60	12.96	1.075	4.58	371
1017	7.0	Non-Piloted	0*	--	--	0	0	347
H751	8.0	Piloted	93.0	45	15.12	2.083	4.8	445
H751	9.0	Piloted	84.0	43	13.38	1.449	8.1	507
H751	10.0	Piloted	60.5	60	12.6	1.263	6.38	497
1017	10.0	Non-Piloted	73.4	50	12.72	2.778	Instantaneous @ 20 s	550
				GRAPHITE/EPOXY				
1008A	5.0	Piloted	87.0	122	12.54	1.515	1.68	406
1012-9	6.0	Piloted	109.7	30	14.64	3.333	4.25	403
1012-9	7.0	Piloted	107.4	36	13.38	2.777	8.33	467
1008A	7.0	Non-Piloted	94.6	97	10.68	4.63	Instantaneous @ 75 s	480
1012-9	8.0	Piloted	98.4	62	12.06	2.137	7.32	482
1012-9	9.0	Piloted	81.0	60	10.38	2.137	15	555
1008A	10.0	Piloted	90.8	90	9.96	2.315	9.52	594
1008A	10.0	Non-Piloted	84.7	90	10.74	3.968	Instantaneous @ 30 s	596

* No Ignition

Total heat release (area under the MHRR curve) at 5 minutes averaged only slightly higher for the graphite/bismaleimide than for the graphite/epoxy. This was consistent with the DSC data which suggested no significant difference between the two materials.

The time-temperature development at the specimen back surface is presented in Appendix Figures 27 through 42. Values at 5 minutes are presented in Table V for comparison. Temperatures were consistently higher at each heat flux level for graphite/epoxy than for graphite/bismaleimide.

Examination of flame travel data in Table V shows that the graphite/bismaleimide sample did not self-ignite under 7.0 W/cm^2 heat flux non-piloted conditions while the graphite/epoxy specimen under the same conditions burst into flames after 75 seconds. Both composites went into the flaming mode at the 10-W/cm^2 non-piloted condition. Flame travel rate (FTR) data were obtained by visually noting the time for the flame to reach the vertical edges of the sample. With such small sample sizes, unavailability of adequate material for replication and relatively high FTR values, measurements were highly subjective. No conclusions should be drawn from the data. The OSU calorimeter is not an appropriate instrument for flame travel determinations for many materials.

Table VI presents the smoke and combustion product release data on the two composites. Curves for each test are presented in Appendix Figures 43 through 74. Under conditions of piloted ignition, the graphite/bismaleimide composite produced significantly lower smoke

than the graphite/epoxy. Carbon monoxide generation rates and total CO release values (Table VI) for the graphite/epoxy material were consistently and significantly greater than those for graphite/bismaleimide in all piloted-ignition cases.

TABLE VI. SMOKE AND COMBUSTION PRODUCTS RELEASE RATES

Sample No.	Heat Flux W/cm^2	Ignition Piloted or Non-Piloted	Max. Smoke Release Rate (SRR) Smoke/min · m^2	Total Smoke Release at 5 min SMOKE/m^2	Max. CO Release Rate ℓ/min · m^2	Total CO Release ℓ/m^2	Max. CO_2 Release Rate ℓ/min · m^2	Max. O_2 Depletion Rate ℓ/min · m^2	Total Weight Loss, g	Percent Weight Loss
					GRAPHITE/BISMALEIMIDE					
1017	5.0	Piloted	1,163	3,252	2.56	9.43	61.40	102.4	26.9	21.8
M751	6.0	Piloted	1,876	2,882	4.09	13.78	81.93	256.0	28.4	23.15
M751	7.0	Piloted	1,292	2,846	4.40	18.77	143.48	307.0	28.15	23.42
1017	7.0	Non-Piloted	301	452	9.22	41.01	20.48	0	25.0	20.3
M751	8.0	Piloted	1,851	5,006	2.46	13.82	215.10	410.0	29.5	24.0
M751	9.0	Piloted	1,938	3,766	4.09	14.00	286.80	512.0	30.1	24.8
M751	10.0	Piloted	1,587	3,390	4.61	13.47	245.80	307.0	29.1	23.7
1017	10.0	Non-Piloted	1,094	4,119	3.07	9.35	245.80	307.0	28.2	23.23
					GRAPHITE/EPOXY					
1008A	5.0	Piloted	5,813	9,939	4.10	14.40	112.70	204.8	24.2	21.34
1012-9	6.0	Piloted	7,965	10,653	8.19	19.19	215.10	410.0	28.0	22.97
1012-9	7.0	Piloted	8,651	10,893	8.71	18.77	215.00	307.0	27.8	22.7
1008A	7.0	Non-Piloted	6,458	10,432	7.68	22.44	184.00	102.0	28.3	24.6
1012-9	8.0	Piloted	6,200	9,724	10.24	25.22	204.80	512.0	28.6	24.1
1012-9	9.0	Piloted	7,319	10,206	12.29	22.45	256.00	512.0	29.1	24.14
1008A	10.0	Piloted	7,319	9,655	11.27	18.48	358.40	307.0	28.4	24.8
1009A	10.0	Non-Piloted	6,674	8,848	9.22	18.23	256.00	307.0	28.2	24.86

D. CONCLUSIONS

Samples of graphite/bismaleimide and graphite/epoxy composites were evaluated by thermo-chemical and heat release rate methods.

Thermogravimetric analyses suggested the graphite/epoxy to be slightly more thermally stable than the graphite/bismaleimide. The total exothermic energy of degradation as measured by differential scanning calorimetry (DSC) showed no significant difference between the two materials.

Both materials possess a high degree of thermal stability, with total heat release values being quite comparable (within ±10 percent of their mean). The graphite/epoxy material has a tendency to auto-ignite at a lower heat flux (about 7 W/cm^2). It also produces about 23 percent higher peak heat release rates, yields approximately 42 percent more carbon monoxide, and considerably more smoke than the graphite/bismaleimide. These differences are based on mean experimental values over the heat flux range studied and under piloted-ignition conditions.

IV. SMOKE TOXICITY OF MATERIALS

A. INTRODUCTION

Assessment of the toxicity of fire gases is still in a stage of development such that appreciable judgement is involved when planning a research program on material evaluation.

The simplest initial approach involves the combustion of a material under specified conditions, exposure of laboratory animals to the smoke produced, and subsequent determination of an appropriate biological endpoint.[3,4] Classically, the endpoint is mortality which is applied in the determination of a dose-response relationship. Using conventional statistical treatments, LC_{50} values (concentrations producing 50 percent lethality) are then estimated. The method is widely accepted traditionally and data are available in the literature for cross-comparison purposes.

For a more definitive study, the preferred methodology should consider not only lethality, but also the time required to produce an effect on a learned behavior.[5] Assessment of incapacitation is highly relevant, since it reflects initial responses to toxic agents and has a bearing on the ability of exposed humans to escape from a fire. Choices must be made regarding techniques best suited for any given case.

The protocol developed for this test series was designed to assess the acute smoke toxicity of materials at different heat flux levels. A traditional toxicity measurement, the dose-response derived LC_{50}, and a time-to-response behavioral model, the rotorod, were incorporated into the experimental design.

The rotorod task is an established technique for measuring sensori-motor dysfunction in rats[6,7] and has previously been successfully employed in combustion toxicology studies.[8]

Each rotorod unit consists of three independent compartments (each 15 x 25 x 43 cm) constructed of aluminum sheet and brass rods. Parallel spacing of the brass rods on 1.6-cm centers allows smoke to flow freely through the apparatus during combustion experiments. A 1.27-cm (diameter) wood rod, positioned horizontally 25 cm above the apparatus floor, is driven at 4.0 rpm by an externally mounted motor. Constant-current electric shock generator and scrambler devices connecting all surfaces of the apparatus provide the incentive for the rats to remain balanced on the rotating rod. Sensori-motor incapacitation is indicated by falls from the rotating rod that are sensed by a toggle floor and microswitch arrangement.

Prior to testing, rats are trained to mount and remain balanced on the rotating rod. Ten 60-minute sessions of training for each animal results in extremely stable performance levels; rats so trained, when unstressed by exposure to combustion products, do not voluntarily dismount from the rod and if deliberately dislodged, are easily able to remount within 3 seconds. Given these baseline observations, a multiplicity of reliable, objective indices of behavioral incapacitation are available. In addition, remote monitoring of the animals is possible through the microswitch arrangement. For this test series, an animal was considered incapacitated if, upon falling from the rod, it was unable to remount within 15 seconds.

The combustion-exposure system for this study was specially designed and built at Southwest Research Institute. The rotorod behavioral assessment apparatus was contained in a 329-ℓ acrylic chamber interfaced with a columnar combustion furnace. Heat flux energy was supplied by two 43-cm 6-lamp (1600 T3 quartz lamps) panels mounted at 45° angles with respect to the column. The design permitted heat fluxes incident on a sample specimen placed within the column of up to 10 W/cm^2 to be obtained. Combustion products could rise directly from the furnace into the chamber without dilution and without significant heat stress to exposed animals. The combustion-exposure system is pictured in Figures 1 and 2 and shown diagramatically in Appendix Figure 75.

The experimental system and protocol used were analogous to, but not identical with, the National Bureau of Standards developmental protocol for determining smoke toxicity. The protocol was modified to better meet the fire scenario requirements of the aerospace materials by placing greater emphasis on time-to-effect analysis.

B. EXPERIMENTAL METHODS (Protocol)

Combustion of the graphite/epoxy and graphite/bismaleimide materials was carried out at two heat flux levels, 5 W/cm^2 and 10 W/cm^2, for five smoke concentrations at each heat flux. Smoke concentration is defined in this study as the quantity of material decomposed (weight loss) divided by the volume of the chamber and is expressed in units of milligrams per liter (mg/ℓ). Toxicological assessments are, therefore, based on smoke produced from a material, rather than on the material itself. To avoid physiologically significant temperature elevations in the chamber and still achieve maximum possible smoke concentrations, it was necessary to limit the irradiation period to 23 minutes at 5 W/cm^2 and 5.5 minutes at 10 W/cm^2.

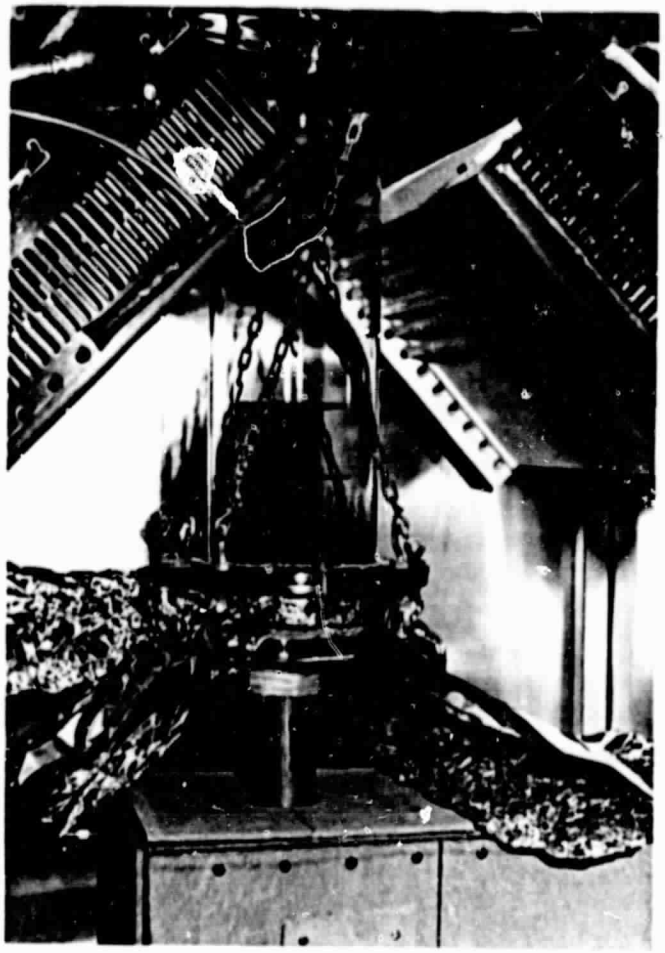

Figure 1. Combustion Apparatus

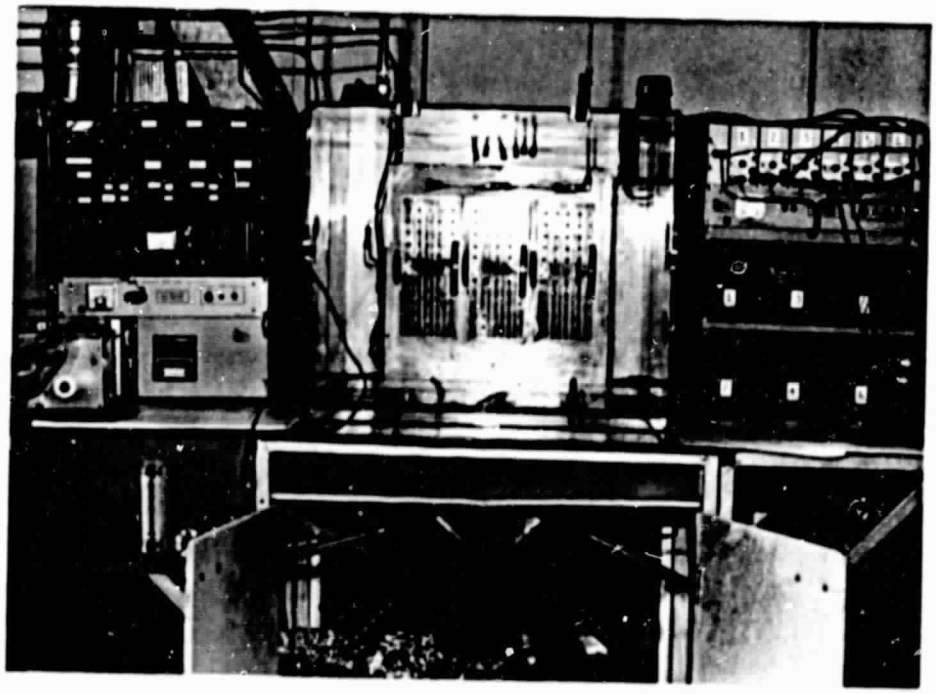

Figure 2. Animal Exposure System

ORIGINAL PAGE IS
OF POOR QUALITY

The smoke toxicity of the materials was assessed from measurements of lethality, incapacitation, and associated blood carboxyhemoglobin (COHb) saturation levels in the following manner.

1. Lethality

Six Sprague-Dawley albino male rats, restrained in individual stainless steel cages, were exposed for 30 minutes to each smoke concentration over the 0 to 100 percent lethality range. Percent lethality, including deaths occurring over a 14-day post-exposure period, was determined as a function of smoke concentration. Estimations of LC_{50} values were made from dose-response data using standard probit analysis techniques.

2. Incapacitation

Three rats per test were employed using the rotorod incapacitation model in which animals are conditioned to remain upon a rotating rod above an electrified grid as an index of sensori-motor capability. Animals were considered to be incapacitated if, upon falling from the rod, they were unable to remount within 15 seconds. Rats were exposed to five smoke concentrations at each heat flux, with mean time-to-response data being obtained for each concentration. Estimations of EC_{50} values were made from time-to-response/concentration plots, rather than from conventional dose-response relationships.

3. Blood Carboxyhemoglobin Saturation

Blood samples were obtained by cardiac puncture from animals expiring during a test. Rotorod animals, immediately after reaching the 15-second end point, were removed through an airlock device and blood obtained by retro-orbital puncture. Percent blood carboxyhemoglobin saturation was determined using an IL-282 CO-Oximiter.

4. Combustion Atmosphere Analyses

Analyses were made continuously during each experiment for oxygen (Beckman OM-11 Analyzer), carbon monoxide (Beckman 865 Analyzer), carbon dioxide (Beckman 864 Analyzer), and total unburned hydrocarbons expressed as methane (Beckman 402 Hydrocarbon Analyzer). Qualitative assessment of hydrogen cyanide was made both by gas chromatography and indicator tubes.

C. RESULTS AND DISCUSSION

Summaries of experimental data obtained from the graphite/epoxy and graphite/bismaleimide materials are presented in Tables VII and VIII. Probit plots of percent effect (lethality) as a function of smoke concentration for the two materials are shown in Figures 3 and 4. Values of the LC_{50} (30-min) were obtained directly from the dose-response curves.

Time-to-incapacitation as a function of smoke concentration curves are presented in Figures 5 and 6. Also shown on the figures are mathematical equations for the hyperbolic functions derived as a best fit of the experimental data. Estimated EC_{50} (30-min) values (concentrations yielding 50-percent incapacitation response in 30 minutes) were obtained from the curves by identification with smoke concentrations producing mean times-to-incapacitation of 30 minutes. Estimated EC_{50} values can also be obtained from the curves for times other than 30 minutes in a similar fashion.

Table IX contains a summary of 30-minute LC_{50} and EC_{50} values for the two materials evaluated, along with percent blood carboxyhemoglobin saturation associated with both death and incapacitation. Corresponding data are also shown for Douglas fir in order to place the toxicity data in perspective. Additionally, mean carboxyhemoglobin saturation at

TABLE VII

SMOKE TOXICOLOGICAL ASSESSMENT--NASA MATERIALS
SwRI RADIANT FLUX FURNACE/ROTOROD INCAPACITATION MODEL

Graphite/Epoxy 5W/cm² 23-Minute Irradiation Period
GE-1007-050

Test ID	Sample Weight g	Weight Loss Percent	Smoke Concentration mg/ℓ	CO Max. ppm	Mean Time To Incapacitation min:dec s	Mean COHb at Incapacitation	Passive % Lethality (6 rats)	Mean COHb Dead or End of Test
056	15.0	51.3	23.4	2178	27.78 ±3.1	62.8 ±4.7	No Passives	No Passives
055	24.7	45.2	33.9	~3000	21.08 ±0.9	68.2 ±2.4	1/6 16.7	74.1
054	31.6	42	40.3	4000	19.45 ±1.0	68.1 ±1.1	6/6 100	80.0 ±0.9
053	46.3	39.5	55.6	5800	14.12 ±1.02	68.4 ±3.3	6/6 100	81.1 ±2.9
052	66.7	33.2	67.6	6600	12.1 ±1.5	60.8 ±4.3	6/6 100	80.9 ±3.4
					Graphite/Epoxy 10 W/cm² 5.5-Minute Irradiation Period **GE-1012-100-9**			
102	30.3	30.4	28	N/A	22.75 ±2.25	58.1 ±1.0	0	58.5 (end)
103	44.3	27.3	36.8	1750	19.02 ±8.65	54.7 ±8.3	0	61.8 (end)
104	47.9	25	37.1	1870	9.0 ±1.0	34.9 ±6.1	3/6 50	60.1 ±3.0
105	46	27.4	38.3	2240	6.63 ±0.06	33.7 ±3.7	6/6 100	59.0 ±2.1
101	53.5	26.8	43.4	2490	6.57 ±1.8	30.5 ±4.4	6/6 100	65.0 ±2.4

TABLE VIII

SMOKE TOXICOLOGICAL ASSESSMENT--NASA MATERIALS
SwRI RADIANT FLUX FURNACE/ROTOROD INCAPACITATION MODEL

Graphite/Bismaleimide 5 W/cm^2 23-Minute Irradiation Period
GB-1013-050

Test ID	Sample Weight g	Weight Loss Percent	Smoke Concentration mg/ℓ	CO Max. ppm	Mean Time To Incapacitation min:dec s	Mean COHb at Incapacitation	Passive % Lethality (6 rats)	Mean COHb Dead or End of Test
055	13.1	53.4	21.6	2423	25.5 ±1.33	64.0 ±1.3	No Passives	No Passives
053	21.1	49.6	31.8	~3500	19.82 ±1.07	69.0 ±2.3	3/6 50	72.5 ±3.4
052	34.4	46.5	48.6	5000	15.4 ±0.4	70.9 ±2.3	6/16 100	81.3 ±3.4
054	44.4	42.9	57.9	~5000	14.73 ±1.10	65.3 ±6.4	No Passives	No Passives

Graphite/Bismaleimide 10 W/cm^2 5.5-Minute Irradiation Period
GBM-751-133-100

105	20.5	33.7	21.0	2108	26.44 ±4.43	62.8 ±1.7	0	60.8 (end)
103	25.3	31.2	24.0	27-2800	19.33 ±4.05	67.1 ±1.0	1/6 16.7	69.1
101	37.7	28.4	32.5	3200	13.62 ±1.92	68.2 ±1.8	2/6 33.3	72.1 ±0.5
104	46.8	28.3	40.3	~4000	11.08 ±1.34	67.0 ±1.4	3/6 50	77.0 ±1.7
102	57.0	26.9	46.5	4200	9.83 ±1.52	64.6 ±2.6	5/6 83.3	78.7 ±2.9

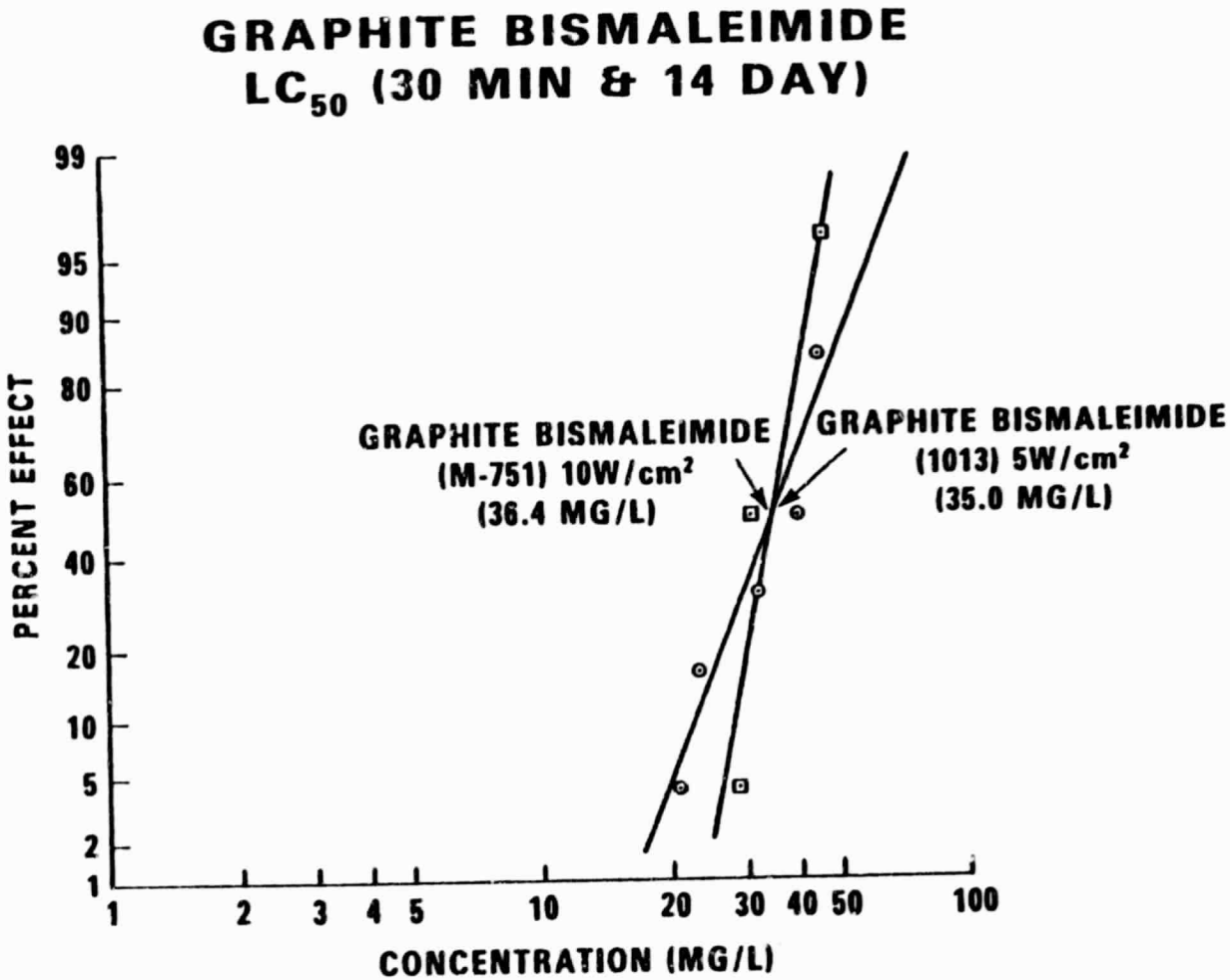
GRAPHITE BISMALEIMIDE
LC50 (30 MIN & 14 DAY)
PERCENT EFFECT
99
95
90
80
60
40
20
10
5
2
1
GRAPHITE BISMALEIMIDE
(M-751) 10W/cm²
(36.4 MG/L)
GRAPHITE BISMALEIMIDE
(1013) 5W/cm²
(35.0 MG/L)
1
2
3
4
5
10
20
30
40
50
100
CONCENTRATION (MG/L)

Figure 3

GRAPHITE EPOXY
LC_{50} (30 MIN & 14 DAY)

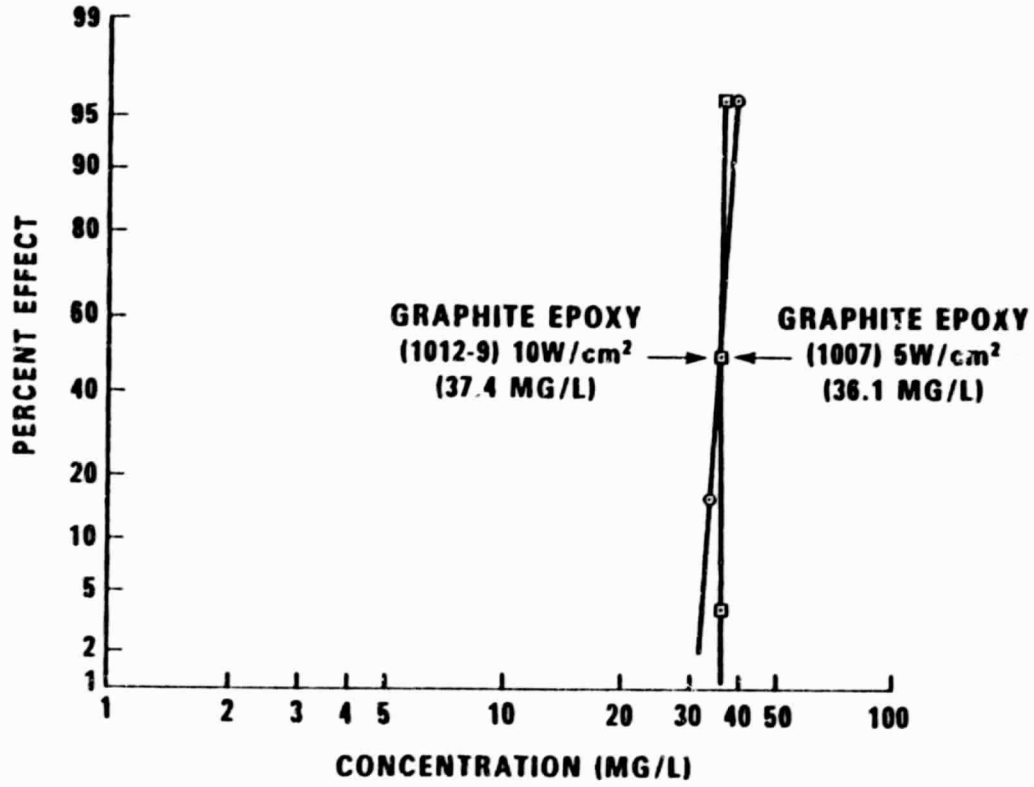

Figure 4

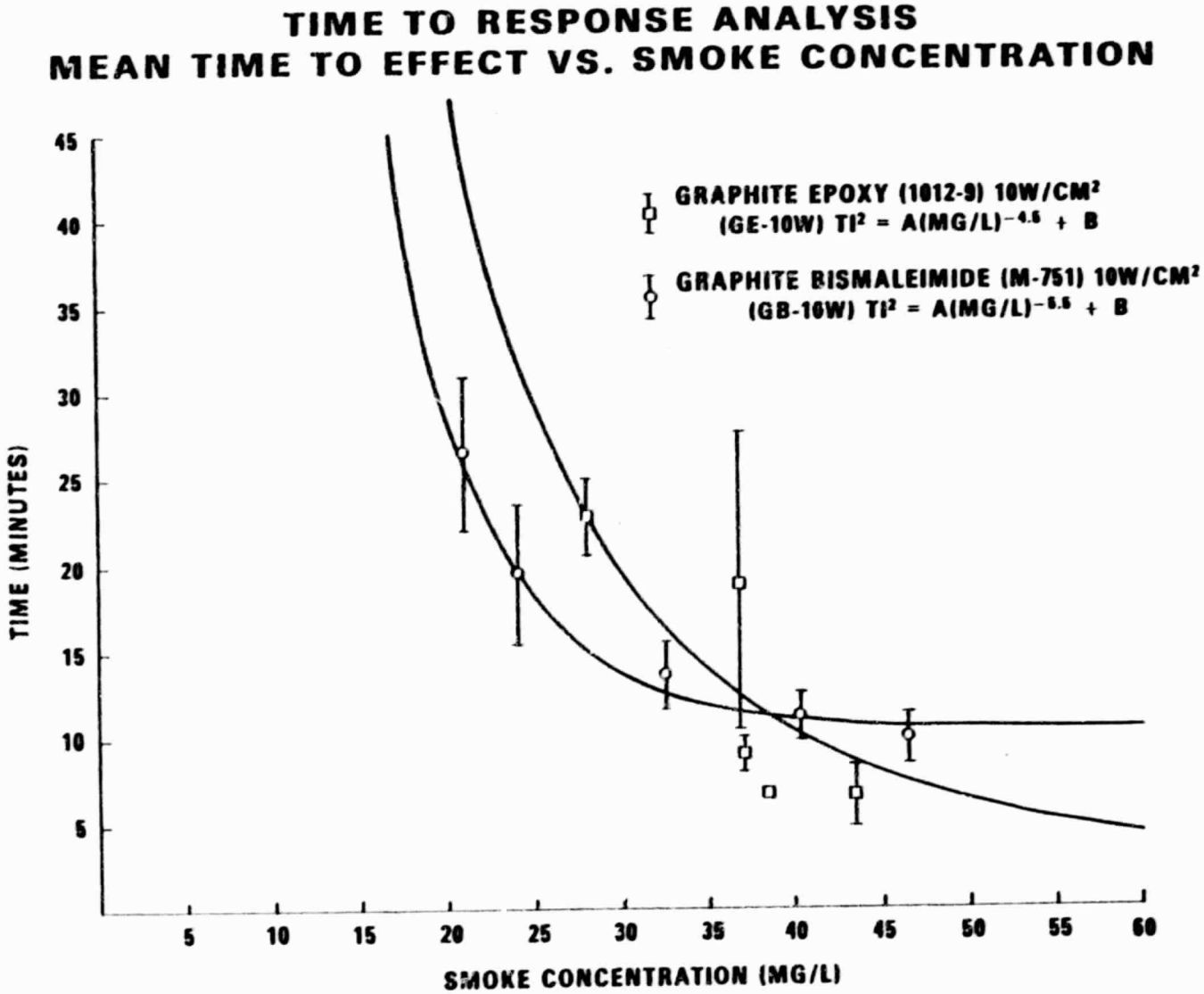
TIME TO RESPONSE ANALYSIS
MEAN TIME TO EFFECT VS. SMOKE CONCENTRATION
GRAPHITE EPOXY (1012-9) 10W/CM²
(GE-10W) TI² = A(MG/L)⁻⁴.⁵ + B
GRAPHITE BISMALEIMIDE (M-751) 10W/CM²
(GB-10W) TI² = A(MG/L)⁻⁵.⁵ + B
TIME (MINUTES)
45
40
35
30
25
20
15
10
5
5
10
15
20
25
30
35
40
45
50
55
60
SMOKE CONCENTRATION (MG/L)

Figure 5

TIME TO RESPONSE ANALYSIS
MEAN TIME TO EFFECT VS. SMOKE CONCENTRATION

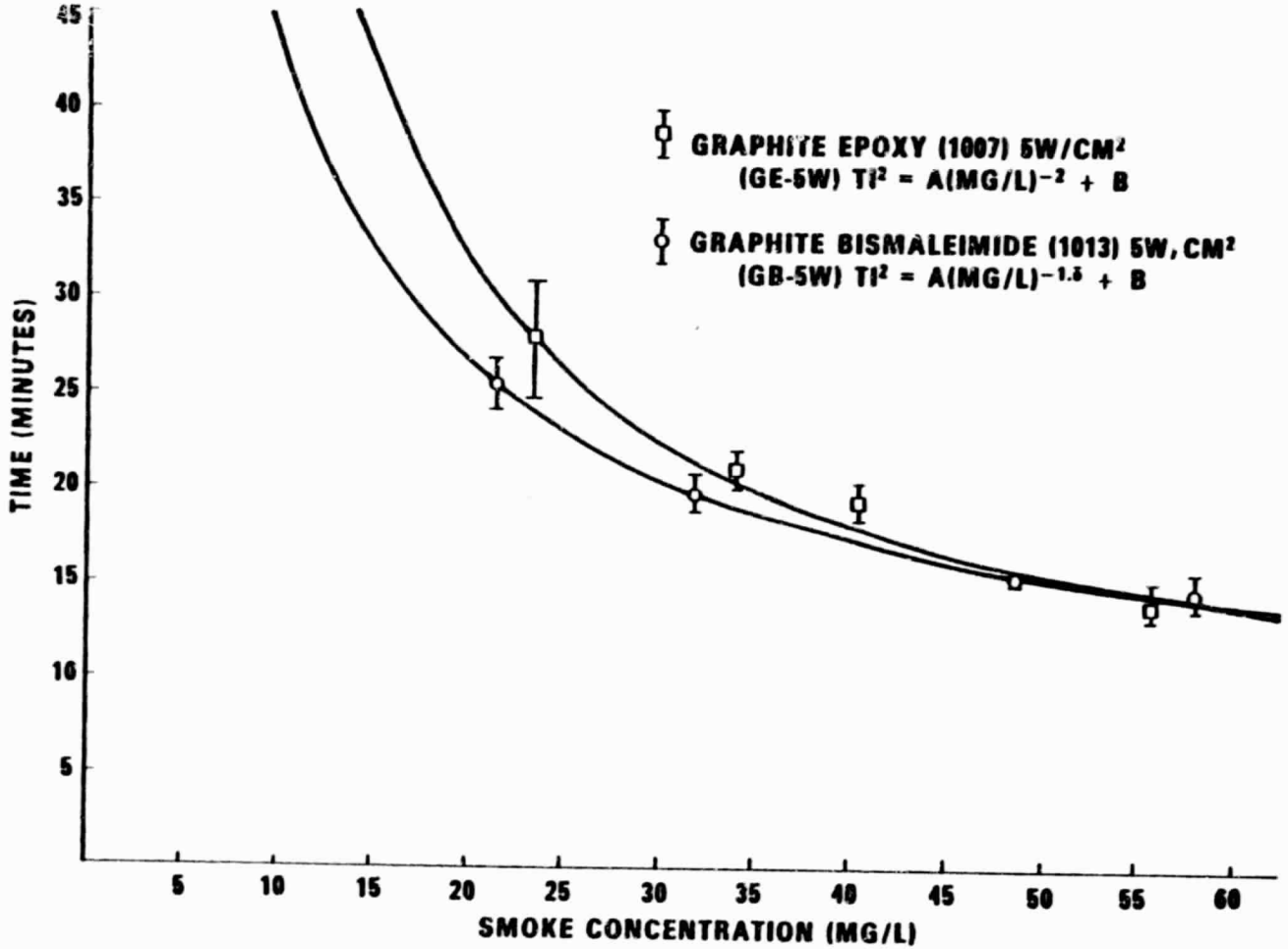

Figure 6

TABLE IX

SMOKE TOXICOLOGICAL ASSESSMENT--NASA MATERIALS
SwRI RADIANT FLUX FURNACE/ROTOROD BEHAVIORAL SYSTEM

Material	Heat Flux (W/cm^2)	LC_{50}, (mg/ℓ) 30 min + 14 days	Percent COHb Death	No. of Rats Sampled	$^2EC_{50}$ (30 min) (mg/ℓ)	Percent COHb at Incapacitation	No. of Rats Sampled
Graphite/ Epoxy	5	36	79.0 ±3.3	19	22	65.9 ±3.6	15
Graphite/ Bismaleimide	5	36	76.9 ±6.2	9	17	67.1 ±3.0	15
Douglas fir	4 (Est.)	36	83.2 ±2.7		18	63.4	
[1] Graphite/ Epoxy	10	37	61.4 ±3.2	15	25	42.4 ±13.0	15
Graphite/ Bismaleimide	10	36	74.2 ±4.4	11	20	65.2 ±2.4	15

1 Flaming Auto Ignition
2 Calculated from mathematical model
3 NBS Experimental Protocol Data-Flaming Mode
Potts Furnace/Leg Flexion Behavioral System

ORIGINAL PAGE IS
OF POOR QUALITY

incapacitation as a function of smoke concentration for the two materials at each heat flux is shown in Figure 7.

Within the limits defined by the protocol, the toxicological potencies of smoke from the graphite/epoxy and graphite/bismaleimide materials are essentially identical for 30-minute exposure times and comparable to those of many common materials, including Douglas fir (Table IX). There were no significant differences in toxicological potency for either material between the two heat flux levels. The 14-day post-test observation period failed to uncover any delayed toxic effects resulting from the 30-minute exposure. No post-test deaths occurred in any of the four-test series, indicating the toxic insults to be primarily limited to within-test exposure.

The data strongly support that carbon monoxide is by far the major toxic insult for both materials at 5 W/cm^2 and for the graphite/bismaleimide at 10 W/cm^2. Carboxyhemoglobin saturation levels and ambient carbon monoxide concentrations produced are consistent with this conclusion and in excellent agreement with carbon monoxide studies.[9]

Although the graphite/epoxy material at 10 W/cm^2 exhibits a toxicological potency comparable to that seen at 5 W/cm^2, significant differences in casuality are suspected, with the suggestion of a secondary toxicant. Blood carboxyhemoglobin saturation values and ambient carbon monoxide levels, while still substantial, are somewhat lower than expected. This is particularly true of higher smoke concentrations as illustrated for incapacitation in Figure 7. It is additionally noteworthy that the graphite/epoxy material did undergo intermittent flaming combustion at 10 W/cm^2.

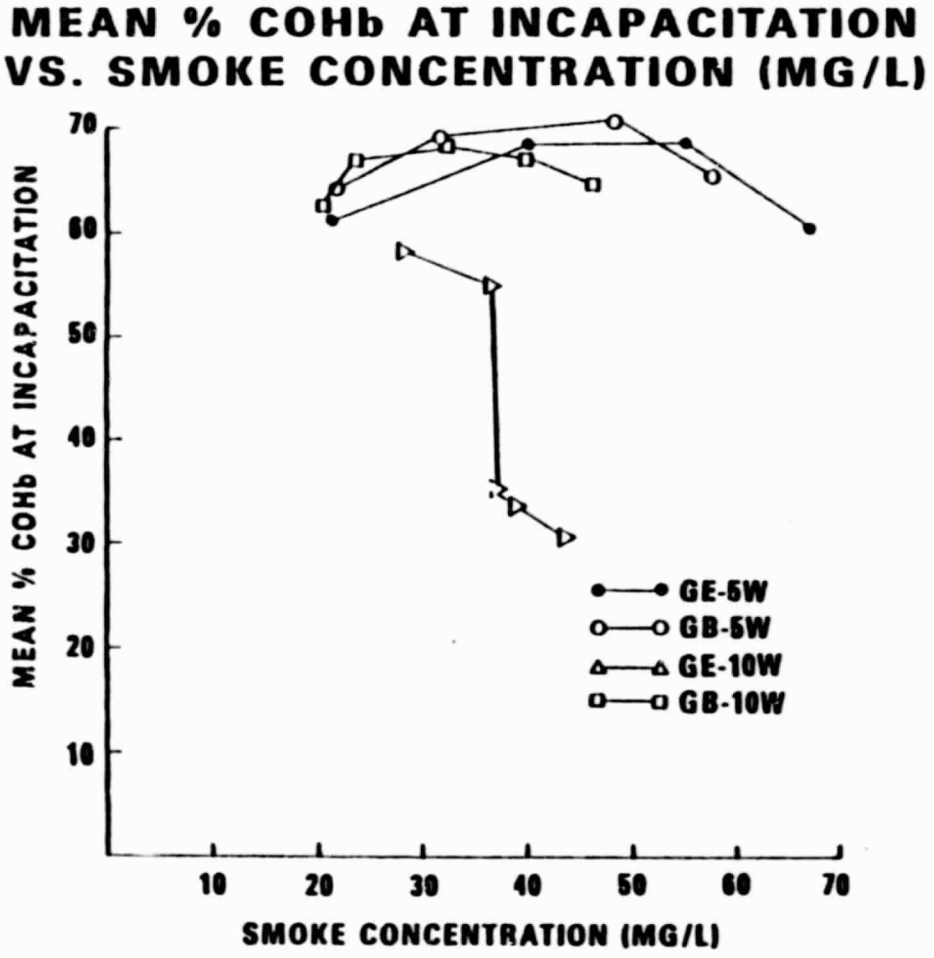
MEAN % COHb AT INCAPACITATION VS. SMOKE CONCENTRATION (MG/L)
MEAN % COHb AT INCAPACITATION
70
60
50
40
30
20
10
10
20
30
40
50
60
70
SMOKE CONCENTRATION (MG/L)
GE-5W
GB-5W
GE-10W
GB-10W

Figure 7

Hydrogen cyanide was confirmed by gas chromatography and the use of Kitagawa indicator tubes as an additional significant toxicant formed from the intermittent flaming of the graphite/epoxy material at 10 W/cm^2. Hydrogen cyanide was also detected analytically from the graphite/epoxy material at 5 W/cm^2 but no discernable toxicological effects were observed.

The contribution of hydrogen cyanide to the toxic insult resulting from the graphite/epoxy at 10 W/cm^2 is also manifest in the somewhat shorter than expected times-to-incapacitation observed at high concentrations of the smoke (Figure 6).

The significance of these observations should be placed in perspective with respect to the overall hazard of the producing condition. The situation was observed under the conditions of what would be a relatively large and intense, hot fire. Moreover, the possible human significance of decreased time to escape due to a contribution of hydrogen cyanide cannot be adequately assessed from limited data on rodents and the state of current knowledge of carbon monoxide-hydrogen cyanide combined insults.

The LC_{50} (30-min + 14-days) value is primarily a measurement of acute toxicological potency. It posesses toxicological significance in a classical sense and should be determined on the basis of acutal smoke produced, as was done in this project. However acceptable this measurement is in a traditional sense, it has limited value in assessing relative potential safety margins between alternate materials to be used in aircraft construction. Toxicological potency (LC_{50}) is often related to, but not a measurement of, limitations on escape potential. Relevant fire hazard parameters all possess the element of time as a variable

(e.g., flame spread rate, heat release rate, smoke development rate, etc.). To address the evaluation of aircraft materials within appropriate fire scenarios, toxicological impact as a function of time is a highly critical parameter which may well be more sensitive than the use of simple toxicological potencies. Expression of all relevant fire parameters as functions of time also offers the opportunity for the modeling of overall hazard since factors limiting escape can be treated mathematically. Simple LC_{50} or EC_{50} dose-response values cannot be assessed in conjunction with time-related fire parameters. It is, therefore, recommended that time-to-effect toxicological studies (i.e., incapacitation) be carried out more extensively in future material evaluation programs.

Although toxicologically unorthodox, the expression of toxic insults on the basis of surface area of material exposed would be much more relevant and translatable to the assessment of relative materials' performance. Thus, material toxicity, rather than smoke toxicity, is a more practical concept, particularly if used as a basis for time-related biological effects.

This study was basically conducted in a classical sense. However, sufficient utilization and analysis of time-related effects were made to justify recommendations that future programs utilize time-to-incapacitation as a function of material surface exposed to radiant heat as the basis for assessment of relative potential safety margins between alternate materials.

D. CONCLUSIONS

Toxicological potencies of smoke produced from the two materials, graphite/epoxy and graphite/bismaleimide, are equivalent for incapacitation and lethality (30-min exposure) at both 5 W/cm^2 and 10 W/cm^2. They are also comparable to those of wood and many common materials of commerce. No evidence was seen for the presence of an "unusual toxicant", in that observed toxicological effects were consistent with toxicants known to be present.

Carbon monoxide was the sole toxicant of significance for both materials at 5 W/cm^2, the graphite/bismaleimide at 10 W/cm^2 and a major toxicant in the case of the graphite/epoxy material at 10 W/cm^2. The latter material was observed to undergo intermittent flaming combustion at 10 W/cm^2 with the production of hydrogen cyanide, evidence for which was seen toxicologically, particularly at higher smoke concentrations. Somewhat shorter times-to-incapacitation than would have been anticipated from carbon monoxide alone were observed.

No post-exposure toxicological effects were observed resulting from 30-minute exposure of rats to smoke from either material.

The combustion-exposure system and protocol used for this project were effective in producing data for computation of traditional toxicity indices as well as providing information to investigate other aspects of the time sequence. The combination of measured parameters enabled rational deductions to be made on the nature of the toxic insults and to delineate relatively fine differences in the combustion toxicity of the materials.

It is recommended that future studies make more extensive use of time-to-incapacitation as a function of material surface exposure to radiant heat as the basis for assessment of relative potential safety margins between materials.

REFERENCES

1. Smith, E.E., "Measuring Rate of Heat, Smoke, and Toxic Gas Release," Fire Technology, Vol. 8, p. 237, (1972).

2. Smith E.E., "Heat Release Rate of Building Materials, Ignition, Heat Release and Noncombustibility of Materials," ASTM STP 302, ASTM, 1972, pp. 119-134.

3. Farrar, D.G., Hartzell, G.E., Bland, T.L., and Galsten, W.A., Development of a Protocol for the Assessment of the Toxicity of Combustion Products Resulting from the Burning of Cellular Plastics, Report UTEC 79/130, Salt Lake City; University of Utah, 1979.

4. Potts, W.J., and Lederer, T.S., "A Method for Comparative Testing of Smoke Toxicity,: Journal of Combustion Toxicology 4 (1977: 114-162.

5. National Research Council Committee on Fire Toxicology, Fire Toxicology: Methods for Evaluation of Toxicity of Pyrolysis and Combustion Products, Report No. 2, Washington, D.C.: National Academy of Sciences, 1977.

6. Dunham, N.W., and Miya, I.S., A Note on a Simple Apparatus for Detecting Neurological Deficit in Rats and Mice, J. AN. Pharmacol. Ass., 44 (1957) 208.

7. Geller, I., Campbell, N.D., and Blum, K., Protection Against Acute Alcoholic Intoxication With Diethanolamine-Rutin, Res. Commun. Chem. Pathol. Pharmacol., 1 (1970) 383.

8. Mitchell, D.S., Rodgers, W.R., Herrera, W.R., and Switzer, W.G., "Behavioral Incapacitation of Rats During Full-Scale Combustion of Natural-Fiber and Synthetic Polymeric Furnishings, Fire Research, 1 (1988-78), 187-197.

9. Hartzell, G.E., Packham, S.C., Hileman, F.D., Isreal, S.C., Dickman, M.L.Baldwin, R.C., and Mickelson, R.W., "Physiological and Behavioral Responses to Fire Combustion Products," Fourth International Cellular Plastics Conference, Society of the Plastics Industry, Montreal, Canada, November 18, 1976. (Report FRC/UU-079 available from the Flammability Research Center, University of Utah).

APPENDIX

THERMAL PROPERTIES FIGURES

LIST OF FIGURES

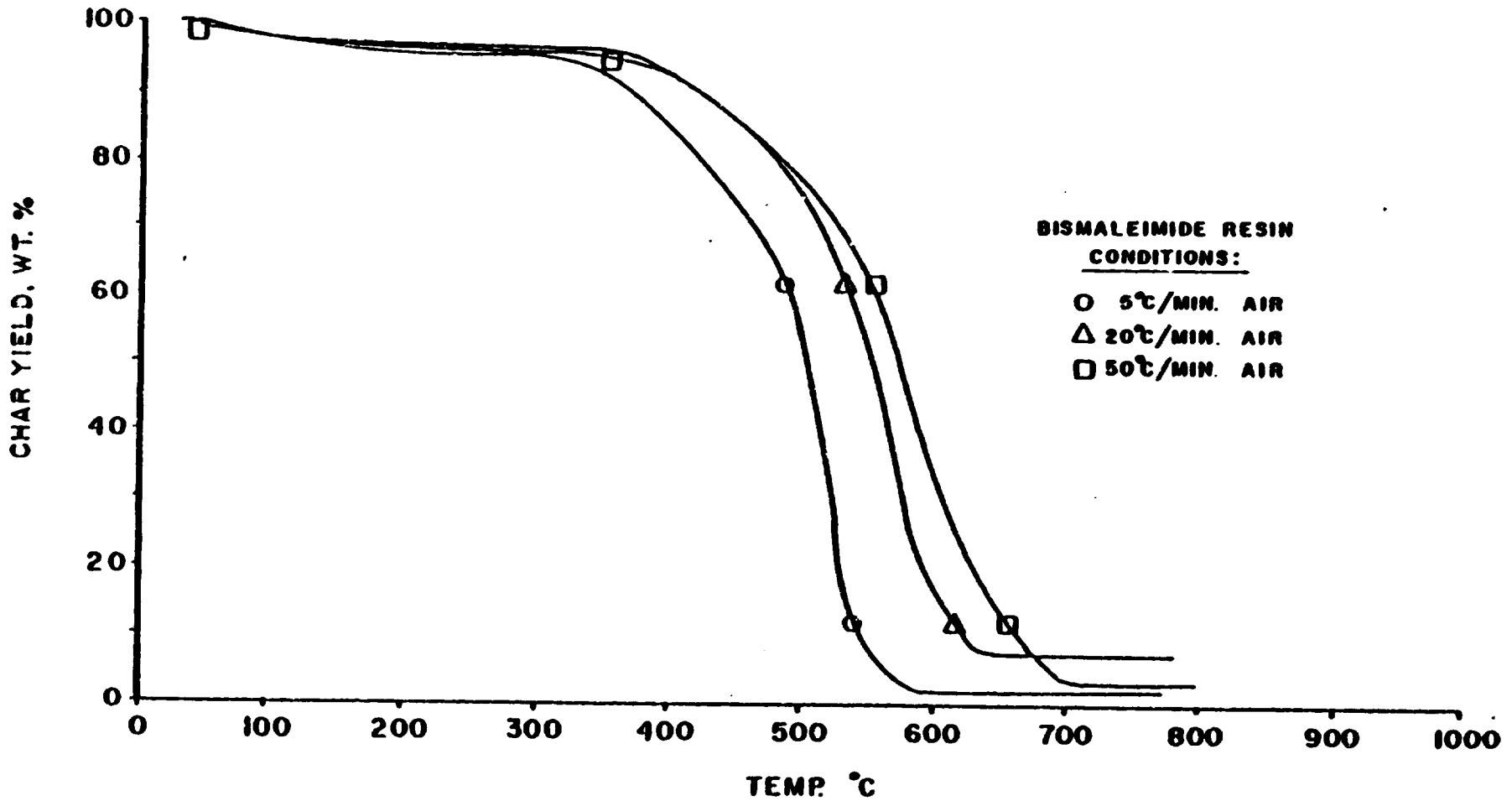

Figure 1. Effect of Heating Rate on Thermal Degradation of Bismaleimide Resin in Air

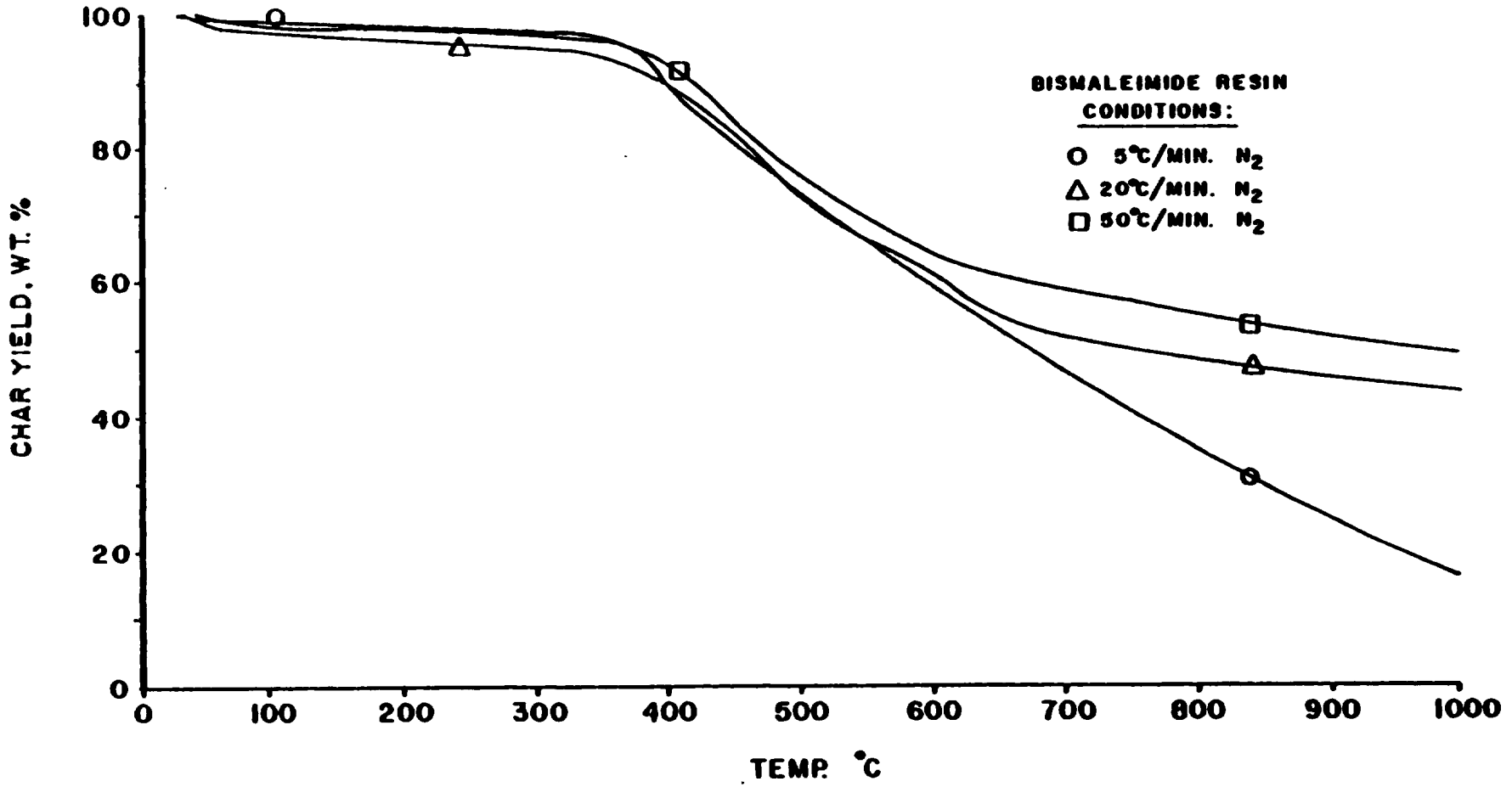

Figure 2. Effect of Heating Rate on Thermal Degradation of Bismaleimide Resin in Nitrogen

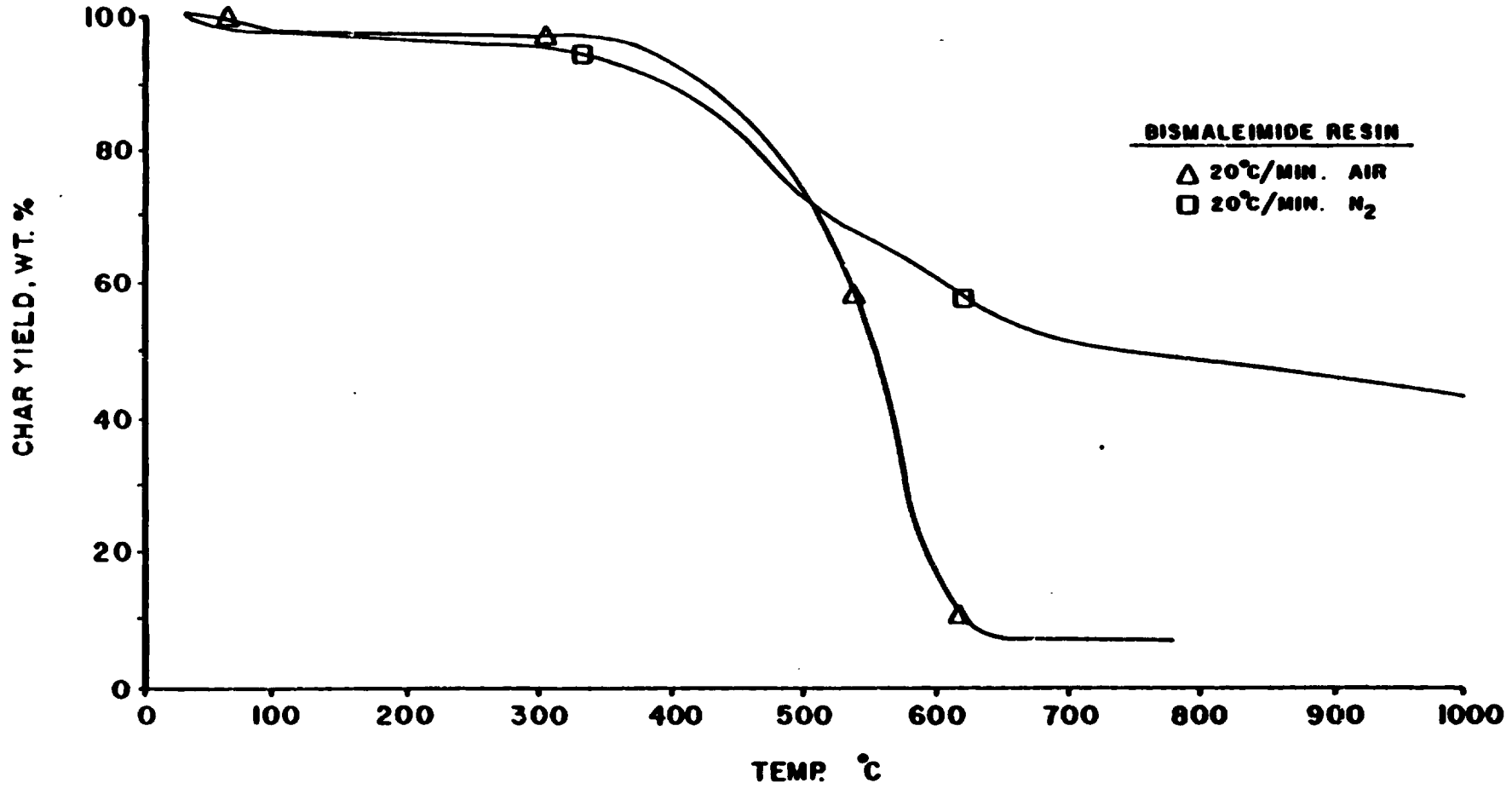

Figure 3. Effect of the Environment on Thermal Degradation of Bismaleimide Resin

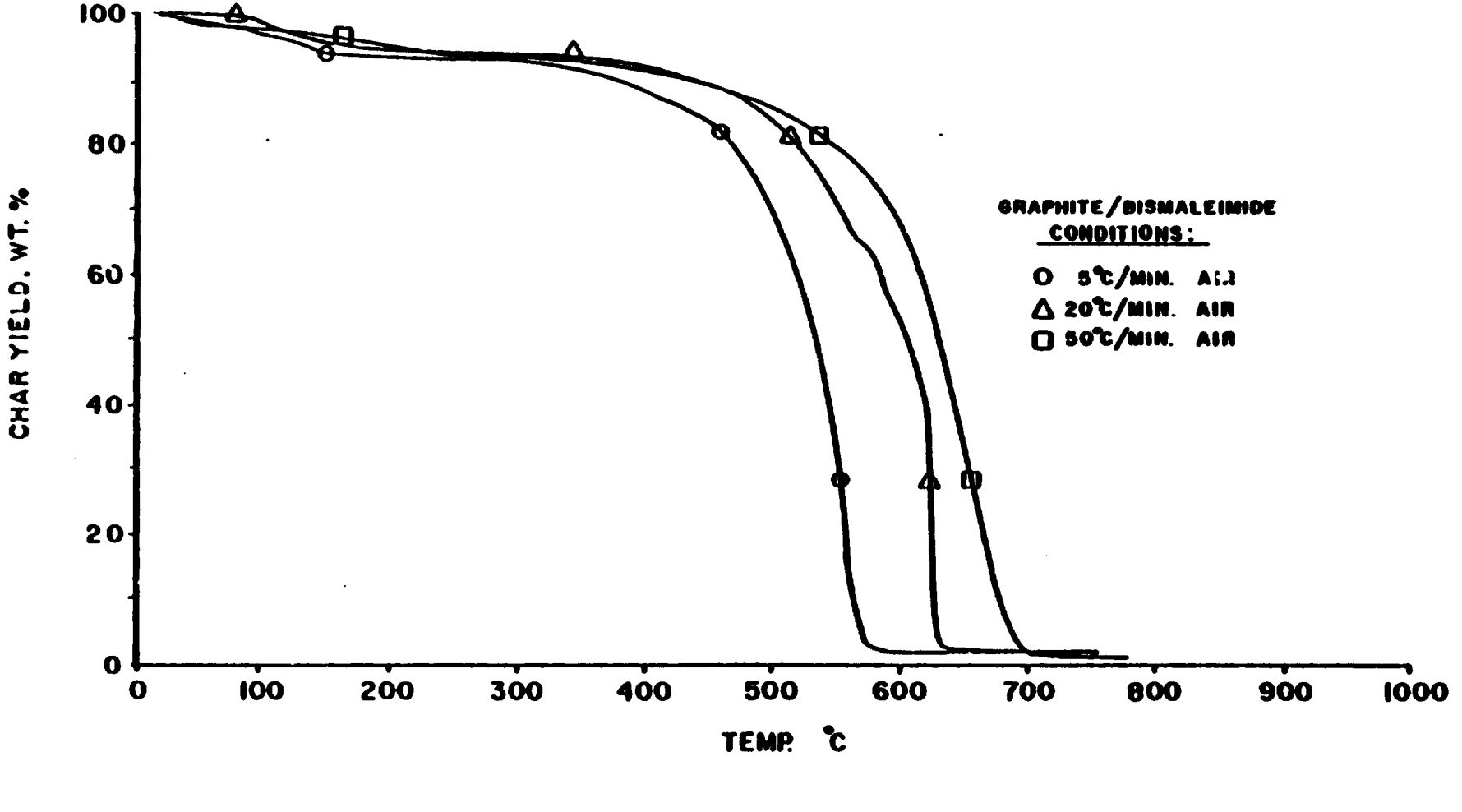

Figure 4. Effect of Heating Rate on Thermal Degradation of Graphite/Bismaleimide Composite

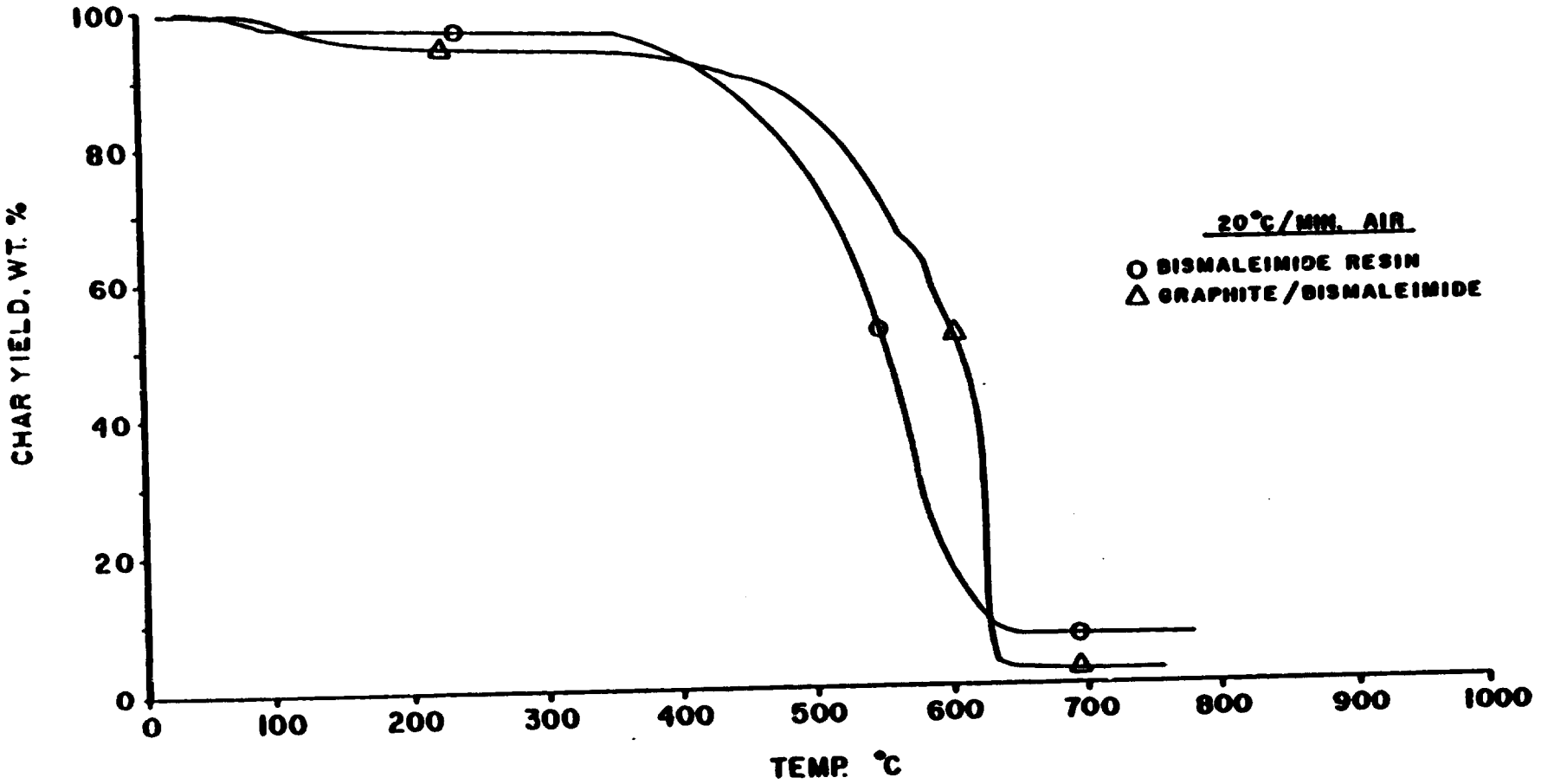

Figure 5. Comparison of Thermograms of Bismaleimide Resin and Graphite/Bismaleimide Composite

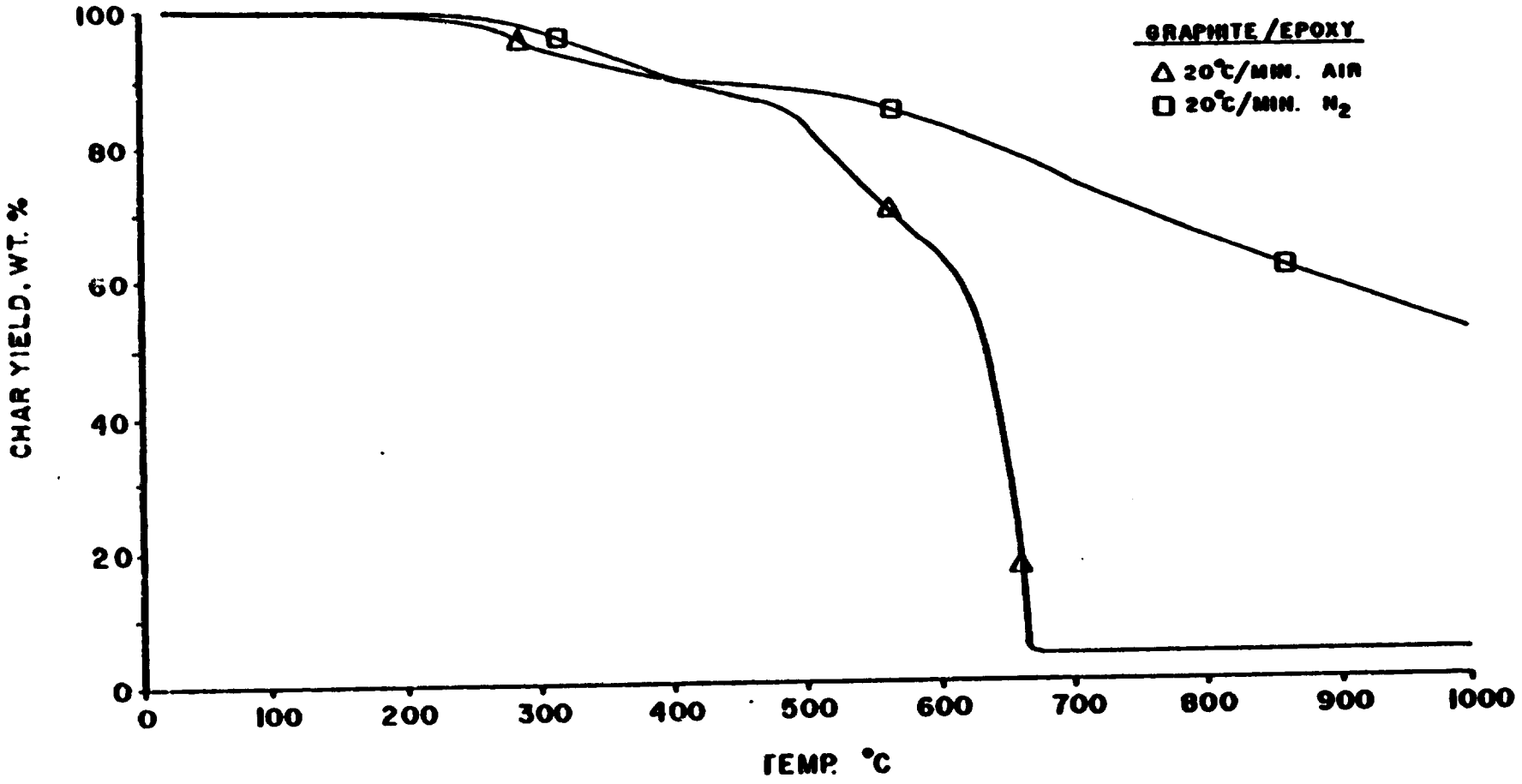

Figure 6. Effect of the Environment on Thermal Degradation of Graphite/Epoxy Composite

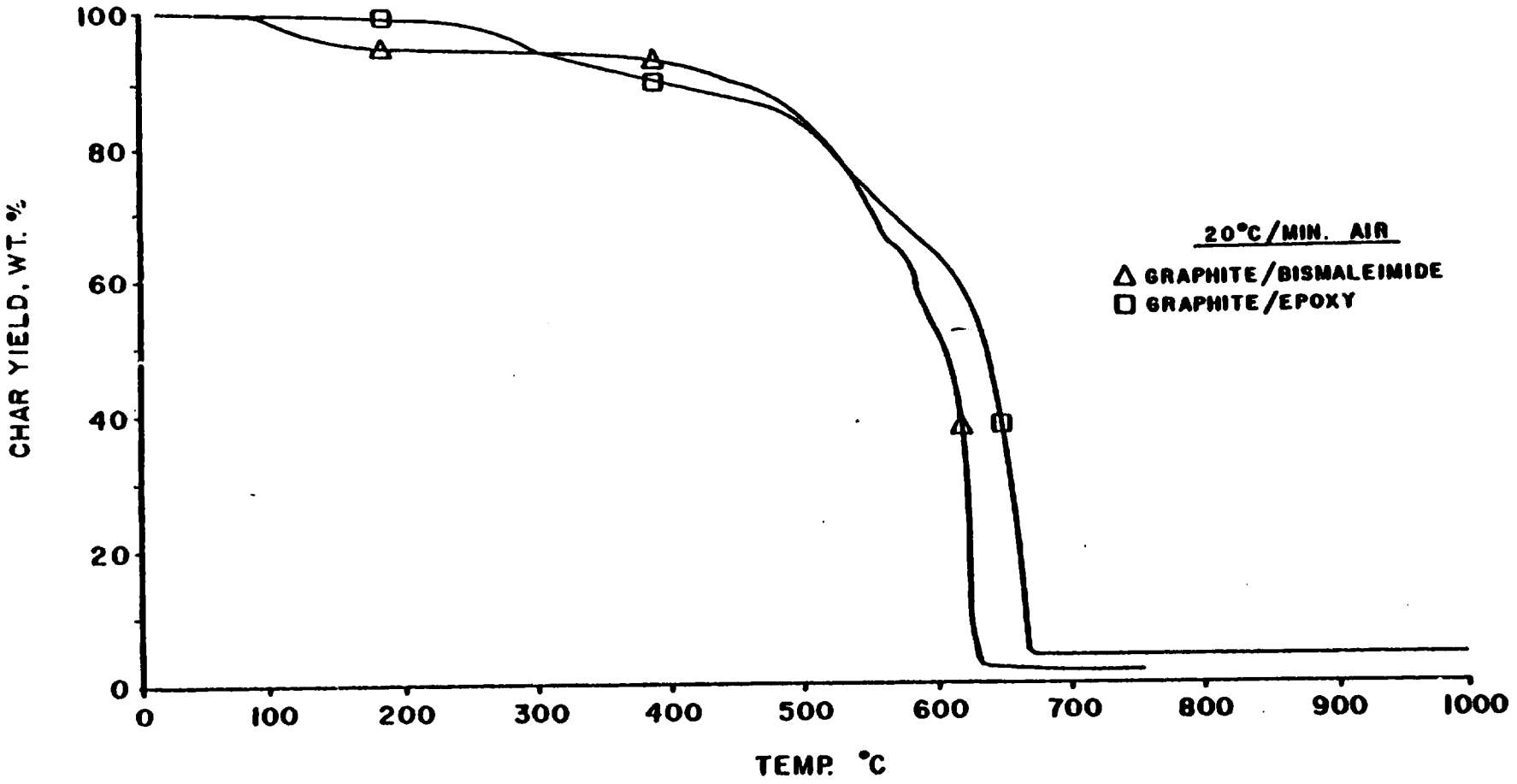

Figure 7. Comparison of Graphite/Bismaleimide and Graphite/Epoxy Degradations in Air

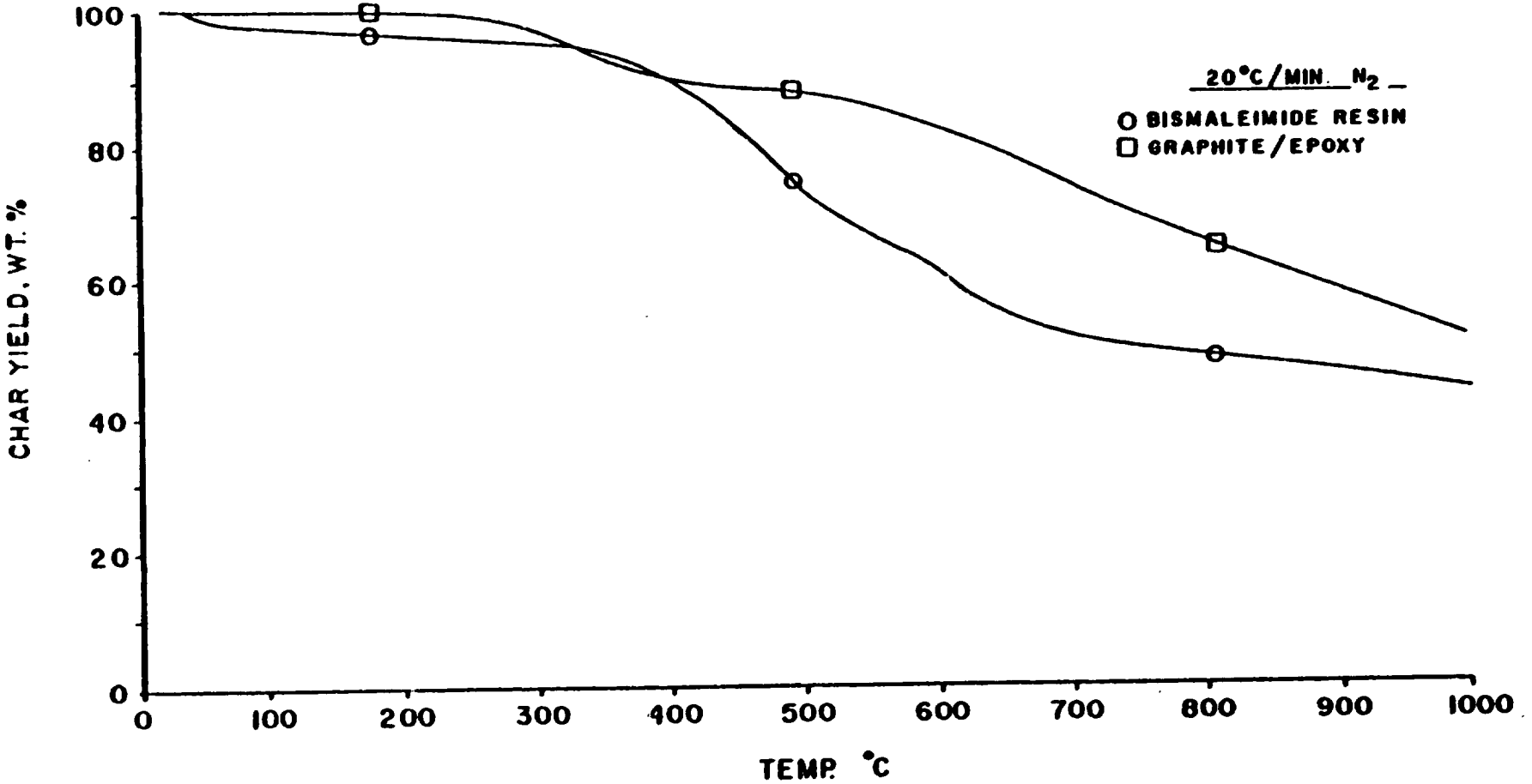

Figure 8. Comparison of Bismaleimide and Graphite/Epoxy Degradations in Nitrogen

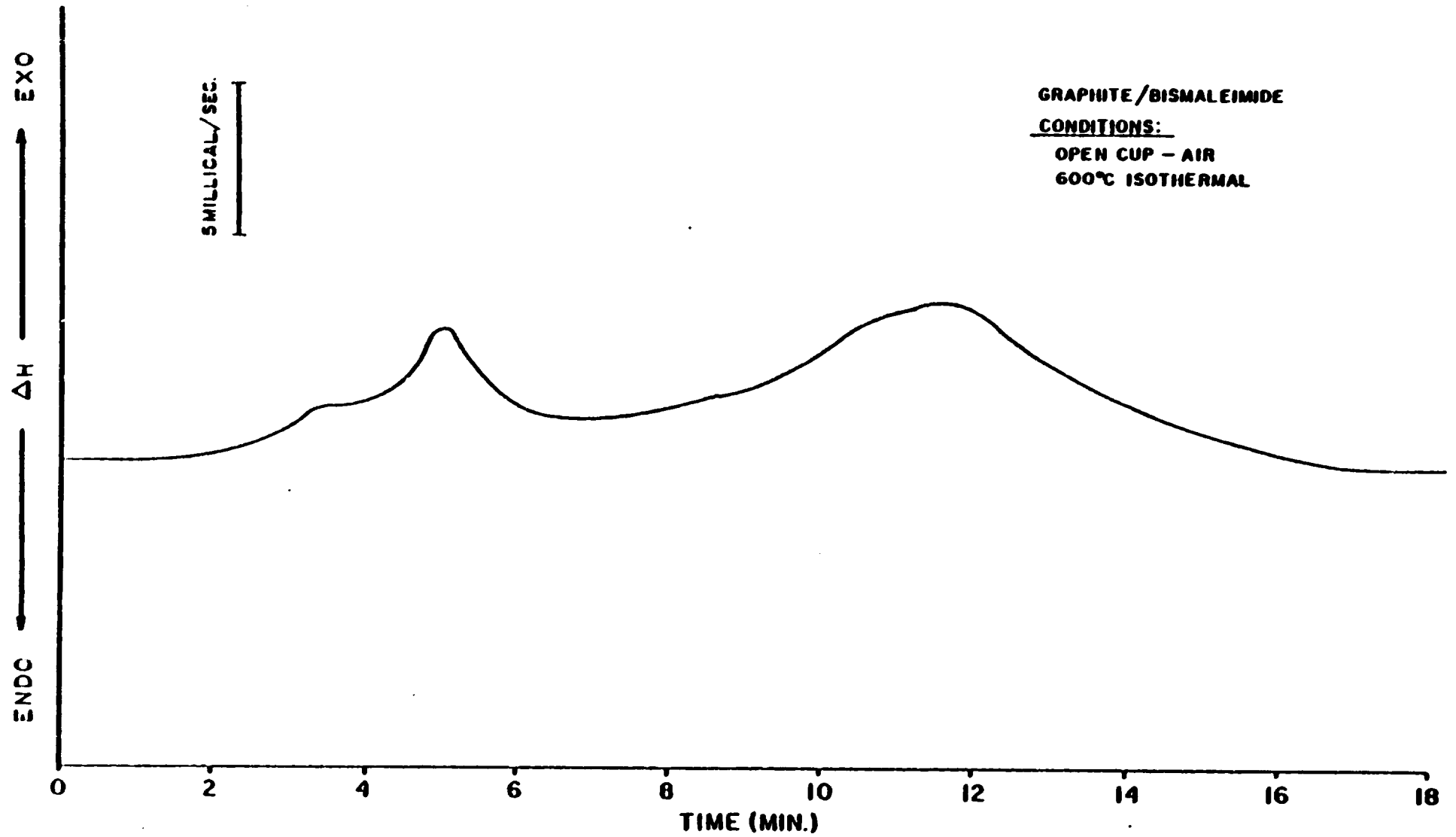

Figure 9. Differential Scanning Calorimeter Thermogram of Graphite/Bismaleimide

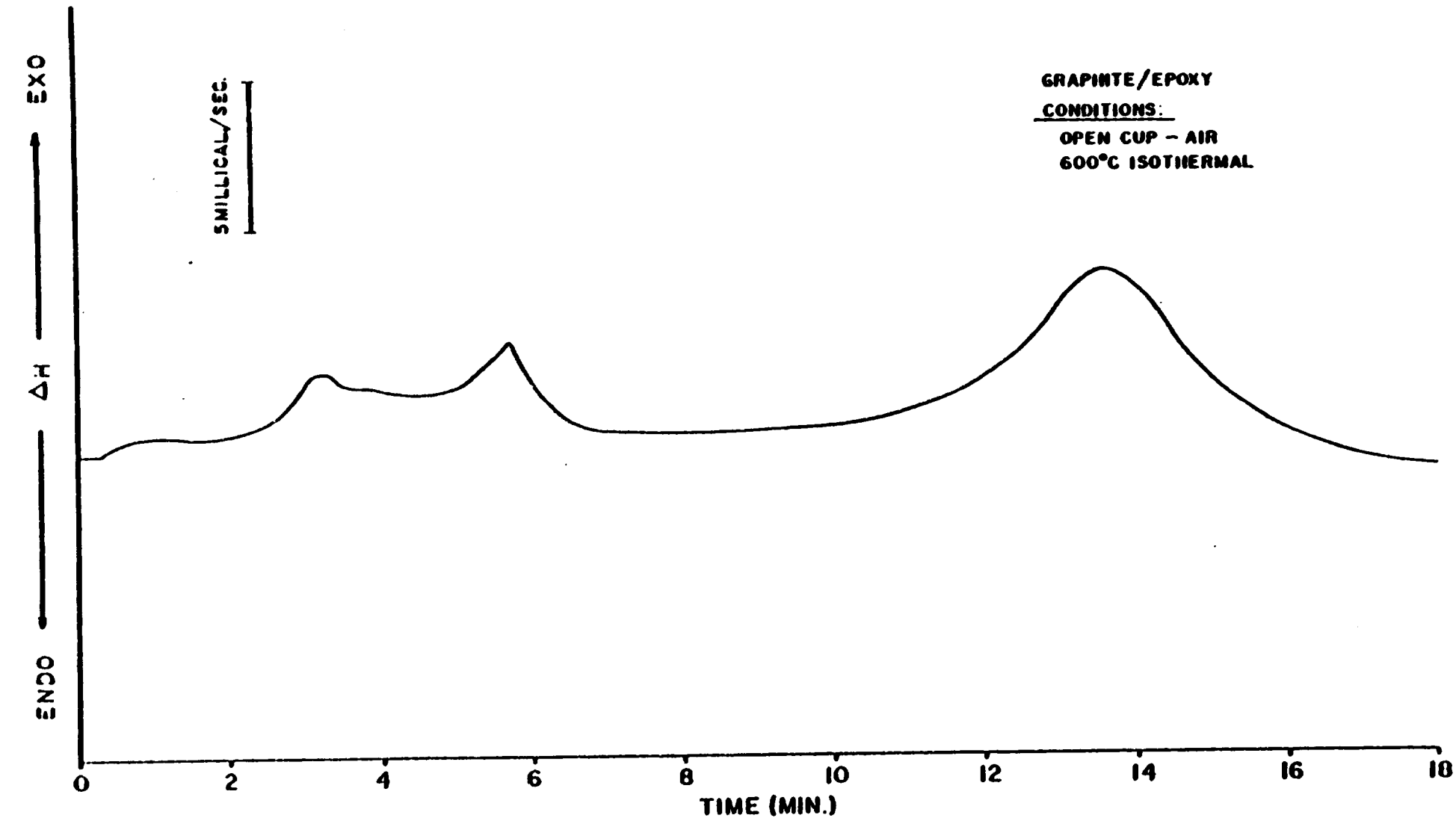

Figure 10. Differential Scanning Calorimeter Thermogram of Graphite/Epoxy

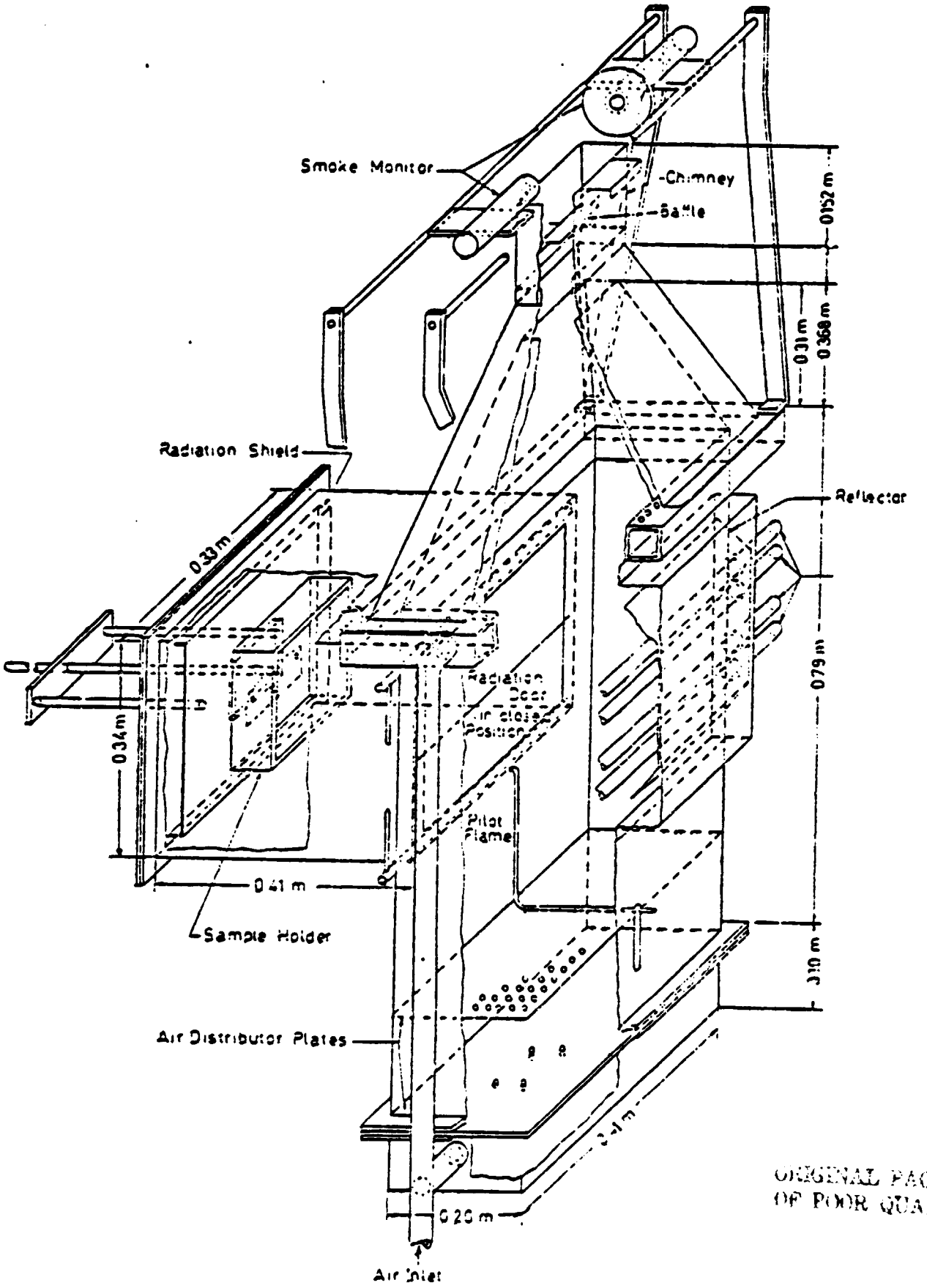

ORIGINAL PAGE IS
OF POOR QUALITY

Figure 11. Ohio State University (OSU) Release Rate Apparatus

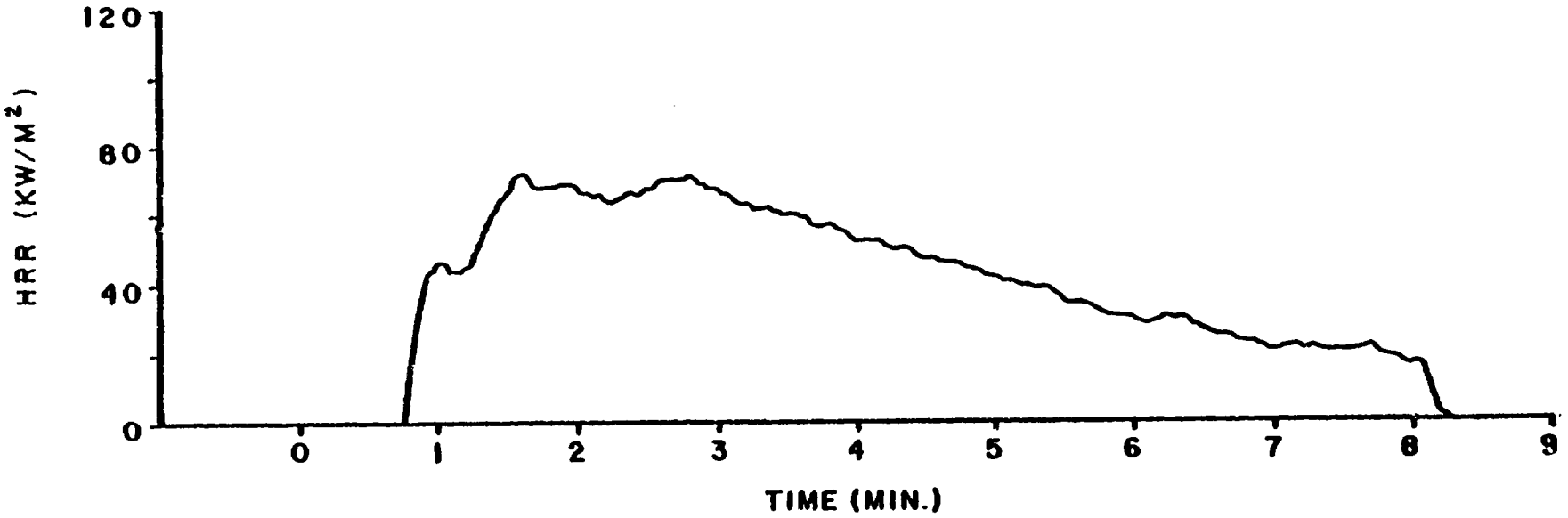

Figure 12. Heat Release Rate of Graphite/Bismaleimide (1017) at 5.0 W/cm^2 With Piloted Ignition

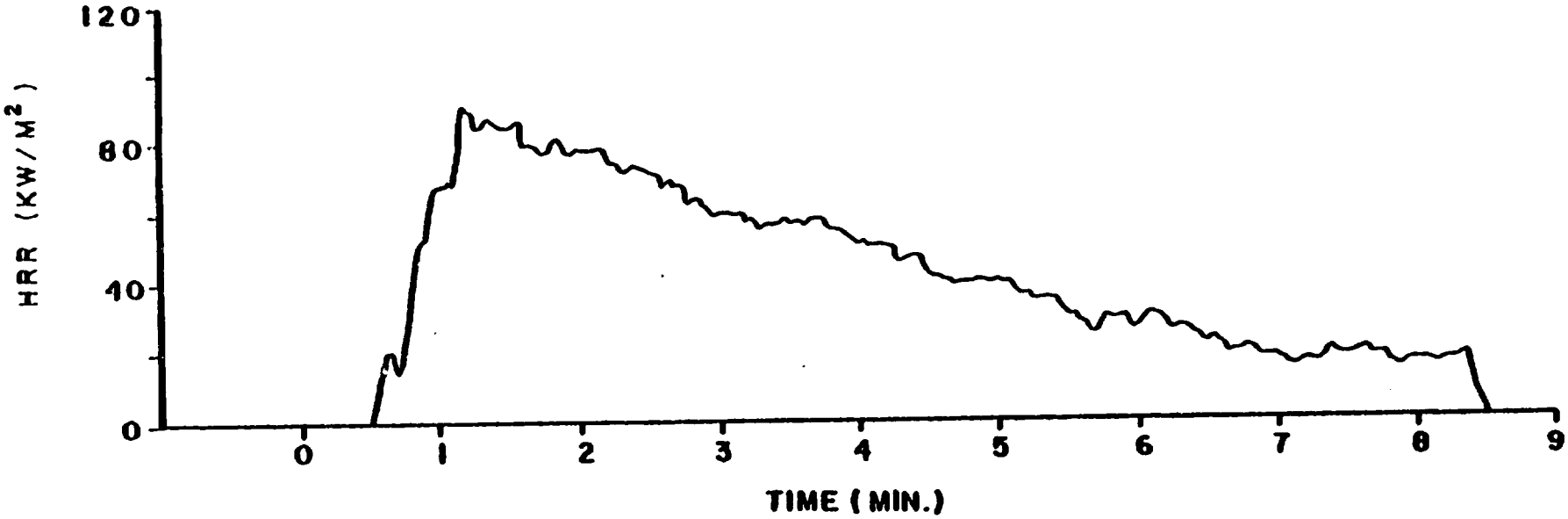

Figure 13. Heat Release Rate of Graphite/Bismaleimide (M751) at 6.0 W/cm^2 With Piloted Ignition

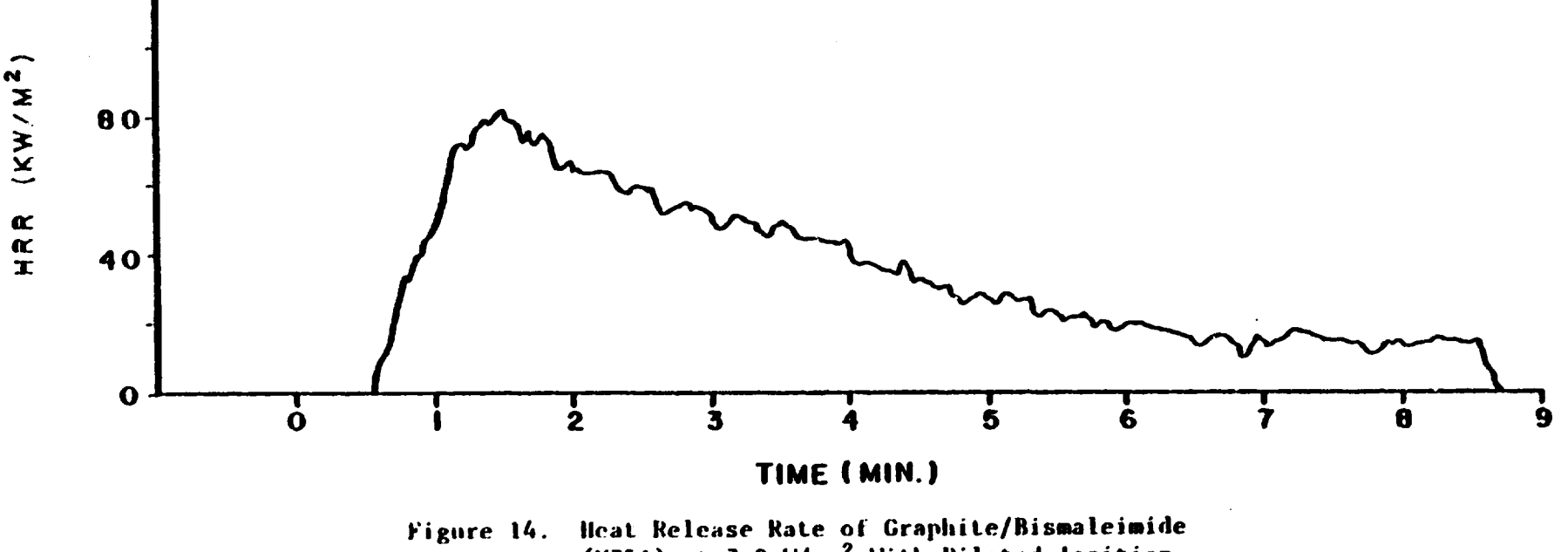

Figure 14. Heat Release Rate of Graphite/Bismaleimide (H751) at 7.0 W/cm^2 With Piloted Ignition

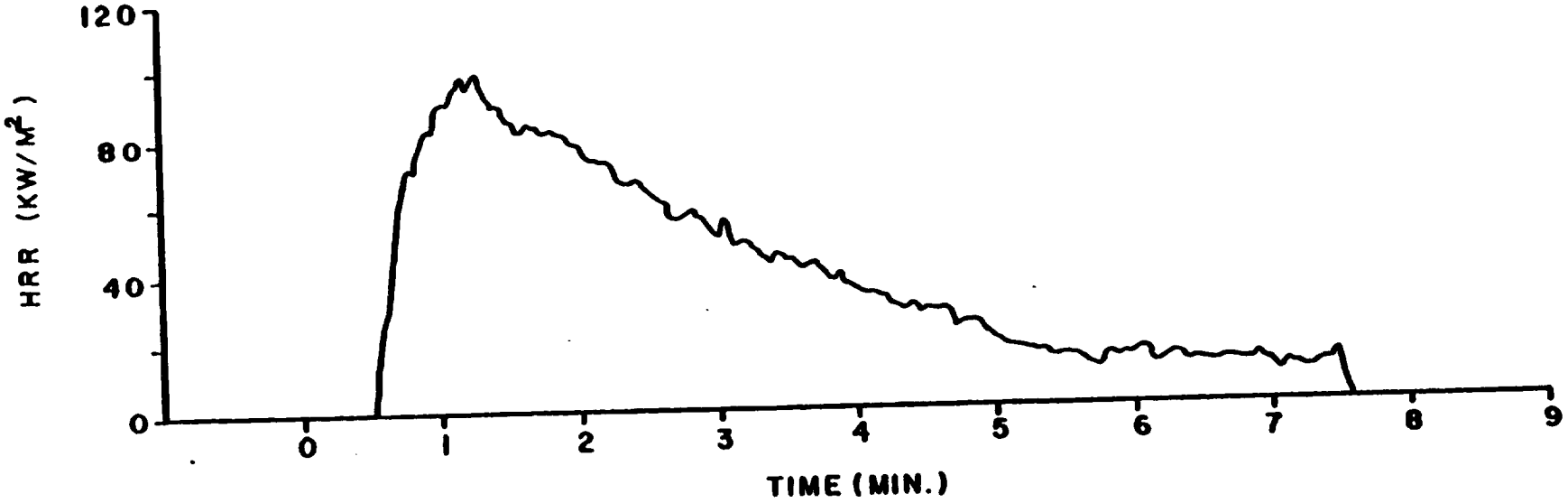

Figure 15. Heat Release Rate of Graphite/Bismaleimide (M751) at 8.0 W/cm² With Piloted Ignition

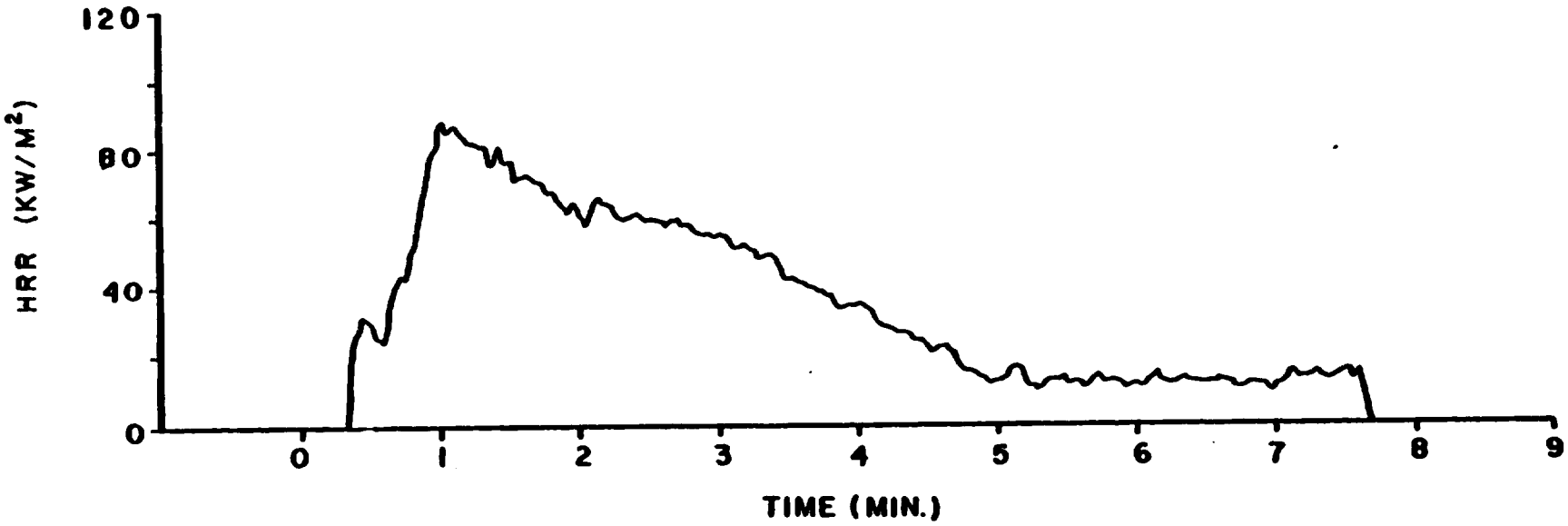

Figure 16. Heat Release Rate of Graphite/Bismaleimide (H751) at 9.0 W/cm^2 With Piloted Ignition

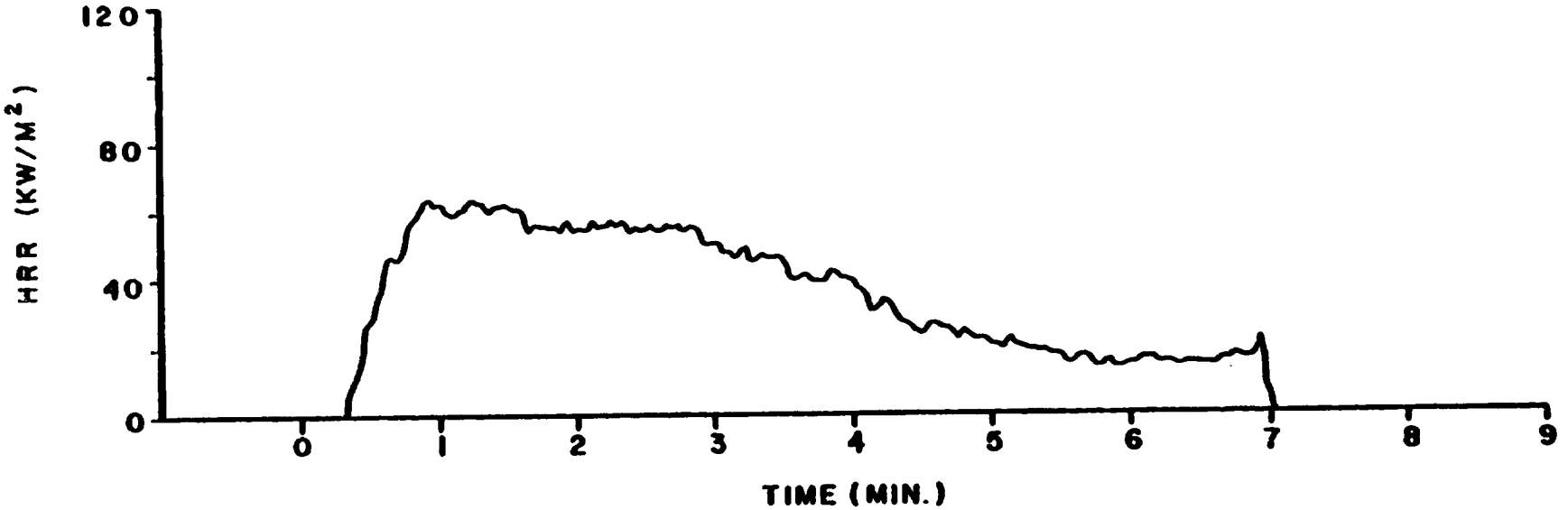

Figure 17. Heat Release Rate of Graphite/Bismaleimide (H751) at 10.0 W/cm^2 With Piloted Ignition

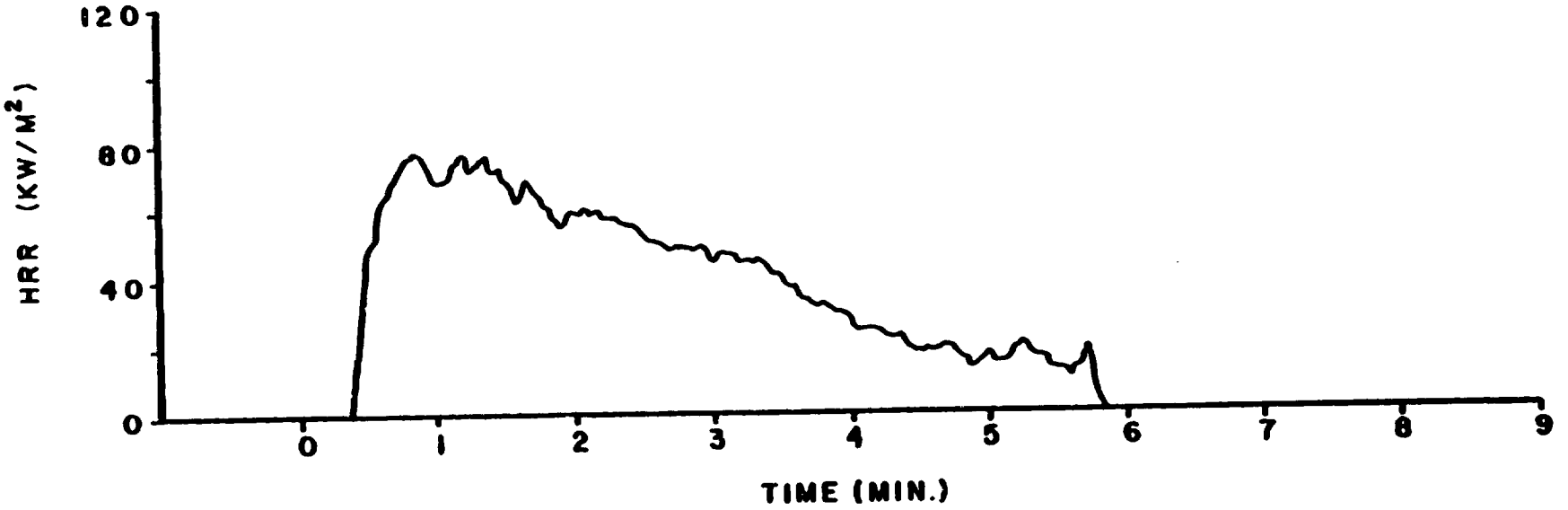

Figure 18. Heat Release Rate of Graphite/Bismaleimide (1017) at 10.0 W/cm^2 With Non-Piloted Ignition

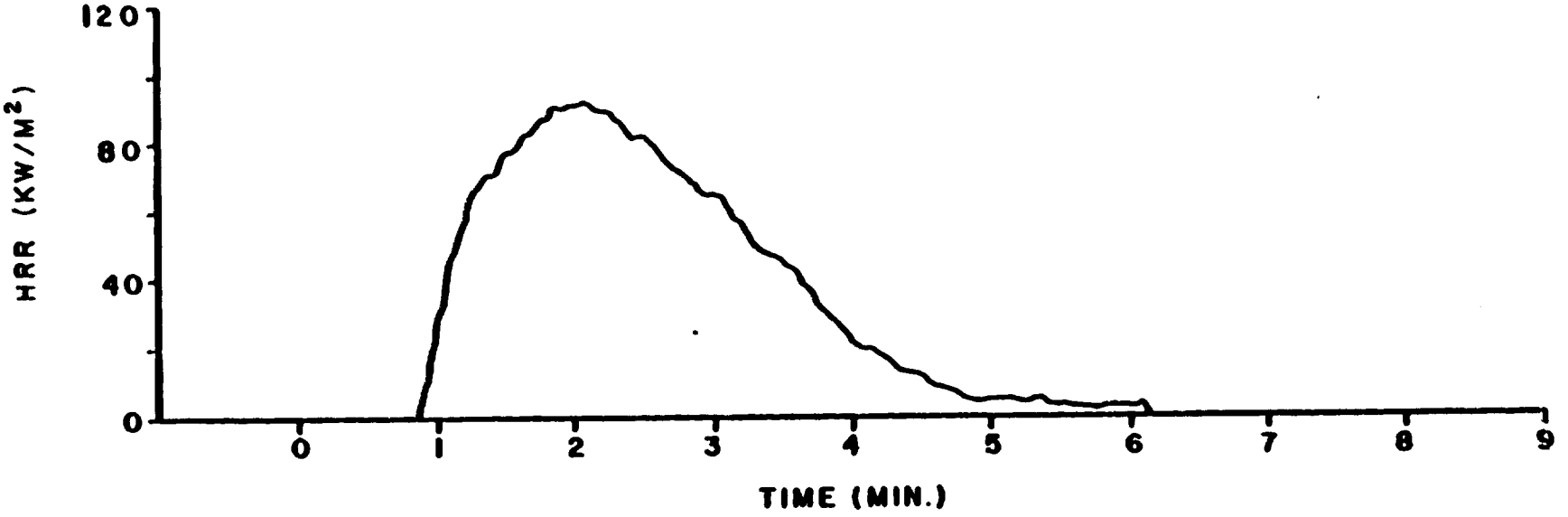

Figure 19. Heat Release Rate of Graphite/Epoxy (1008A) at 5.0 W/cm² With Piloted Ignition

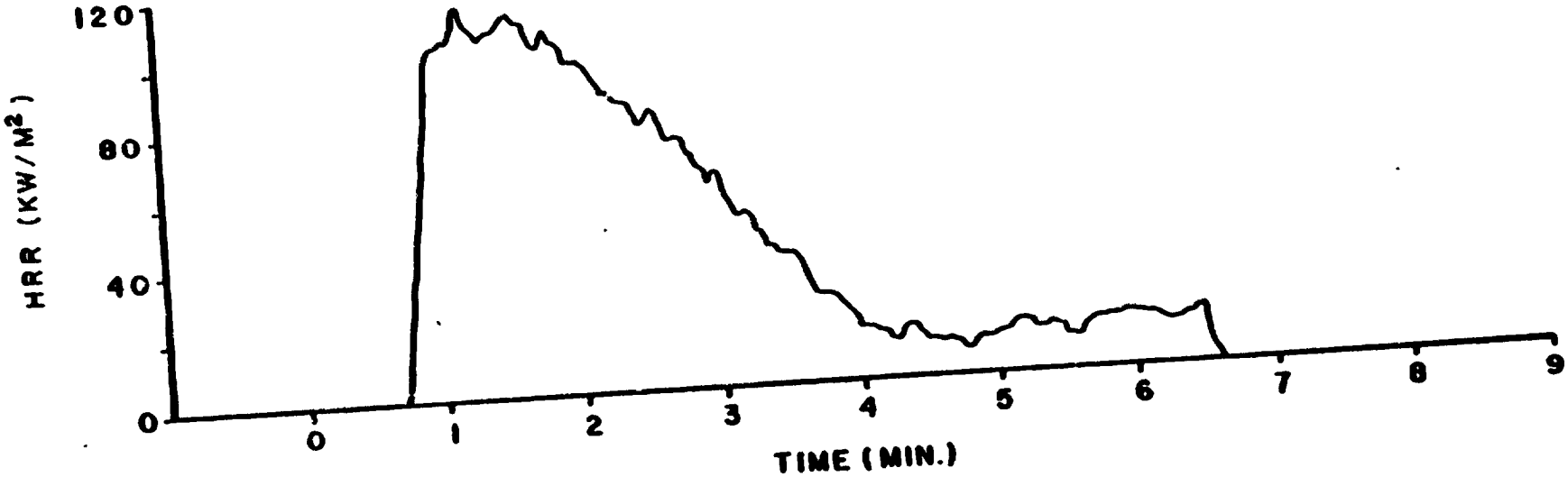

Figure 29. Heat Release Rate of Graphite/Epoxy (1012-9) at 6.0 W/cm² With Piloted Ignition

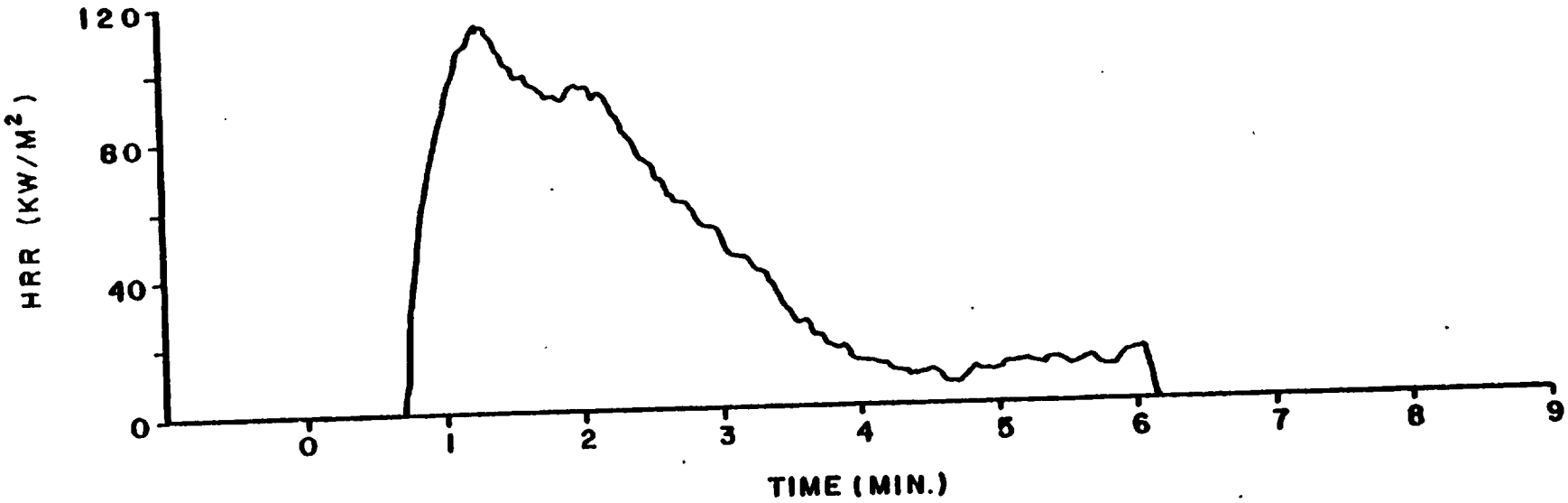

Figure 21. Heat Release Rate of Graphite/Epoxy (1008A) at 7.0 W/cm^2 With Piloted Ignition

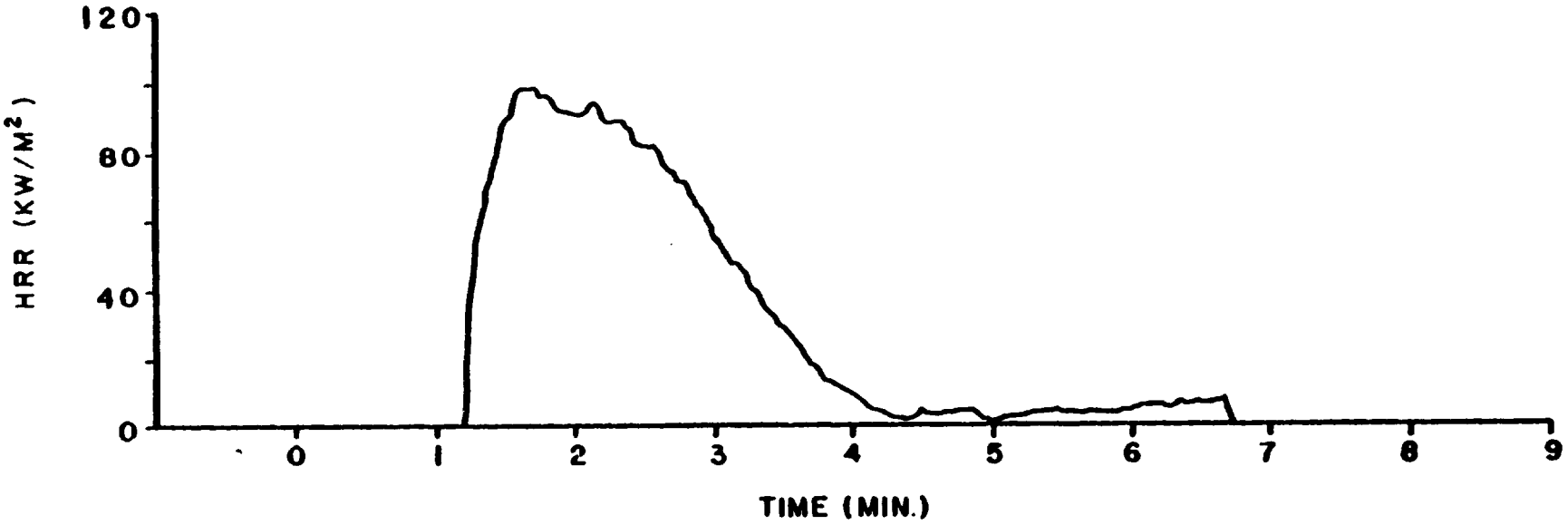

Figure 22. Heat Release Rate of Graphite/Epoxy (1008A) at 7.0 W/cm^2 With Non-Piloted Ignition

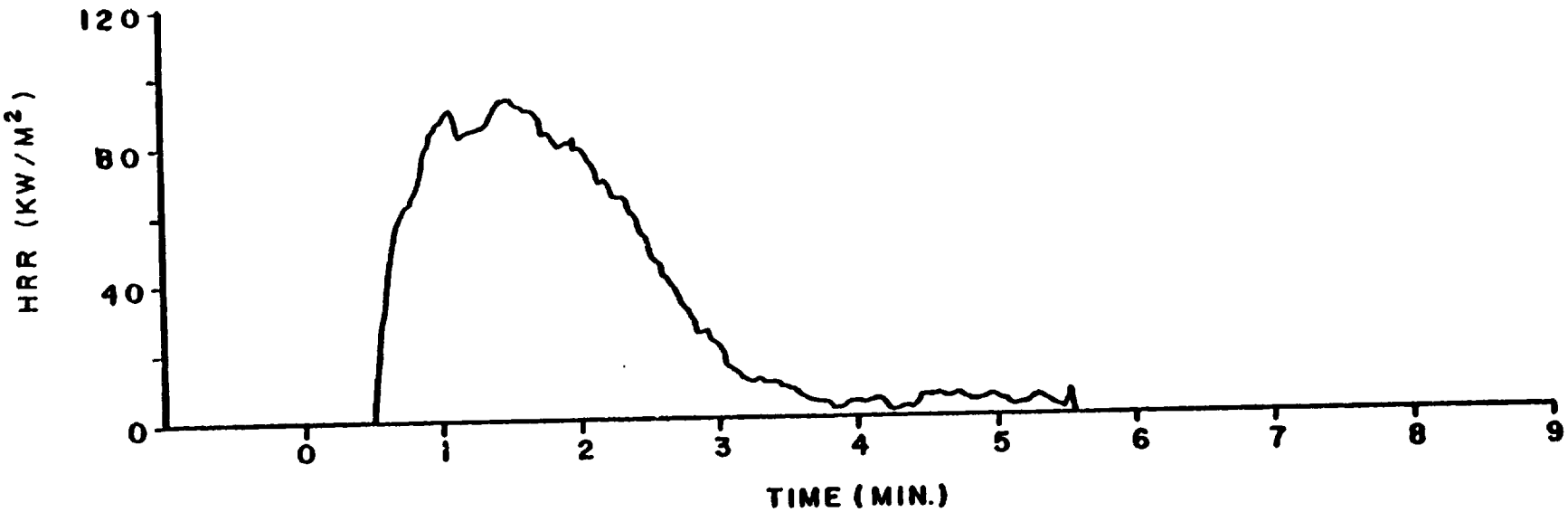

Figure 23. Heat Release Rate of Graphite/Epoxy (1012-9) at 8.0 W/cm^2 With Piloted Ignition

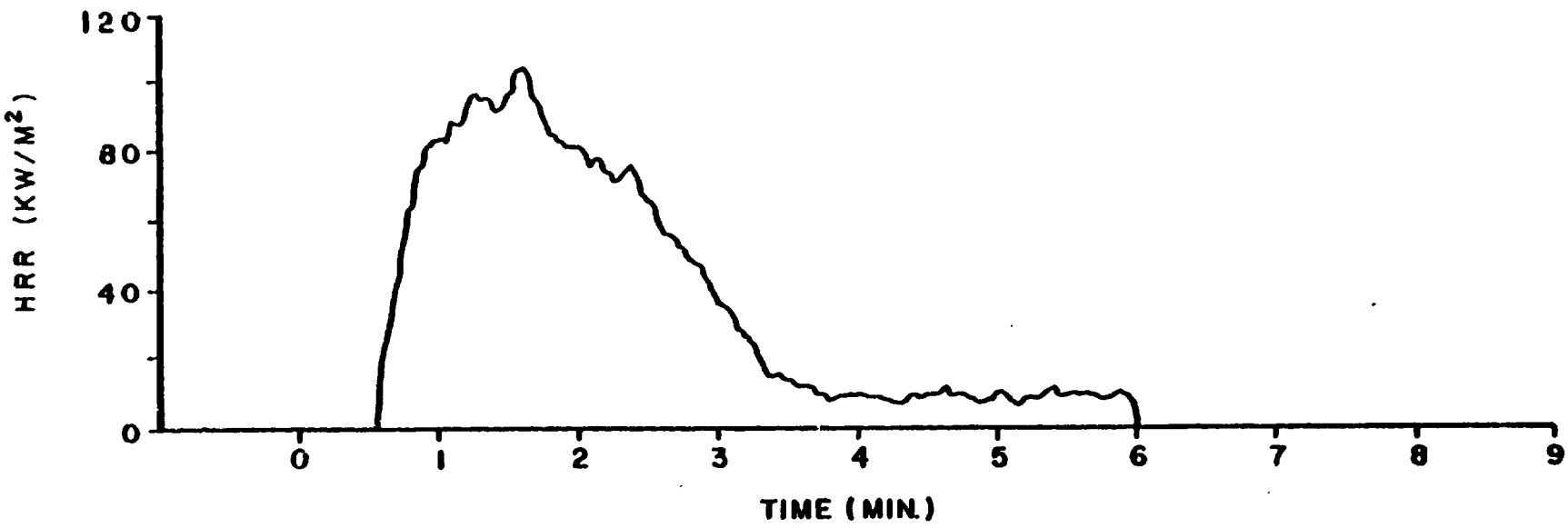

Figure 24. Heat Release Rate of Graphite/Epoxy (1012-9) at 9.0 W/cm^2 With Piloted Ignition

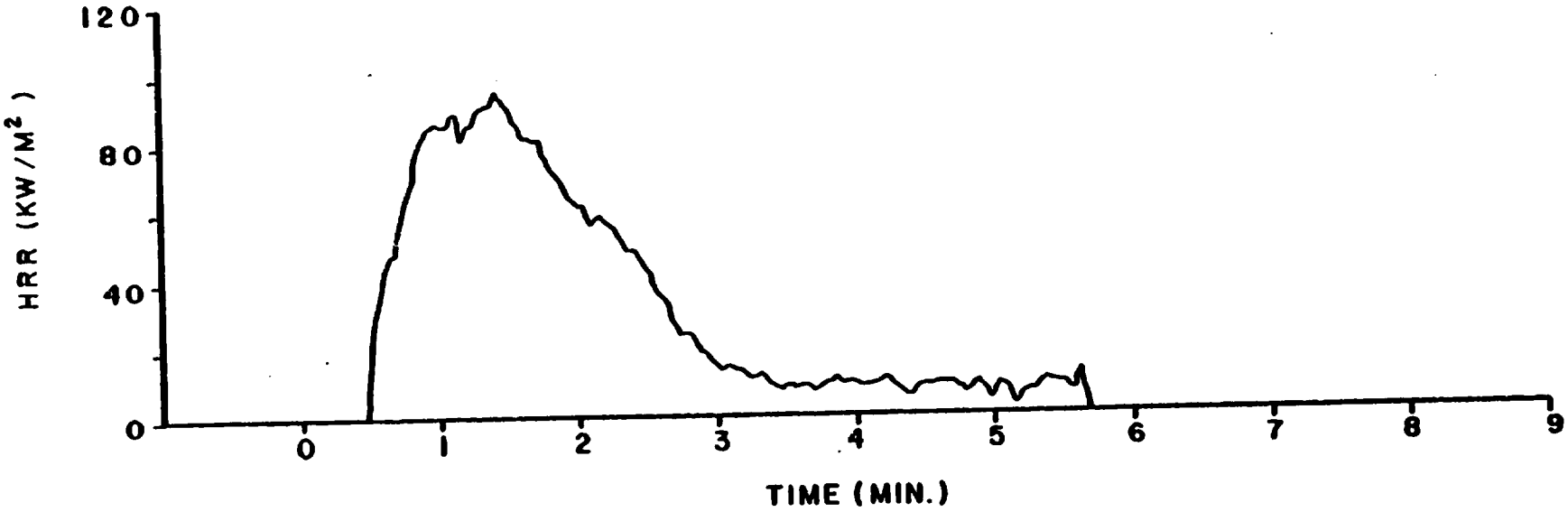

Figure 25. Heat Release Rate of Graphite/Epoxy (1008A) at 10.0 W/cm^2 With Piloted Ignition

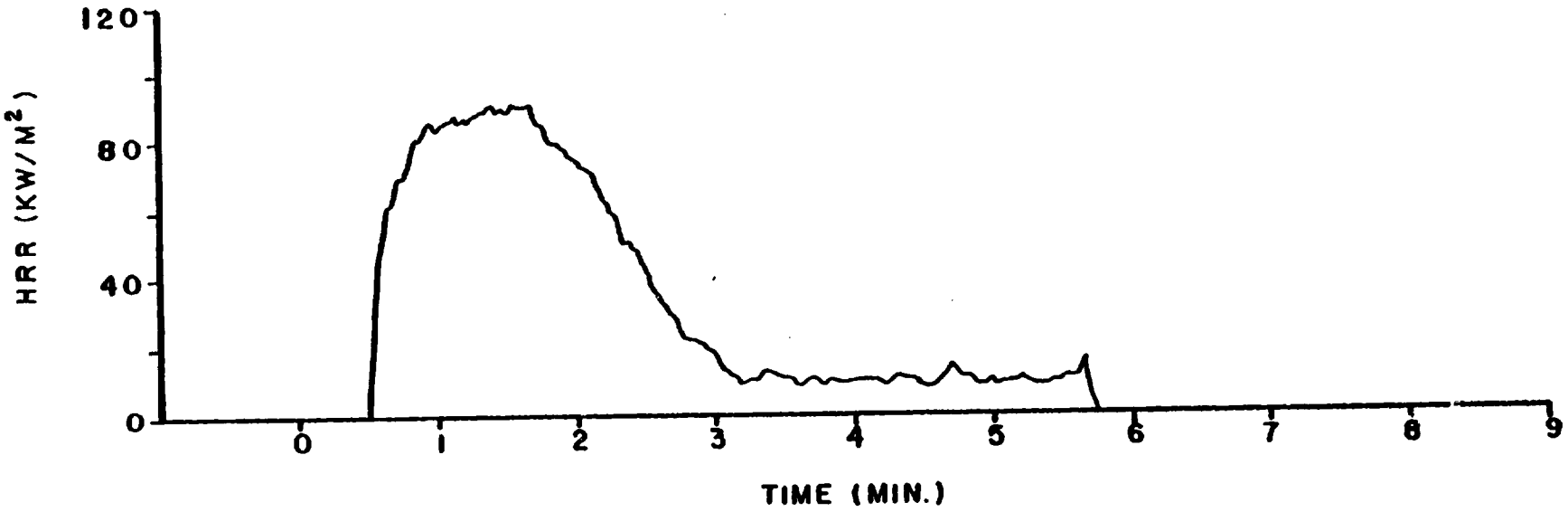

Figure 26. Heat Release Rate of Graphite/Epoxy (1008A) at 10.0 W/cm^2 With Non-Piloted Ignition

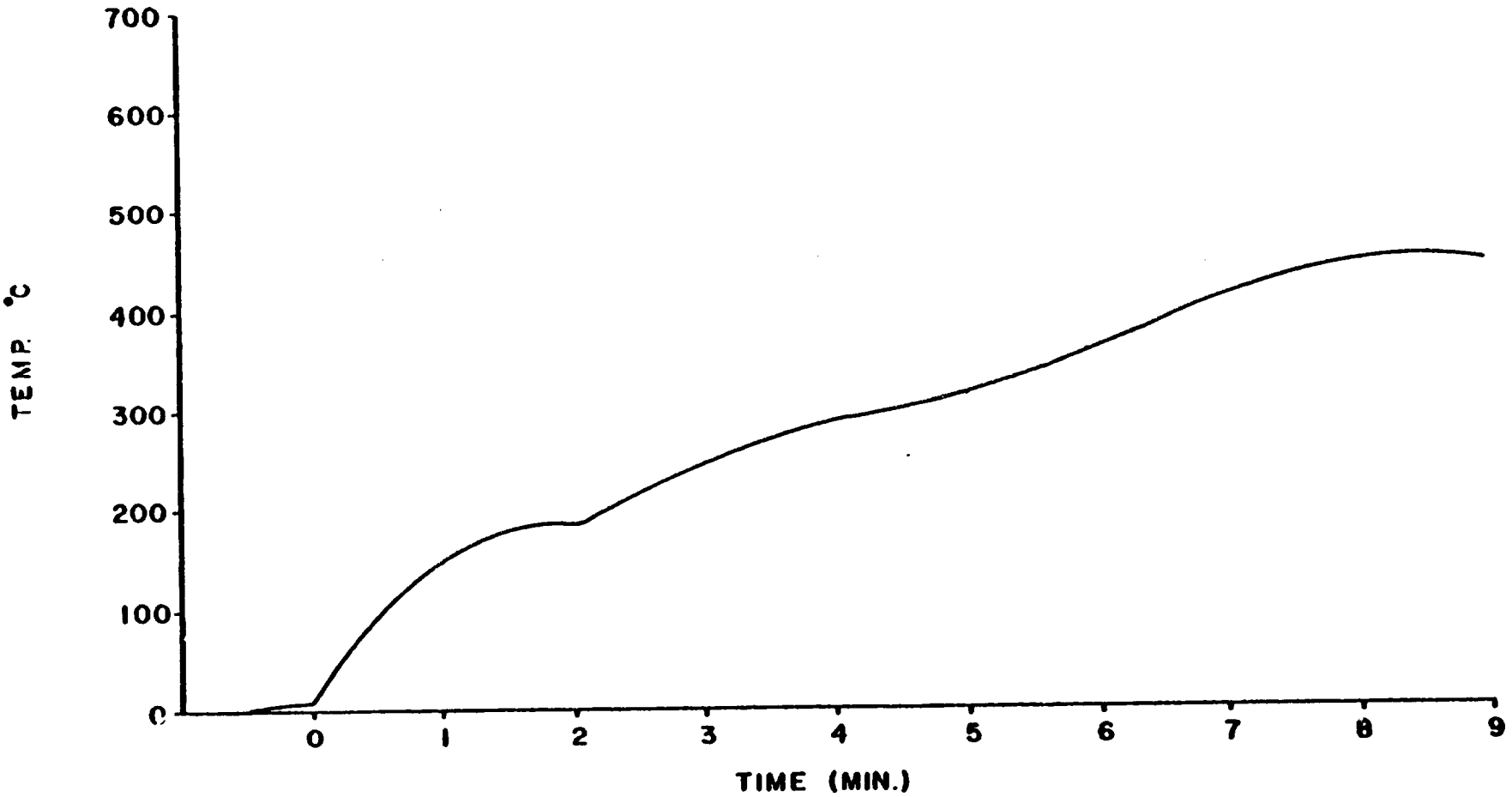

Figure 27. Specimen Back Surface Temperature Rise Graphite/Bismaleimide (1017) at 5.0 W/cm^2 With Piloted Ignition

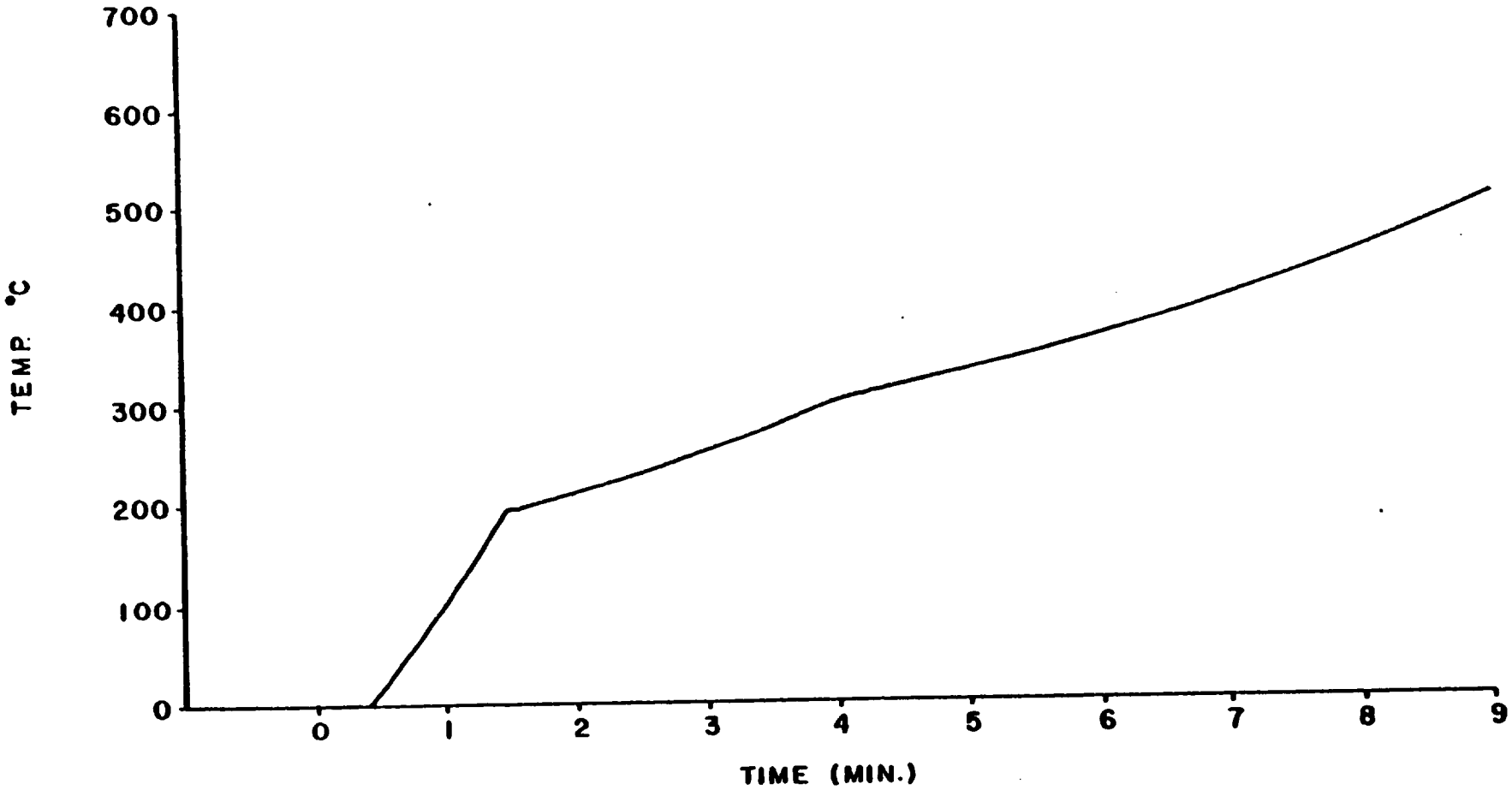

Figure 28. Specimen Back Surface Temperature Rise Graphite/Bismaleimide (M751) at 6.0 W/cm^2 With Piloted Ignition

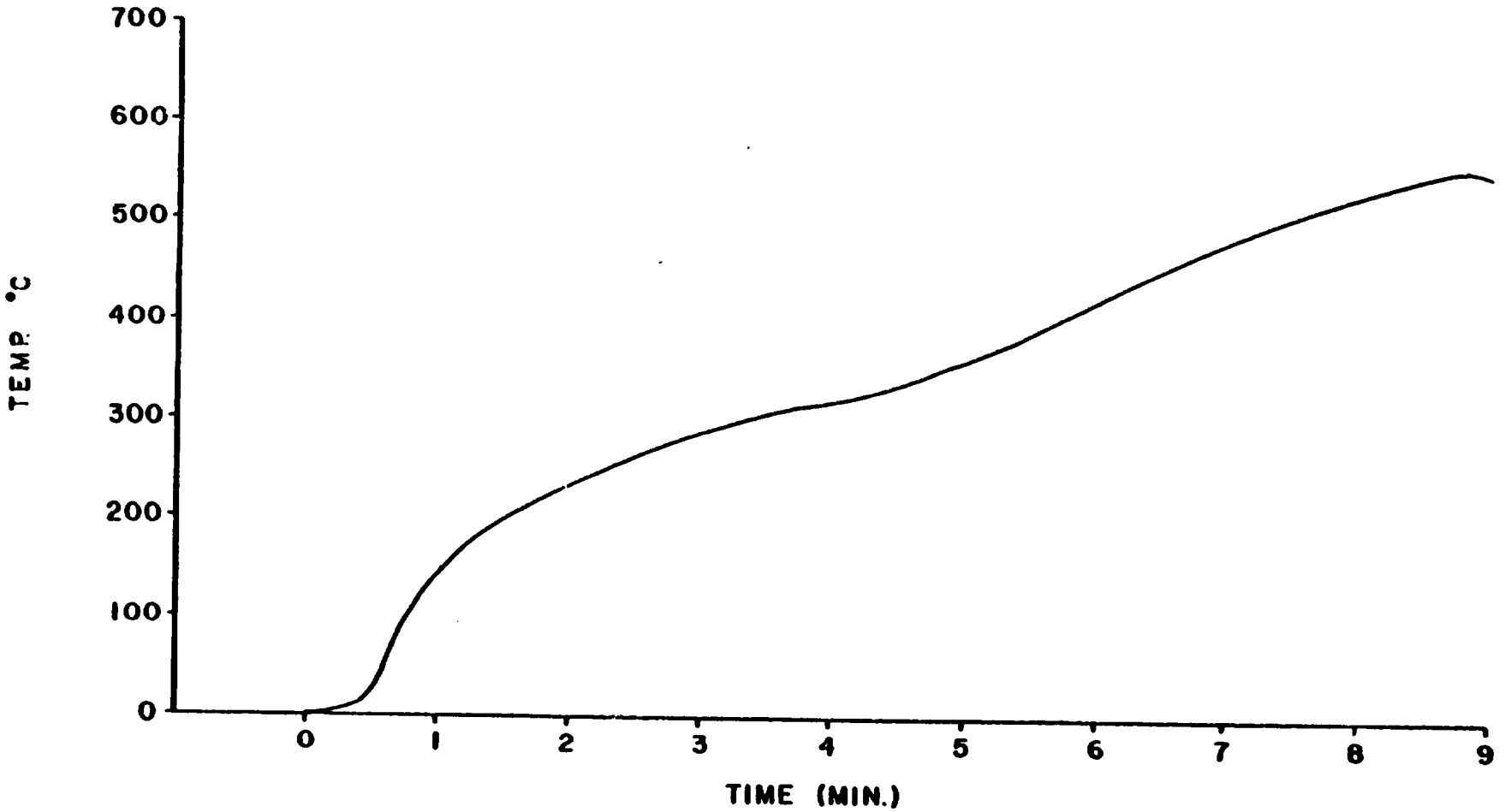

Figure 29. Specimen Back Surface Temperature Rise Graphite/Bismaleimide (M751) at 7.0 W/cm^2 With Piloted Ignition

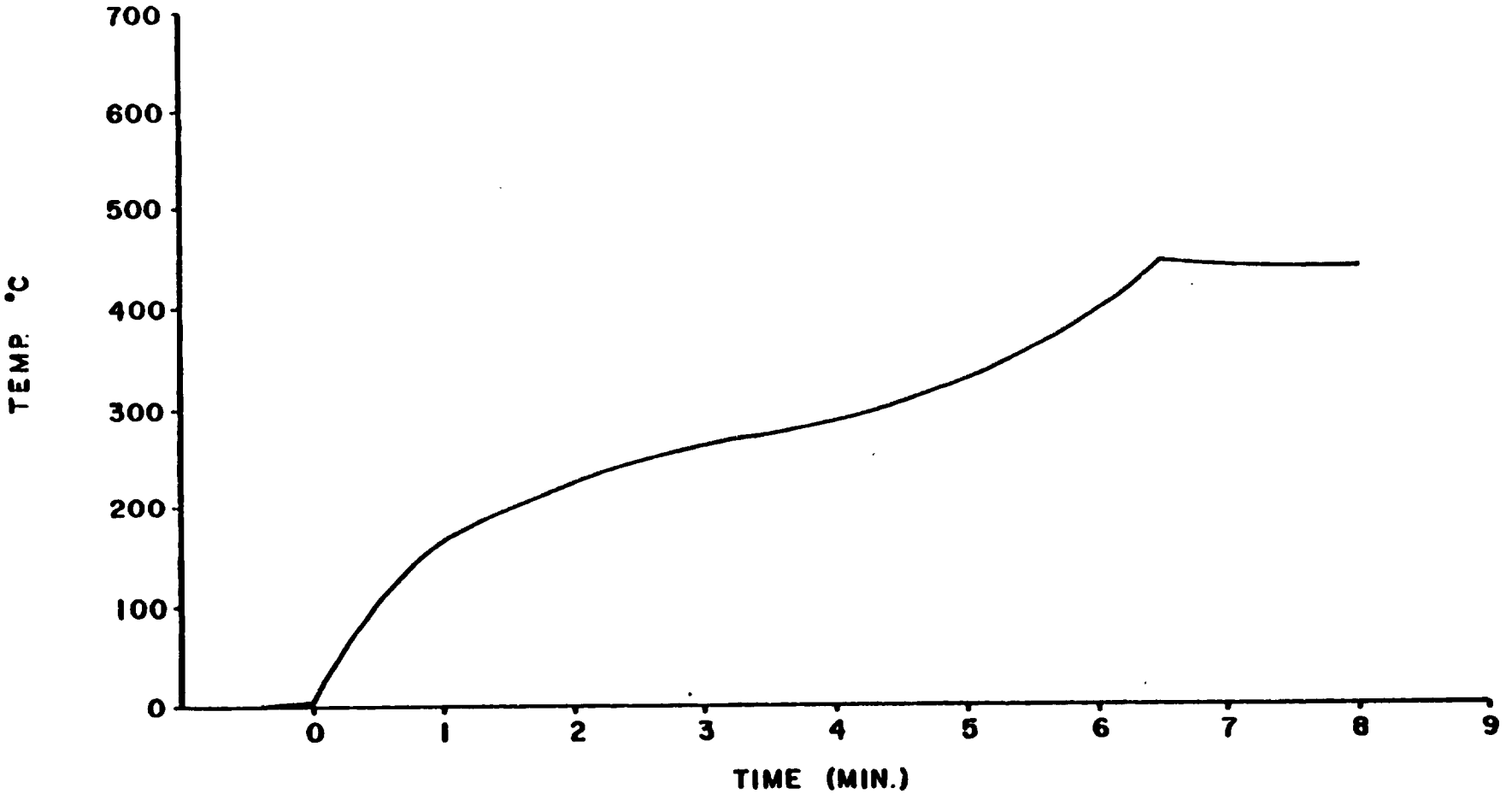

Figure 30. Specimen Back Surface Temperature Rise Graphite/Bismaleimide (1017) at 7.0 W/cm^2 With Non-Piloted Ignition

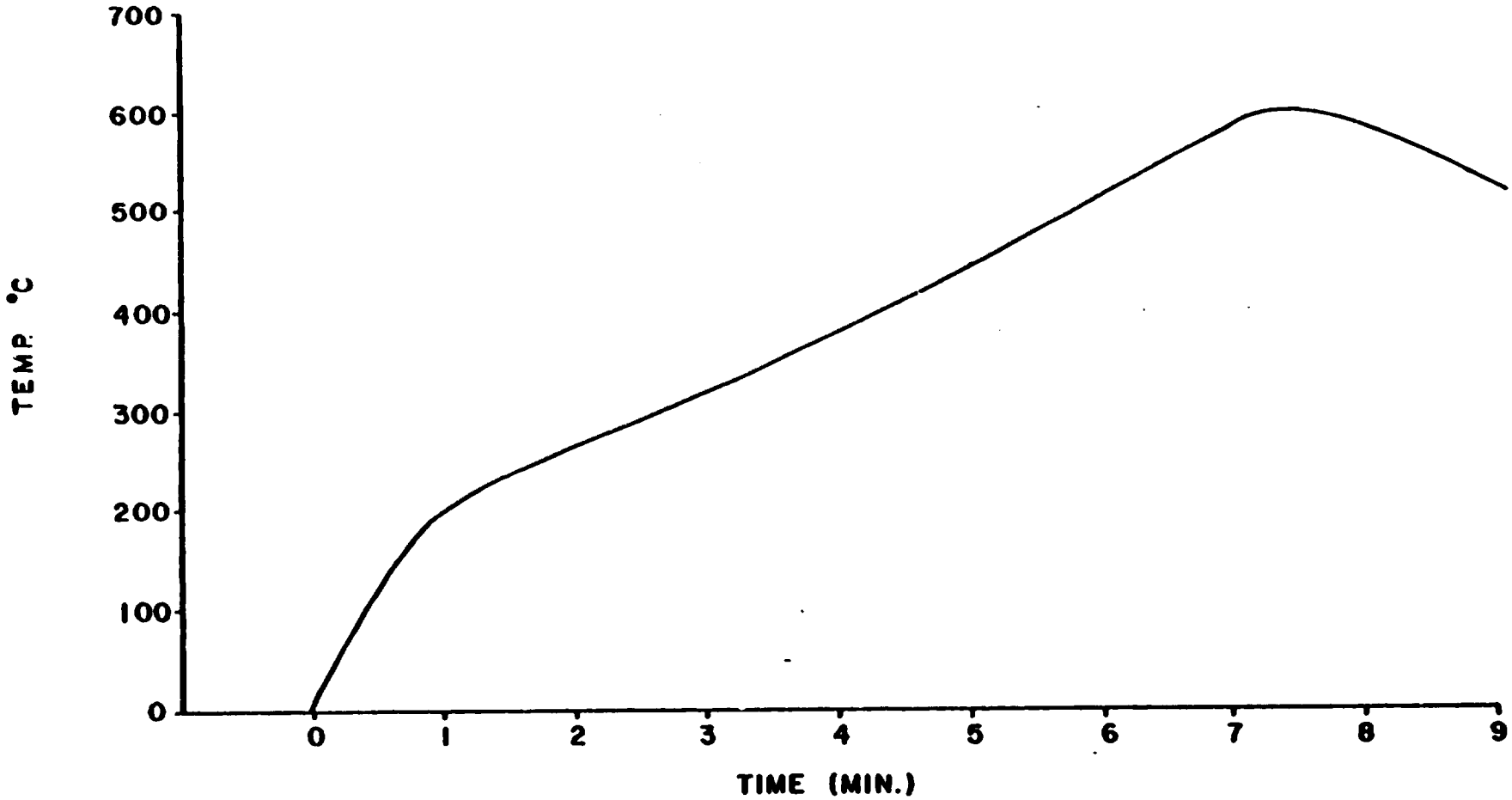

Figure 31. Specimen Back Surface Temperature Rise Graphite/Bismaleimide (H751) at 8.0 W/cm^2

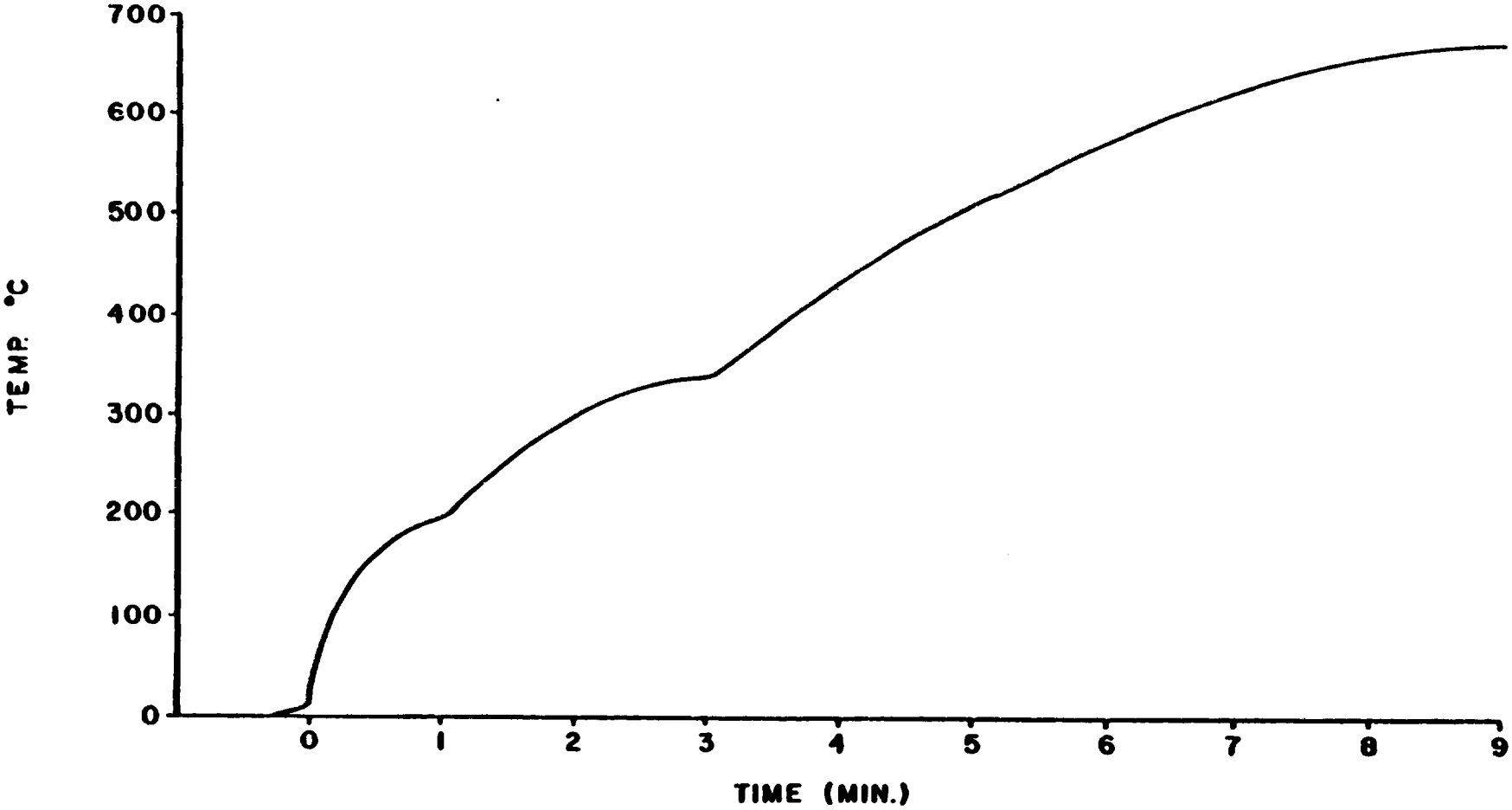

Figure 32. Specimen Back Surface Temperature Rise Graphite/Bismaleimide (M751) at 9.0 W/cm^2 With Piloted Ignition

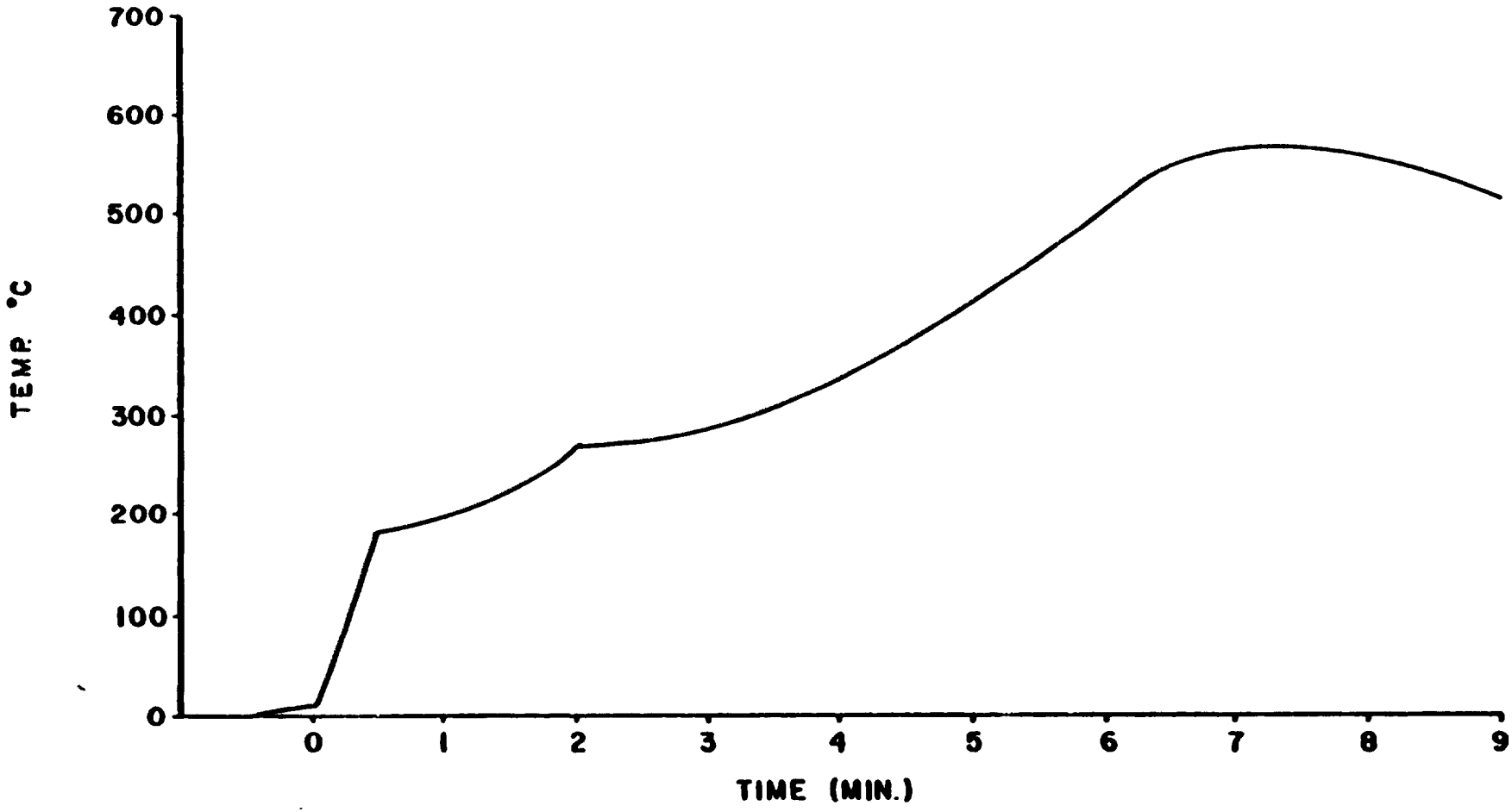

Figure 33. Specimen Back Surface Temperature Rise Graphite/Bismaleimide (H751) at 10.0 W/cm^2 With Non-Piloted Ignition

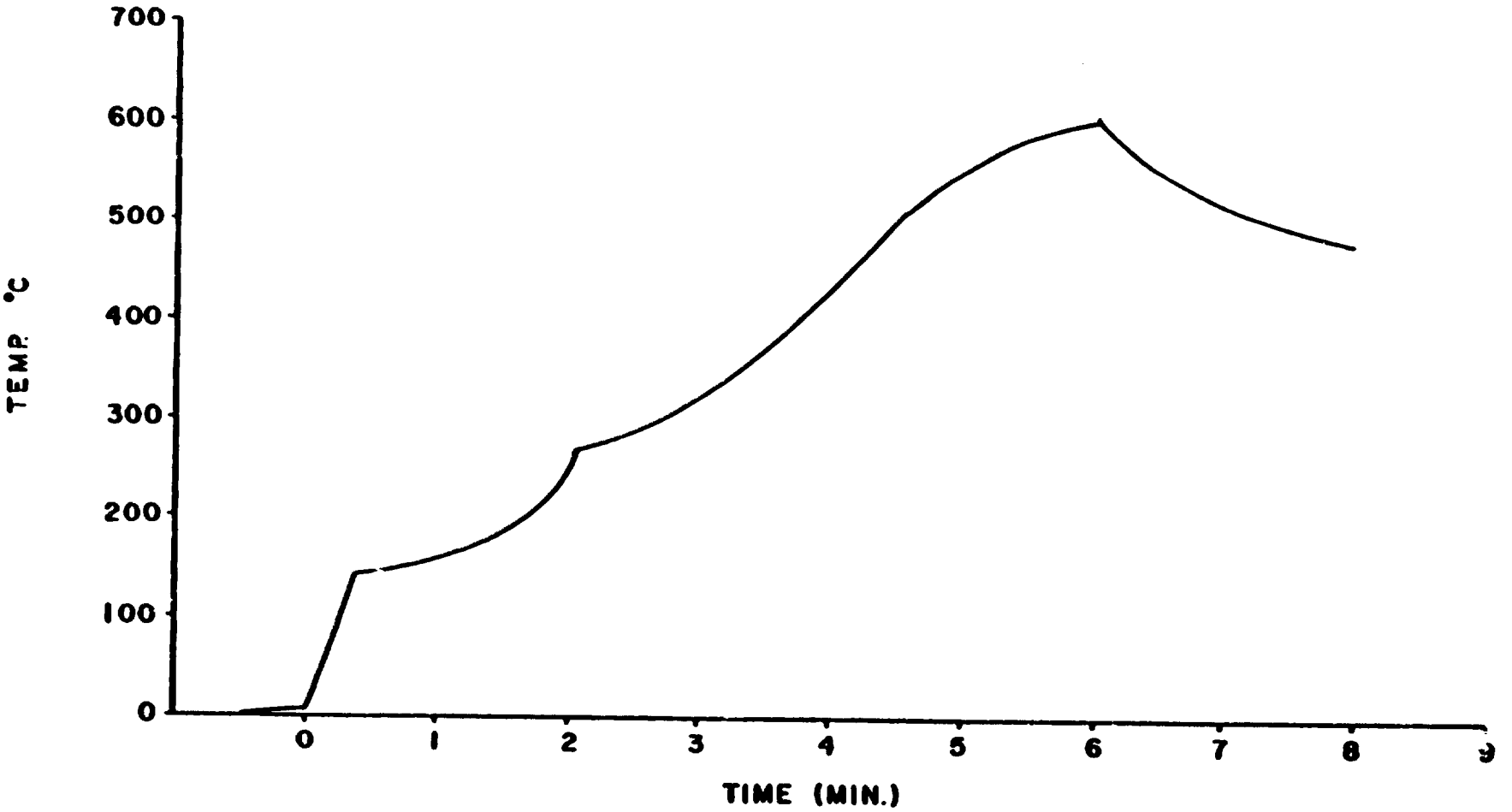

Figure 34. Specimen Back Surface Temperature Rise Graphite/Bismaleimide (1017) at 10.0 W/cm^2 With Non-Piloted Ignition

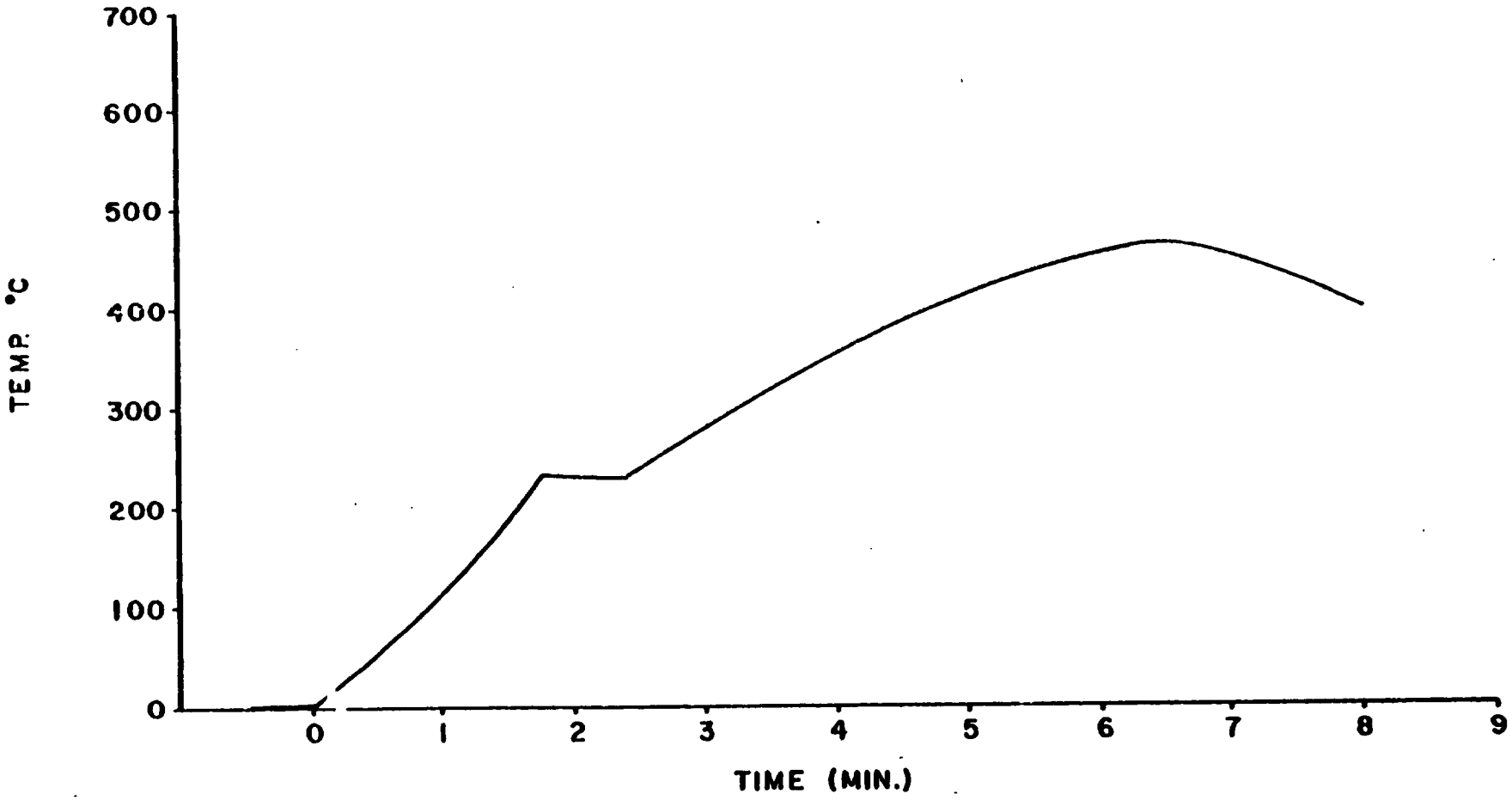

Figure 35. Specimen Back Surface Temperature Rise Graphite/Epoxy (1008A) at 5.0 W/cm^2 With Piloted Ignition

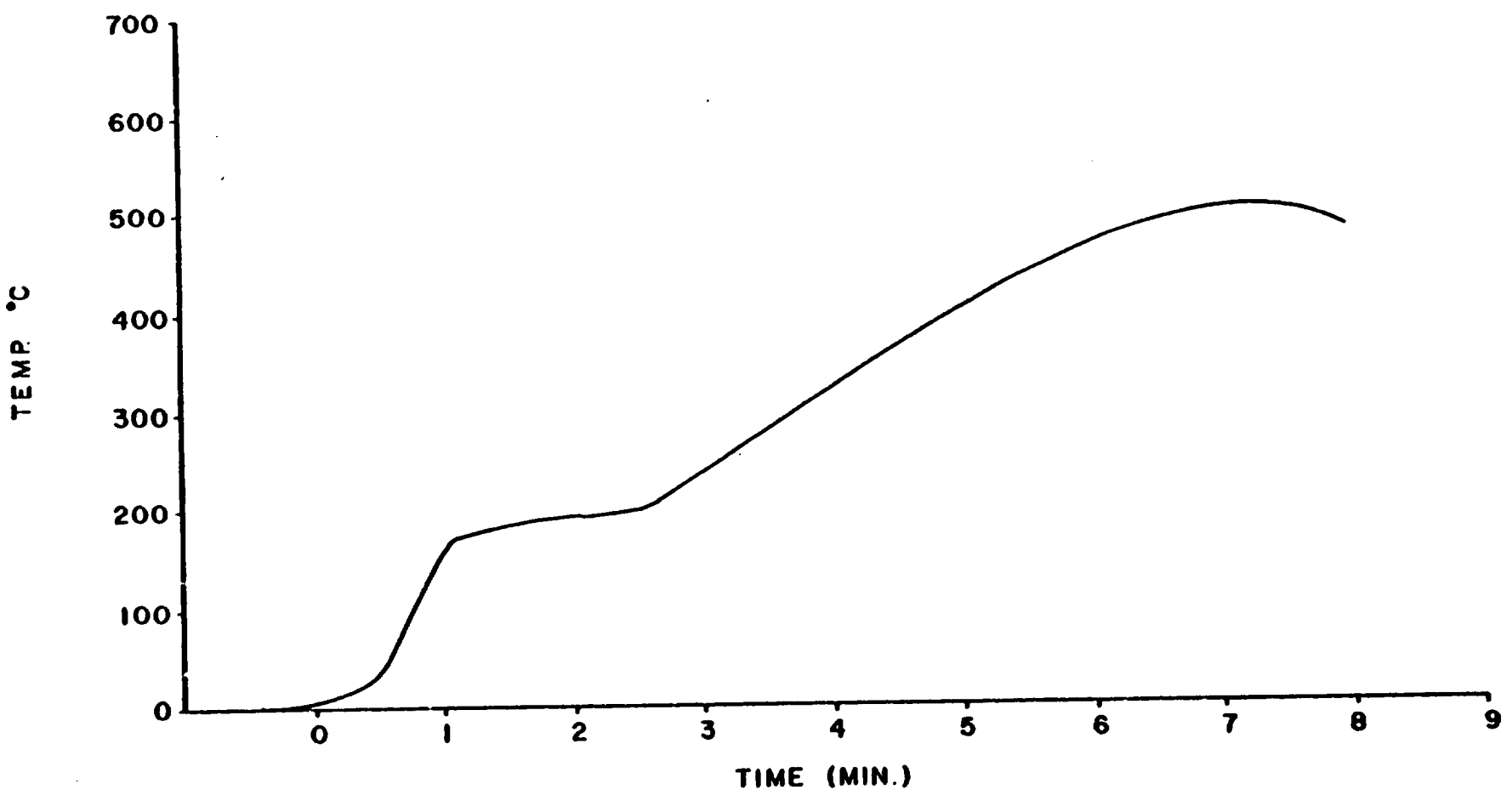

Figure 36. Specimen Back Surface Temperature Rise Graphite/Epoxy (1012-9) at 6.0 W/cm^2 With Piloted Ignition

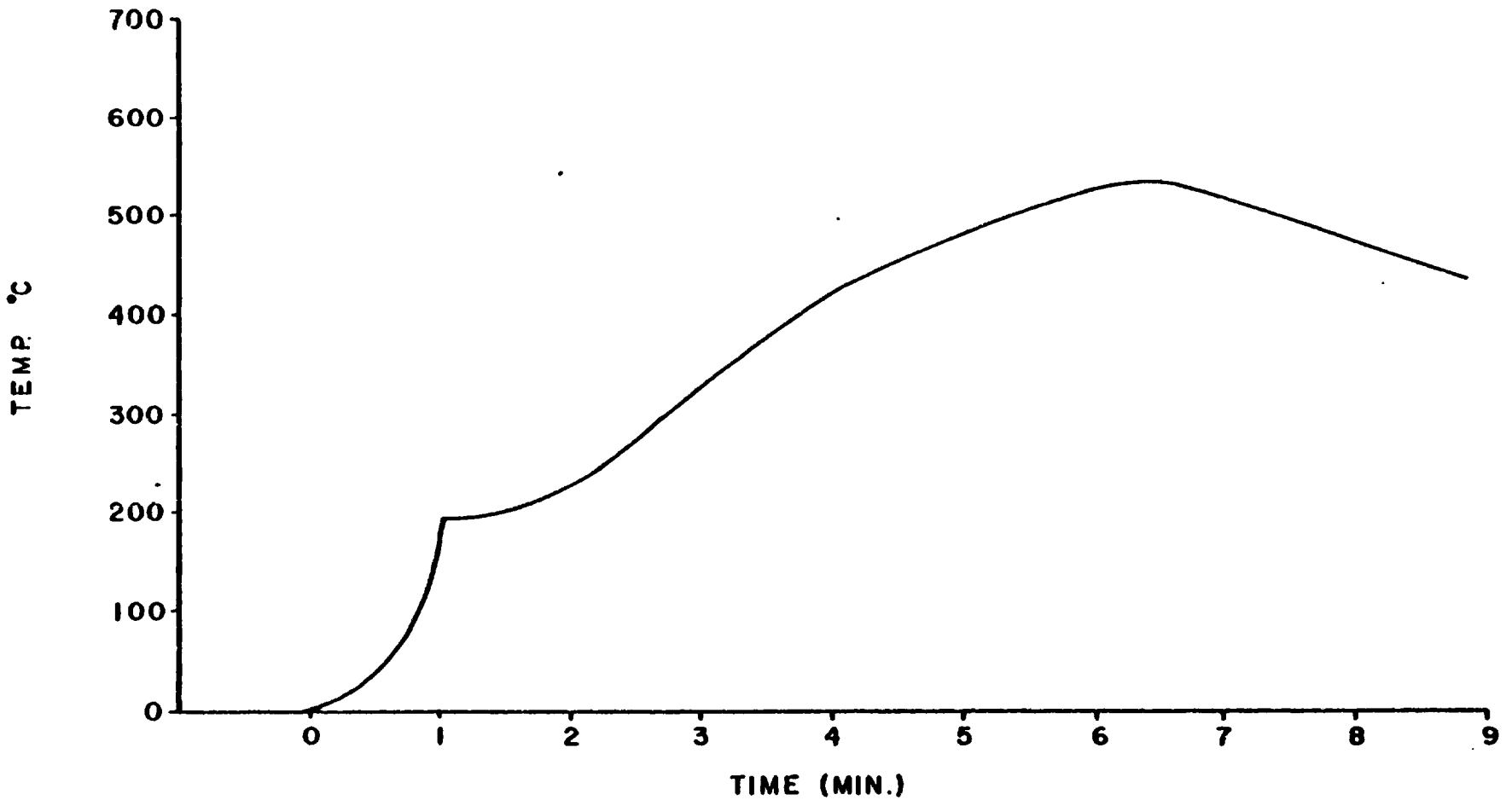

Figure 37. Specimen Back Surface Temperature Rise Graphite/Epoxy (1012-9) at 7.0 W/cm^2 With Piloted Ignition

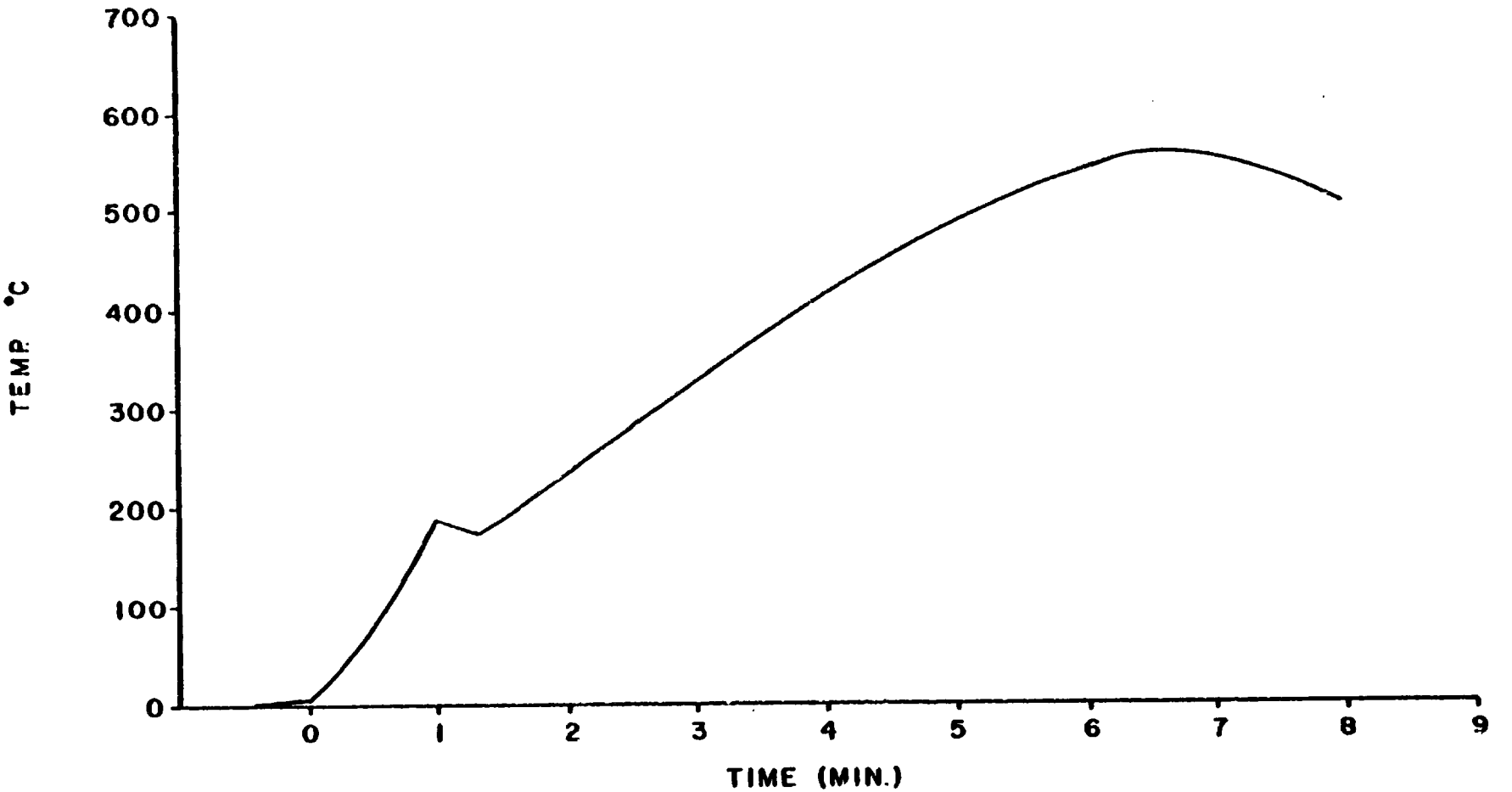

Figure 38. Specimen Back Surface Temperature Rise Graphite/Epoxy (1008A) at 7.0 W/cm^2 With Non-Piloted Ignition

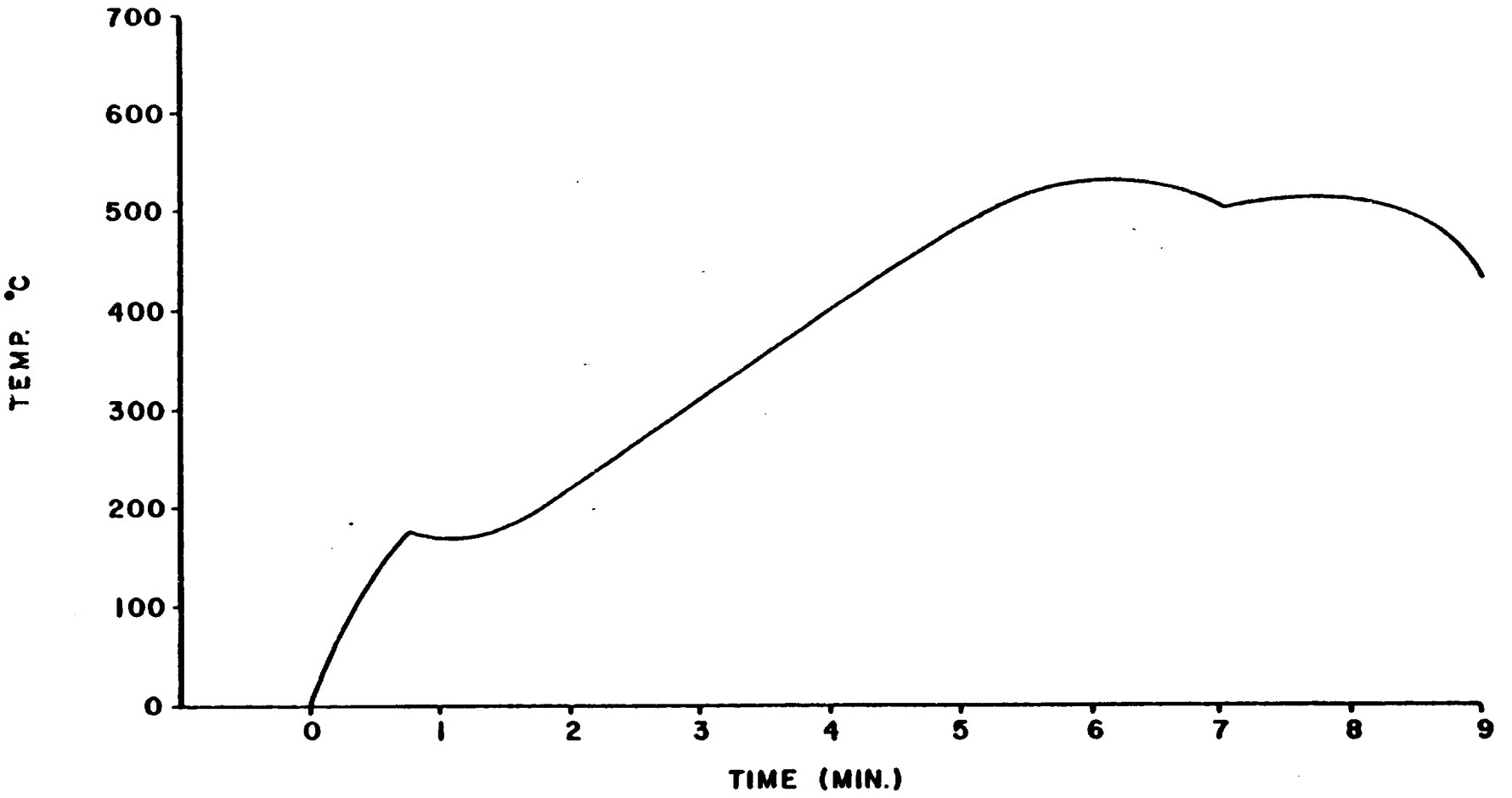

Figure 39. Specimen Back Surface Temperature Rise Graphite/Epoxy (1012-9) at 8.0 W/cm^2 With Piloted Ignition

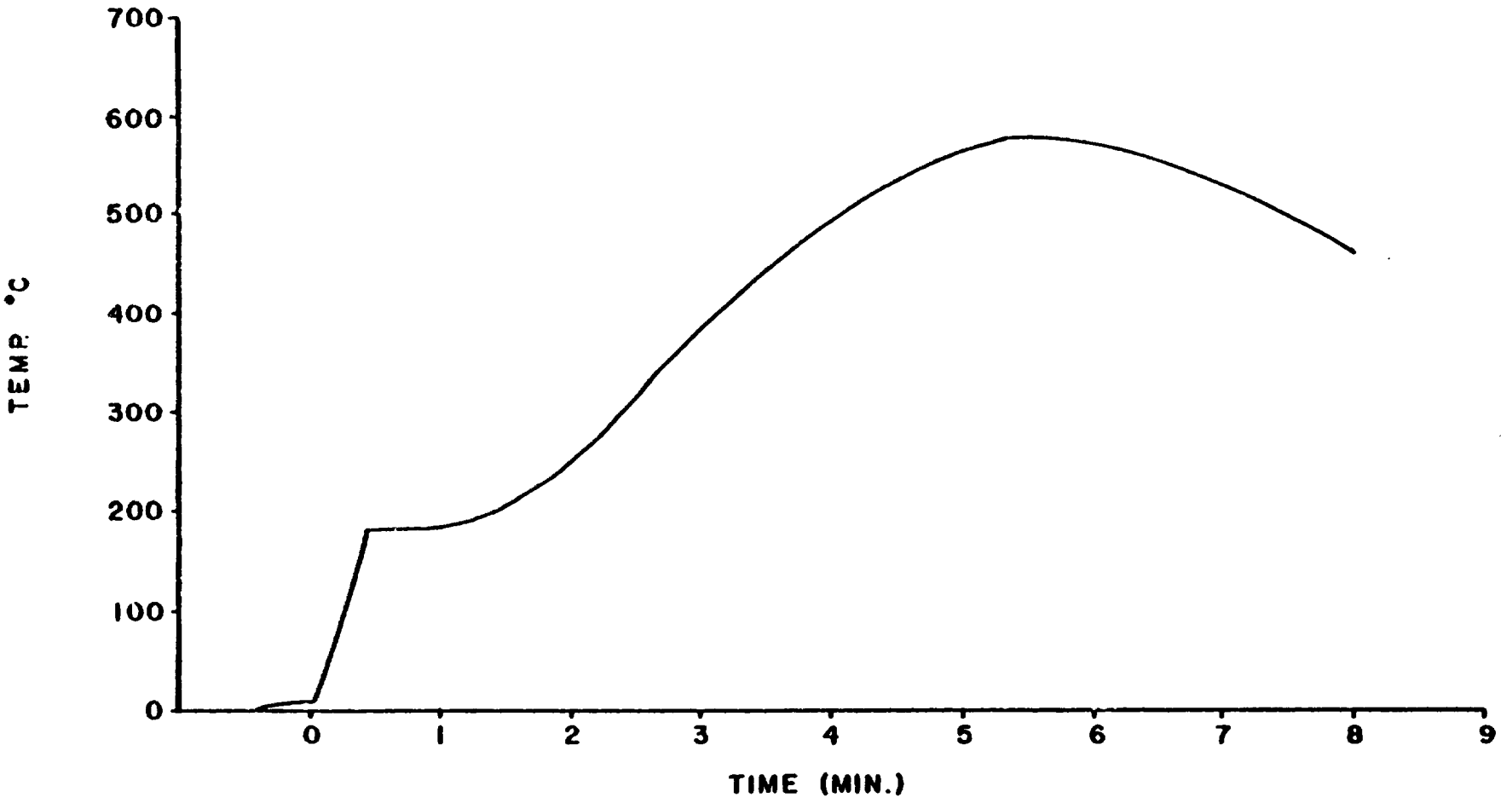

Figure 40. Specimen Back Surface Temperature Rise Graphite/Epoxy (1012-9) at 9.0 W/cm^2 With Piloted Ignition

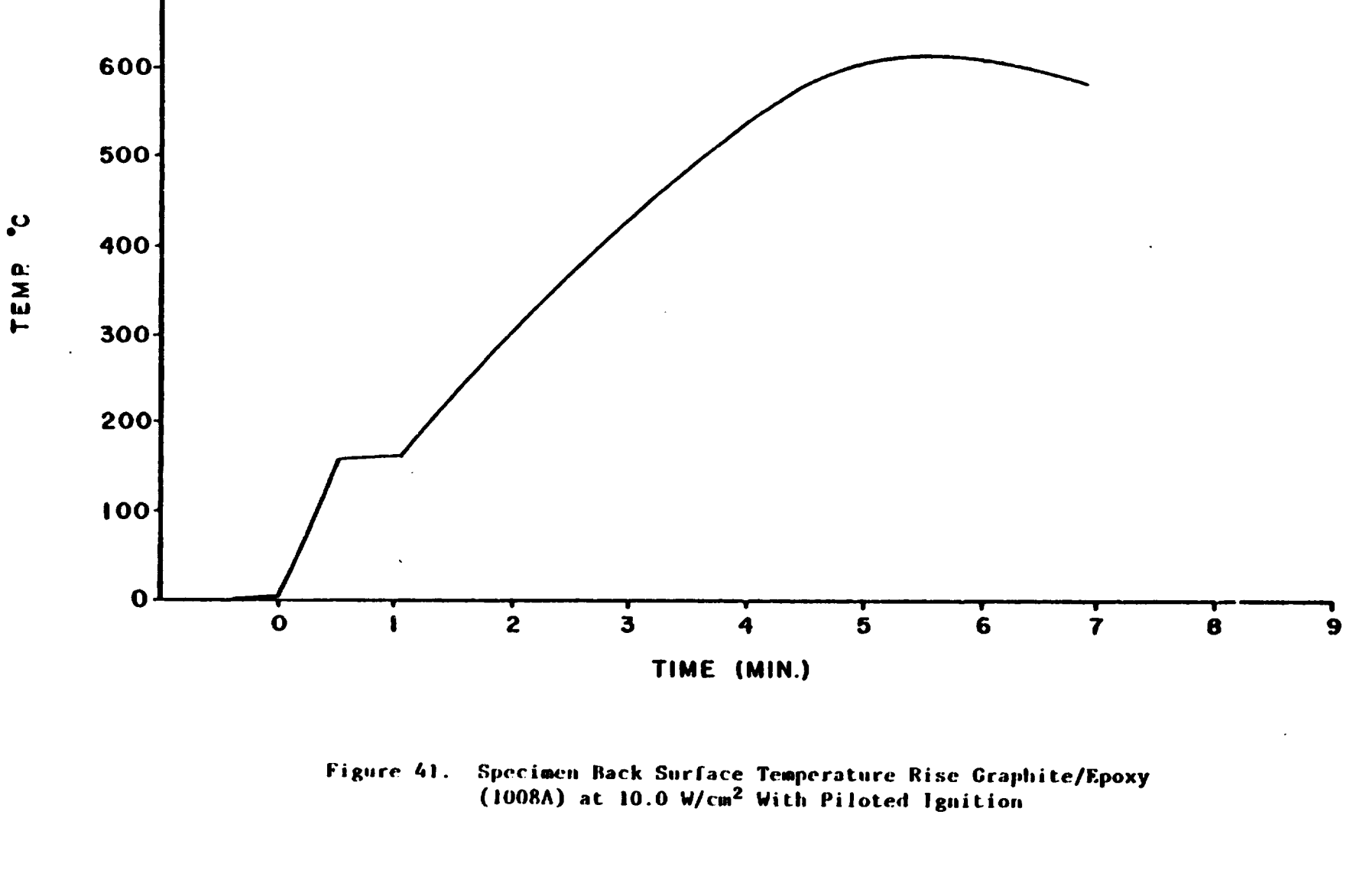

Figure 41. Specimen Back Surface Temperature Rise Graphite/Epoxy (1008A) at 10.0 W/cm^2 With Piloted Ignition

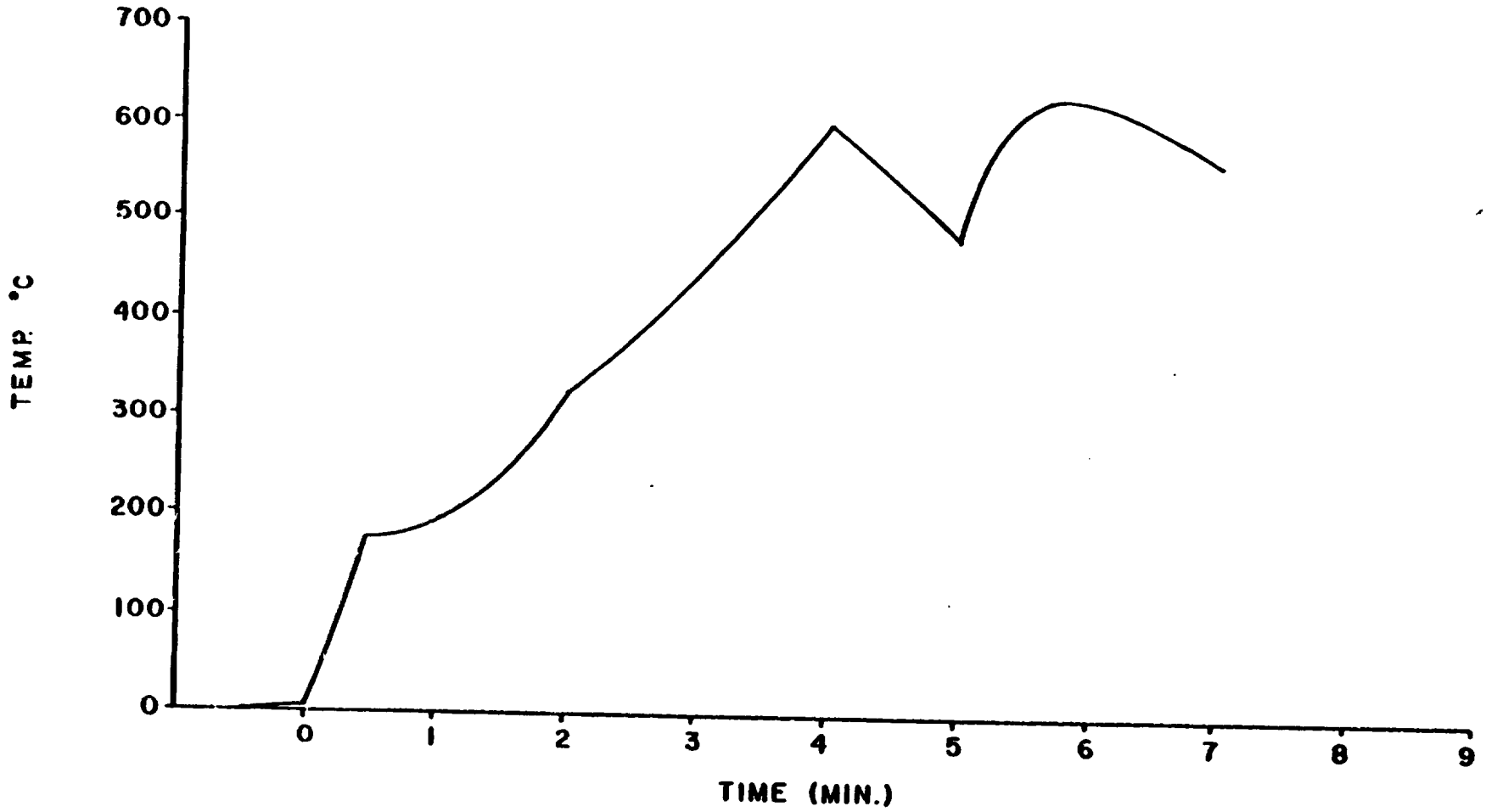

Figure 42. Specimen Back Surface Temperature Rise Graphite/Epoxy (P008A) at 10.0 W/cm^2 With Non-Piloted Ignition

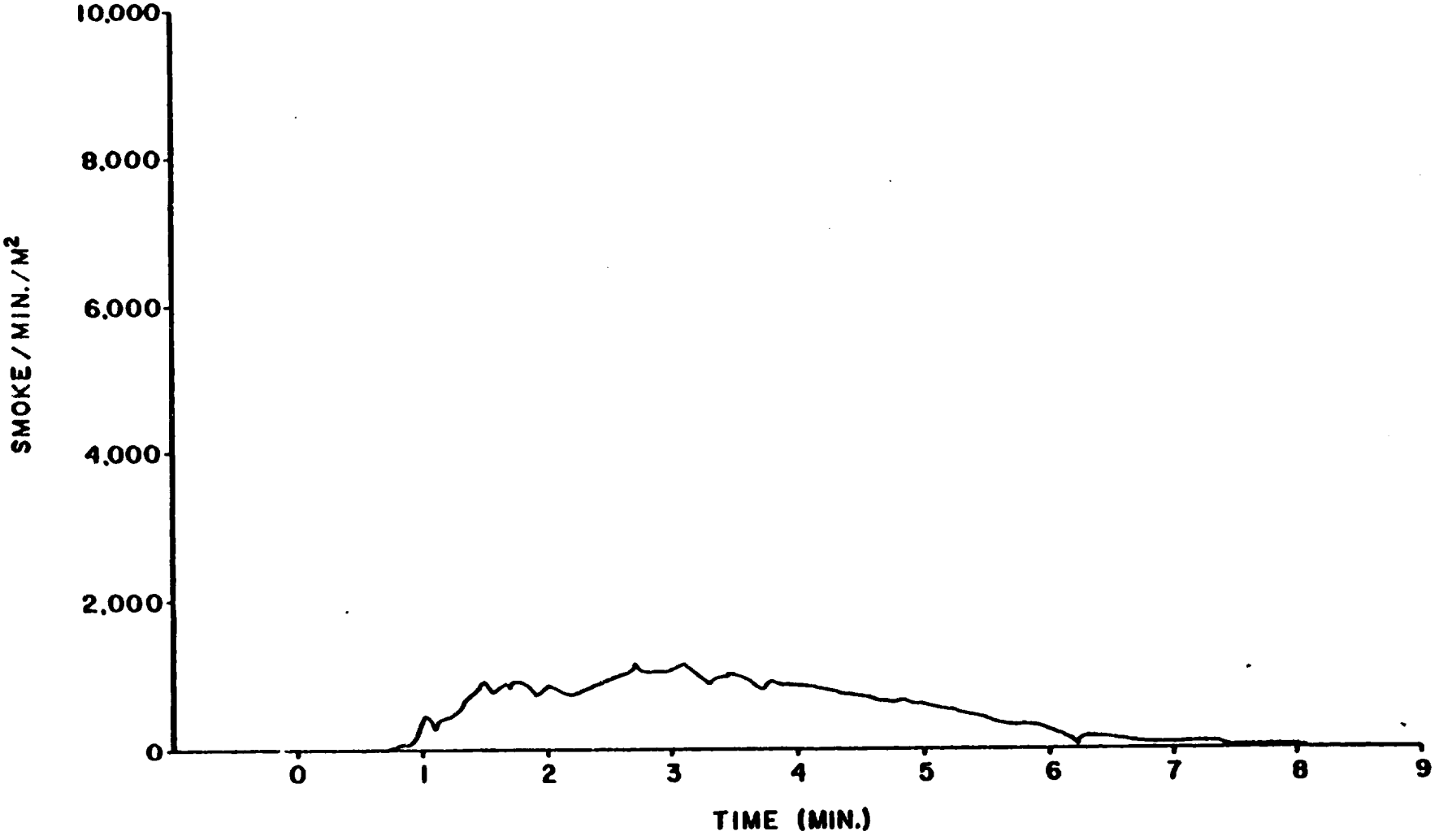

Figure 43. Smoke Release Rate of Graphite/Bismaleimide (M751) at 6.0 W/cm^2 With Piloted Ignition

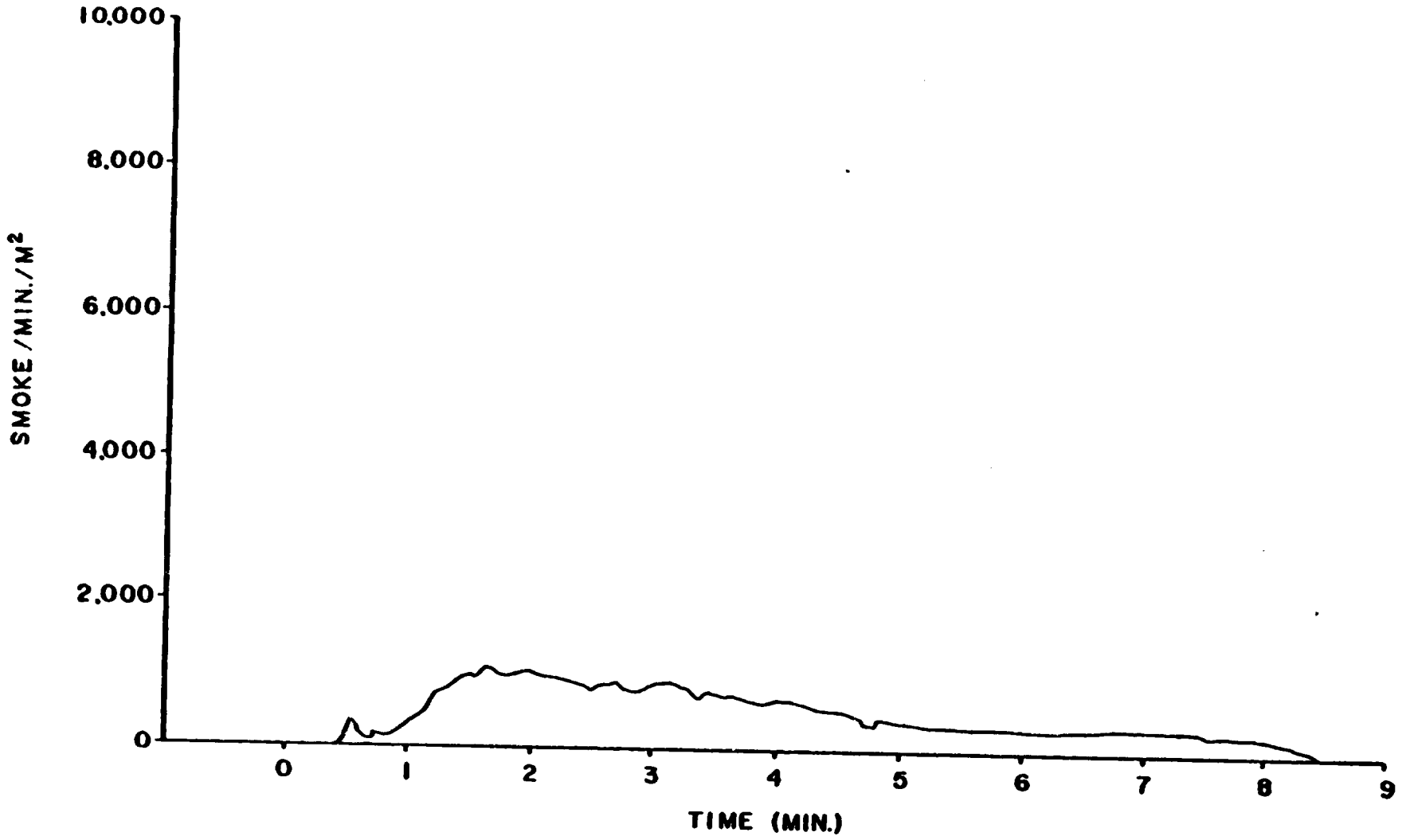

Figure 44. Smoke Release Rate of Graphite/Bismaleimide (M751) at 7.0 W/cm² With Piloted Ignition

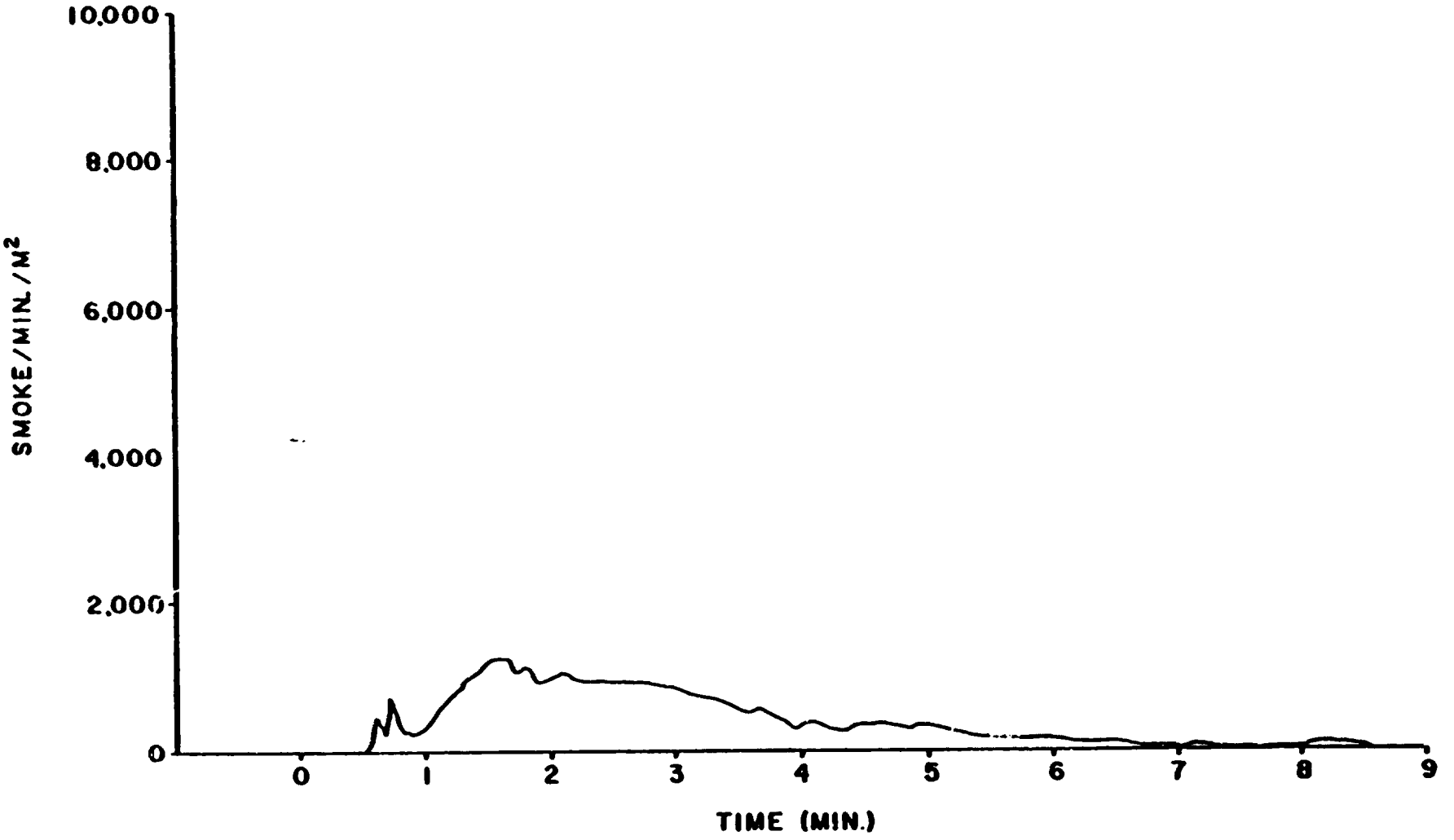

Figure 45. Smoke Release Rate of Graphite/Bismaleimide (H751) at 7.0 W/cm^2 With Piloted Ignition

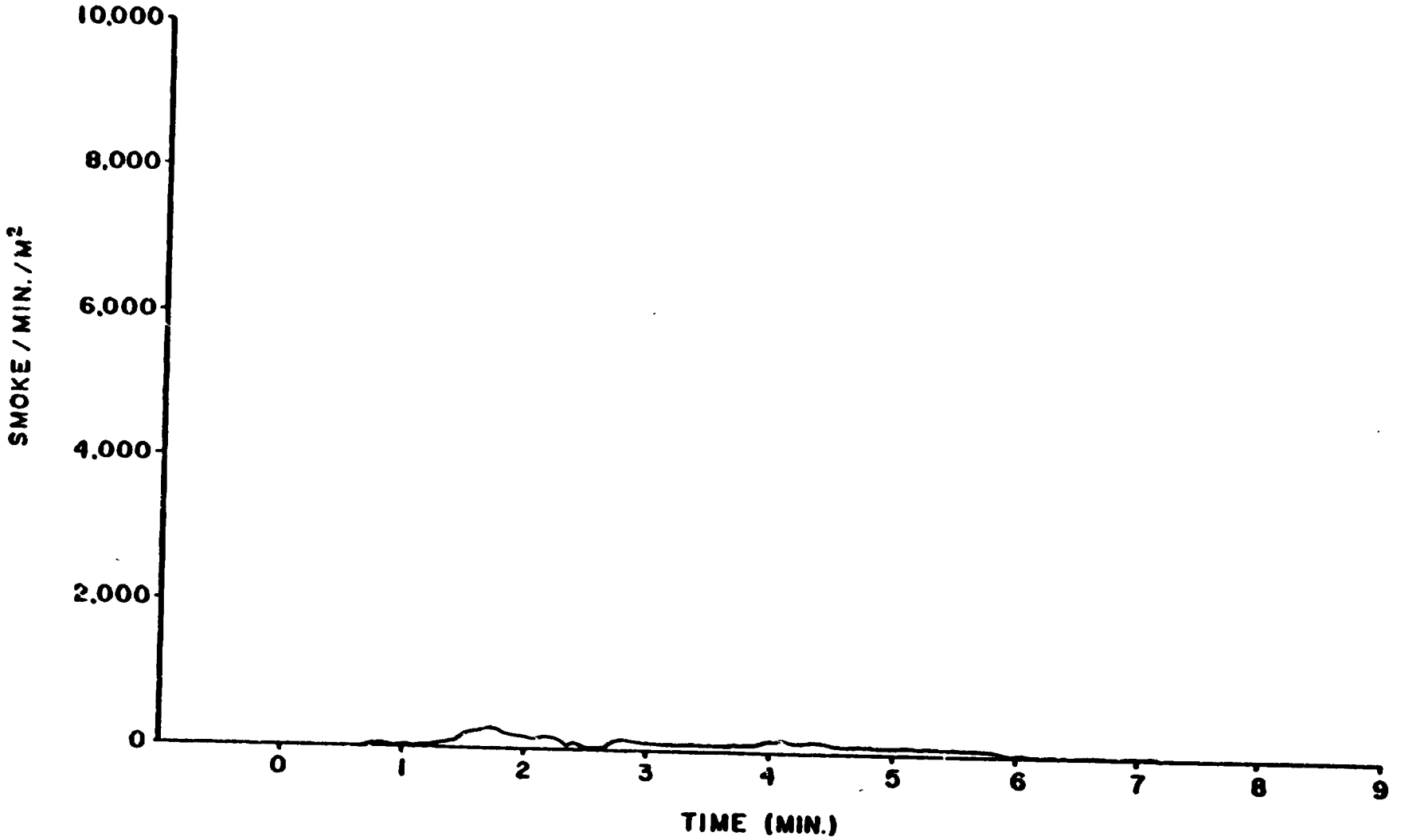

Figure 46. Smoke Release Rate of Graphite/Bismaleimide (1017) at 7.0 W/cm² With Non-Ignition

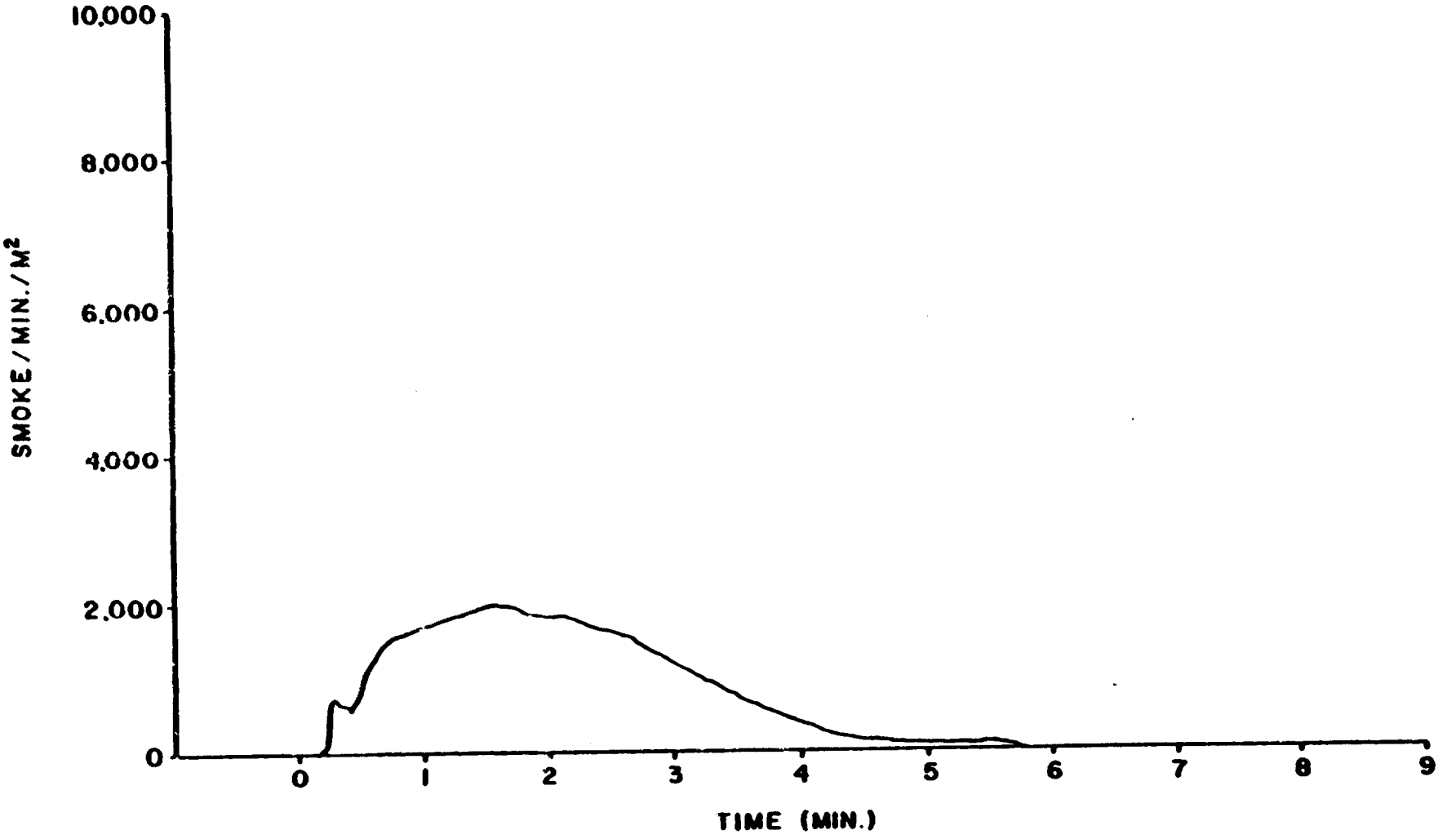

Figure 47. Smoke Release Rate of Graphite/Bismaleimide (M751) at 8.0 W/cm² With Piloted Ignition

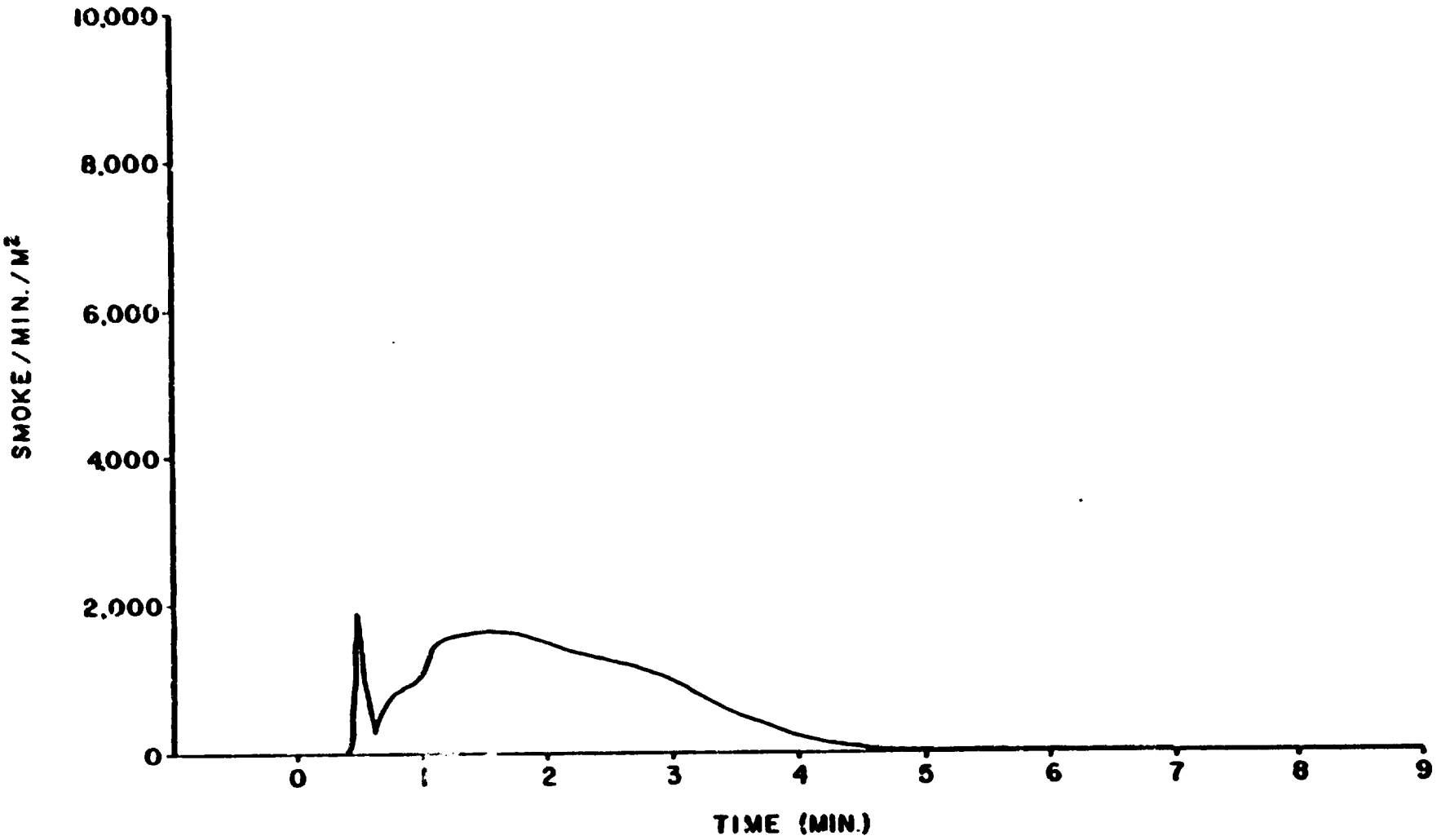

Figure 48. Smoke Release Rate of Graphite/Bismaleimide (H751) at 9.0 W/cm^2 With Piloted Ignition

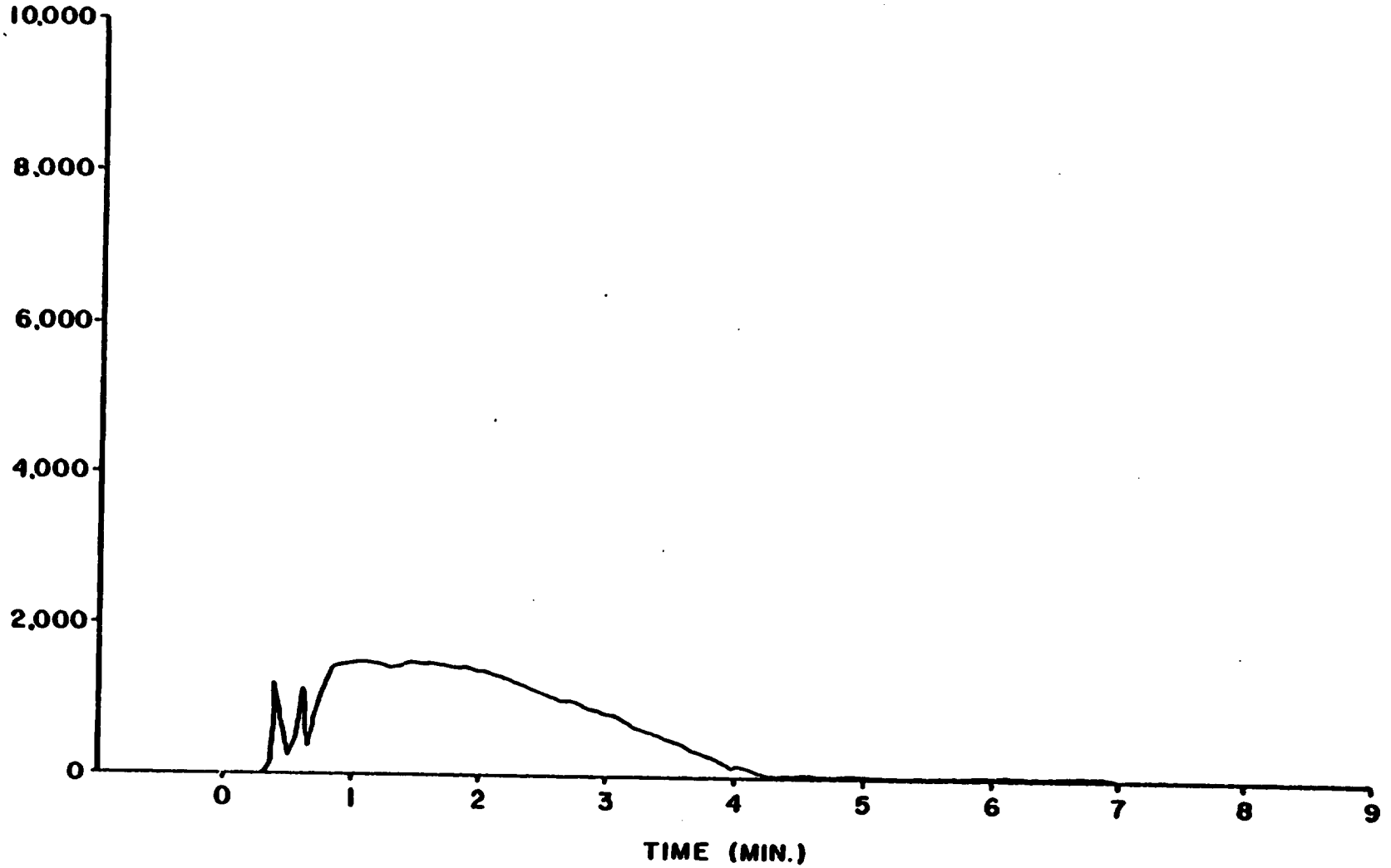

Figure 49. Smoke Release Rate of Graphite/Bismaleimide (M751) at 10.0 W/cm^2 With Piloted Ignition

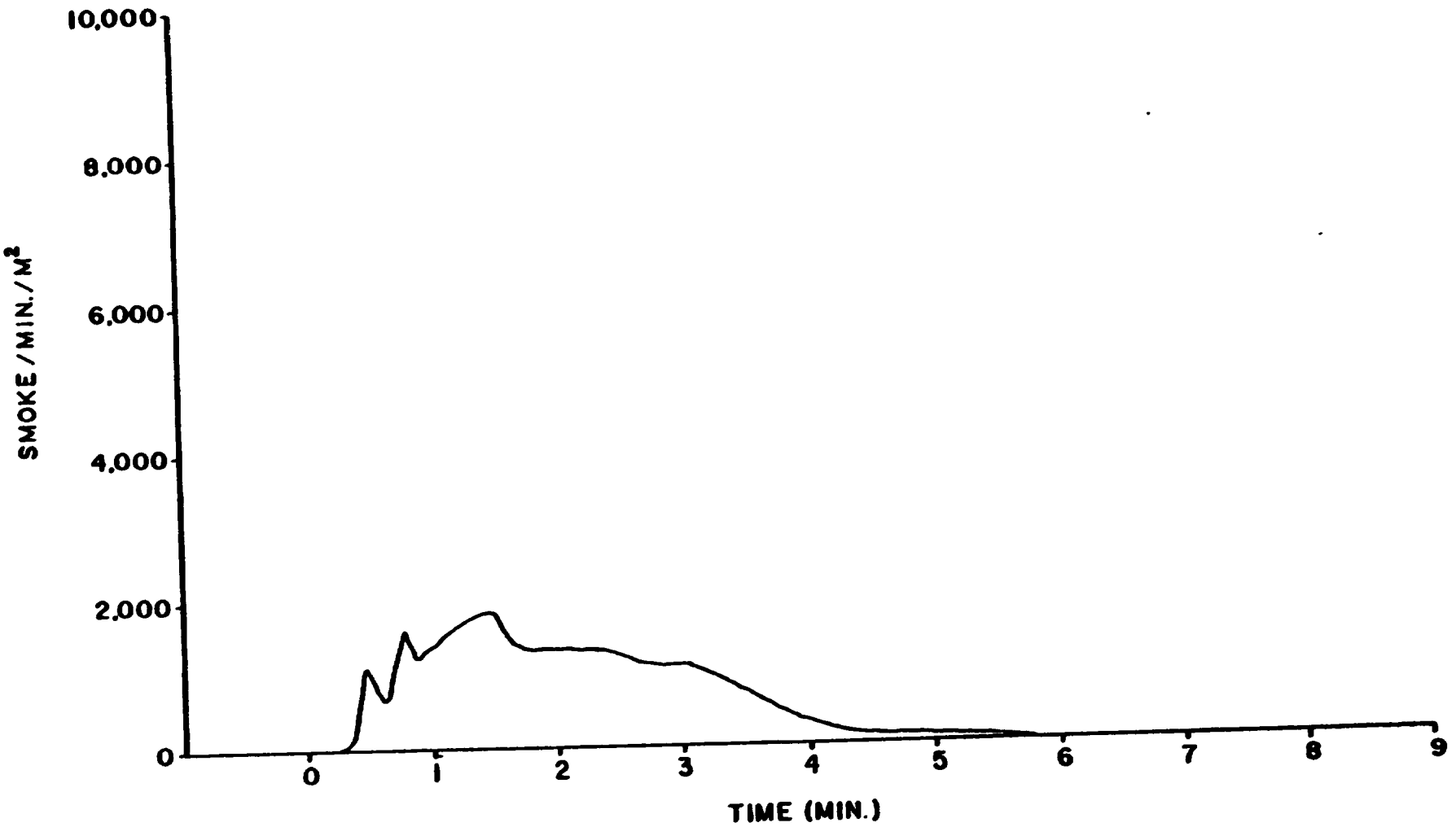

Figure 50. Smoke Release Rate of Graphite/Bismaleimide (M751) at 10.0 W/cm^2 With Non-Piloted Ignition

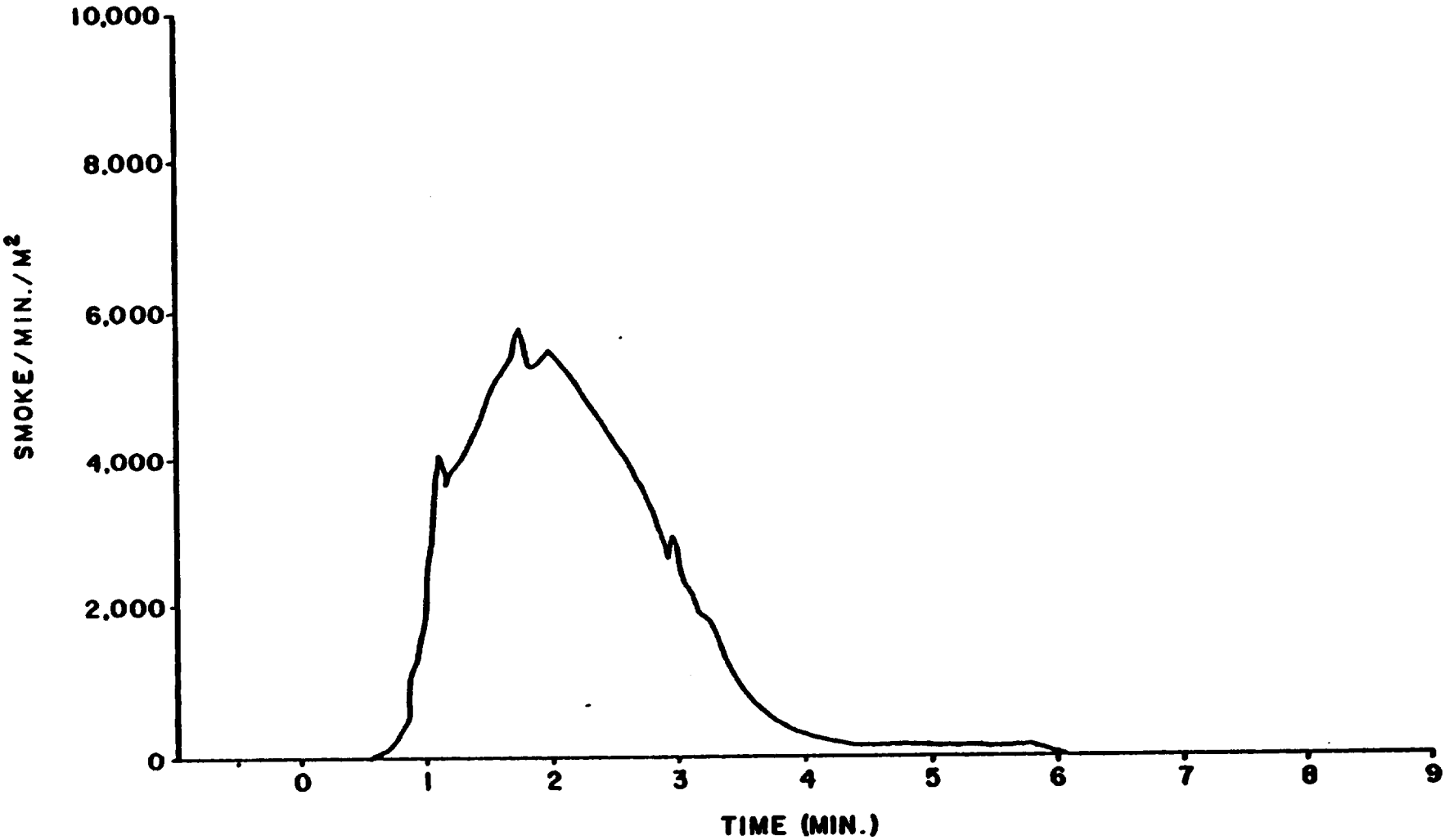

Figure 51. Smoke Release Rate of Graphite/Epoxy (1008A) at 5.0 W/cm^2 With Piloted Ignition

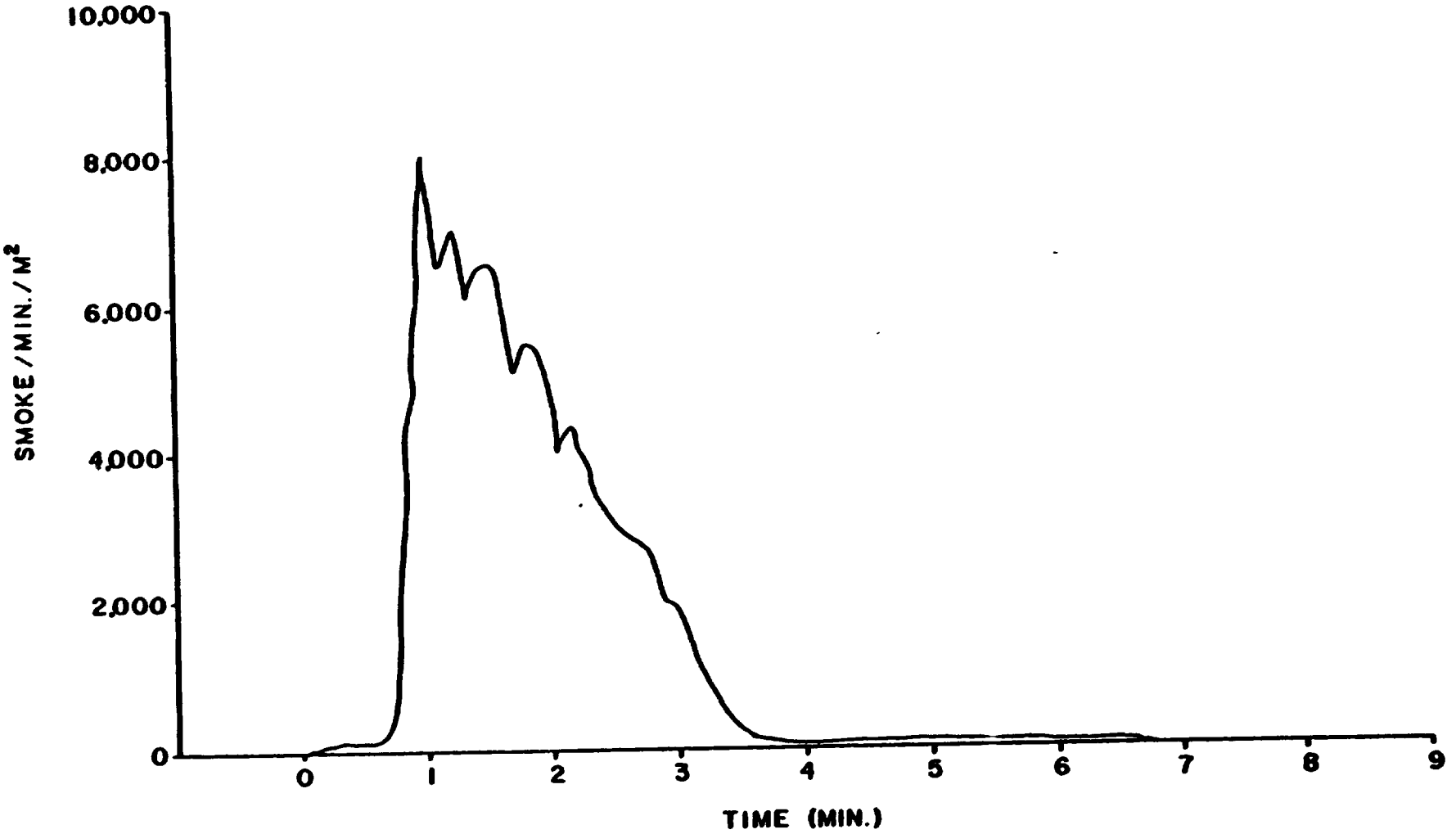

Figure 52. Smoke Release Rate of Graphite/Epoxy (1012-9) at 6.0 W/cm^2 With Piloted Ignition

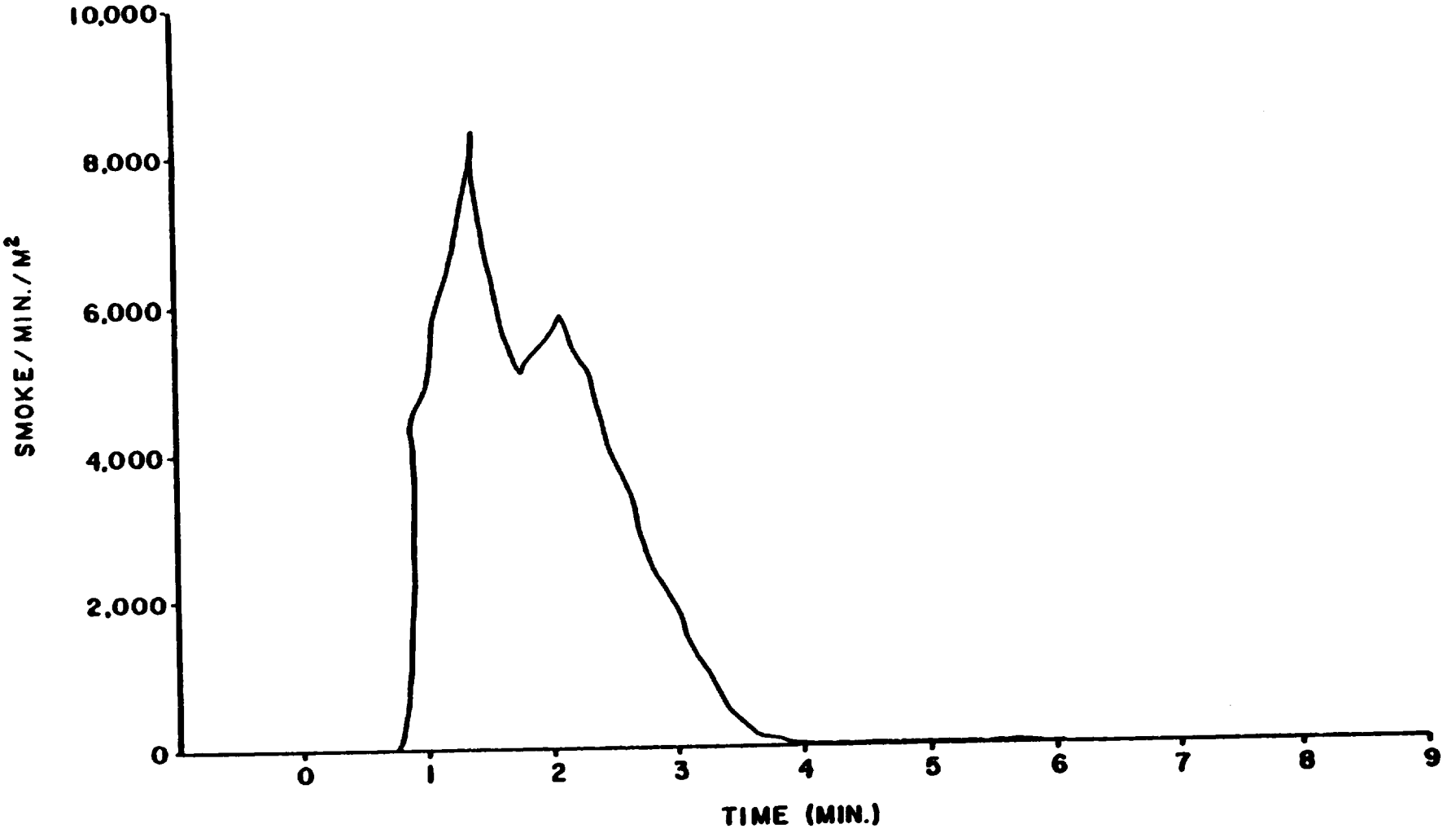

Figure 53. Smoke Release Rate of Graphite/Epoxy (1012-9) at 7.0 W/cm² With Piloted Ignition

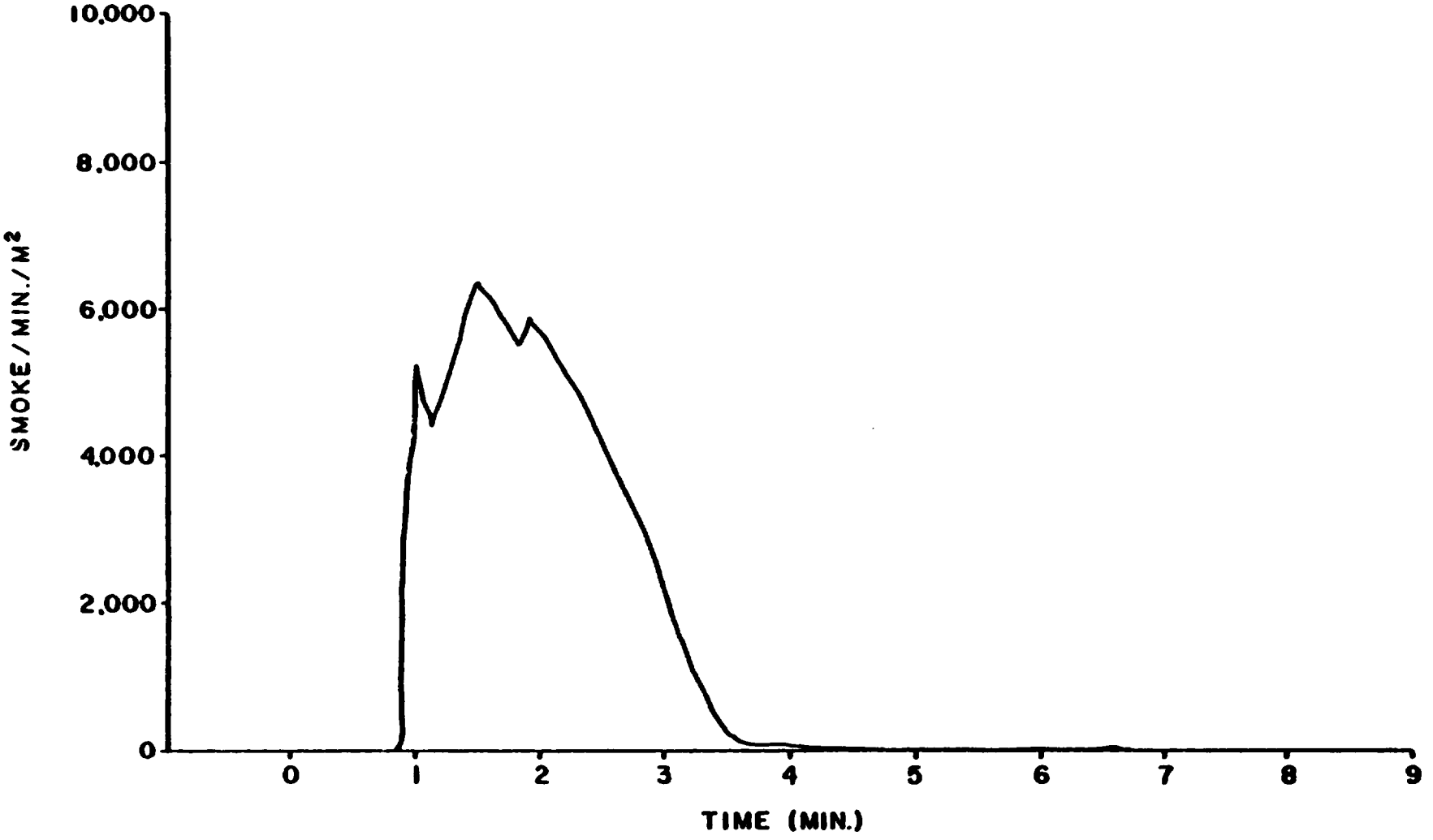

Figure 54. Smoke Release Rate of Graphite/Epoxy (1008A) at 7.0 W/cm² With Non-Piloted Ignition

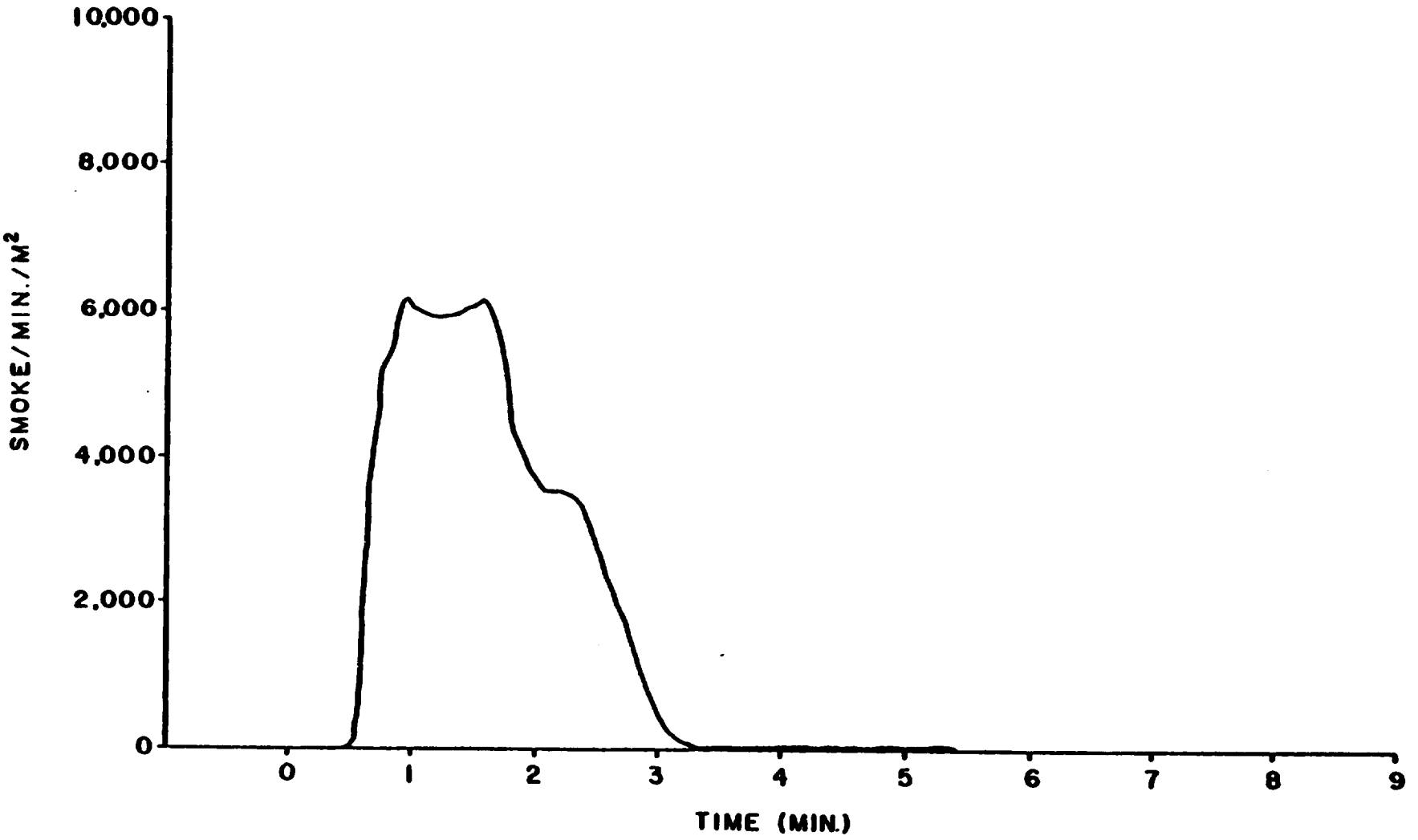

Figure 55. Smoke Release Rate of Graphite/Epoxy (1012-9) at 8.0 W/cm² With Piloted Ignition

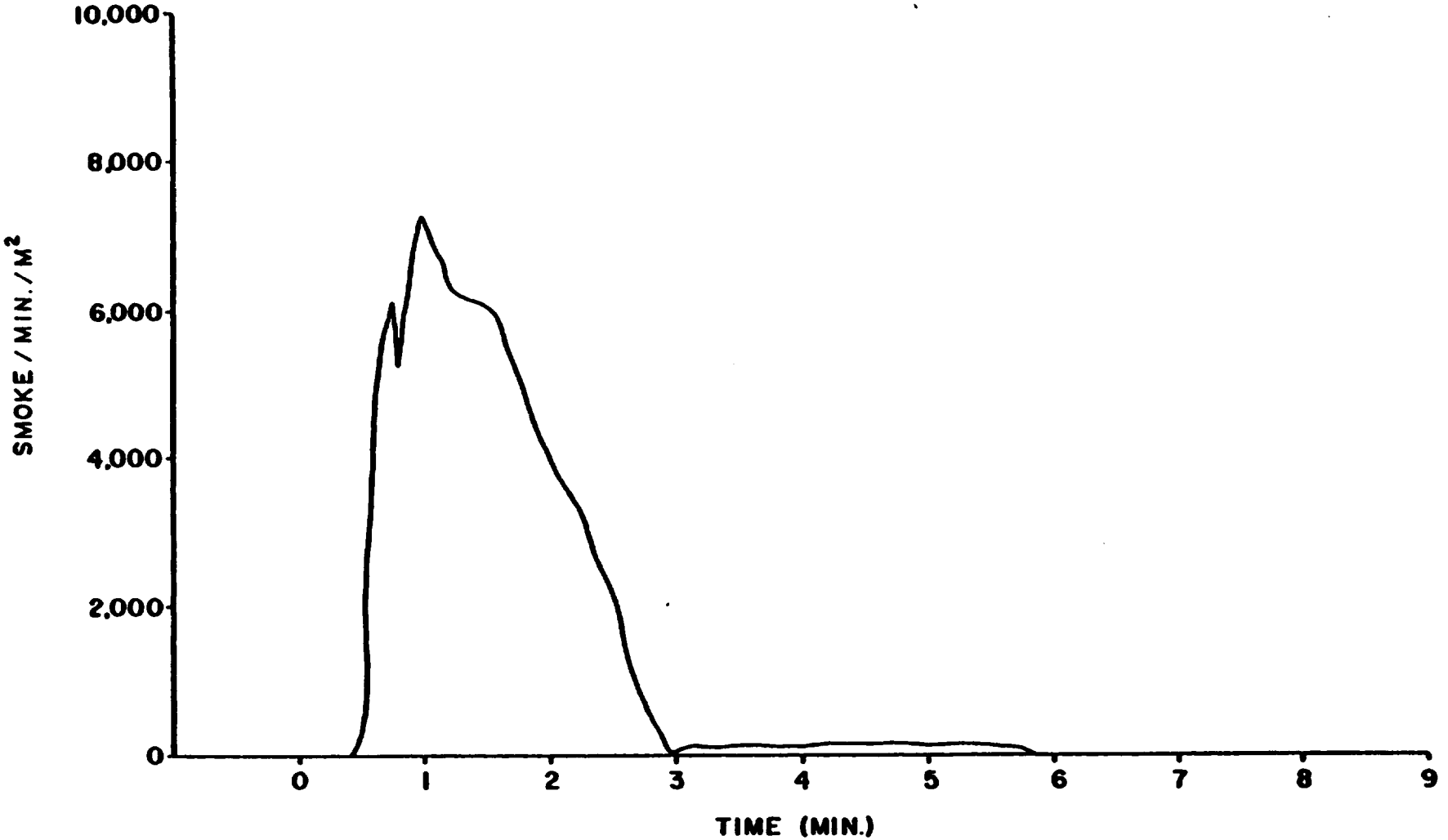

Figure 56. Smoke Release Rate of Graphite/Epoxy (1012-9) at 9.0 W/cm² With Piloted Ignition

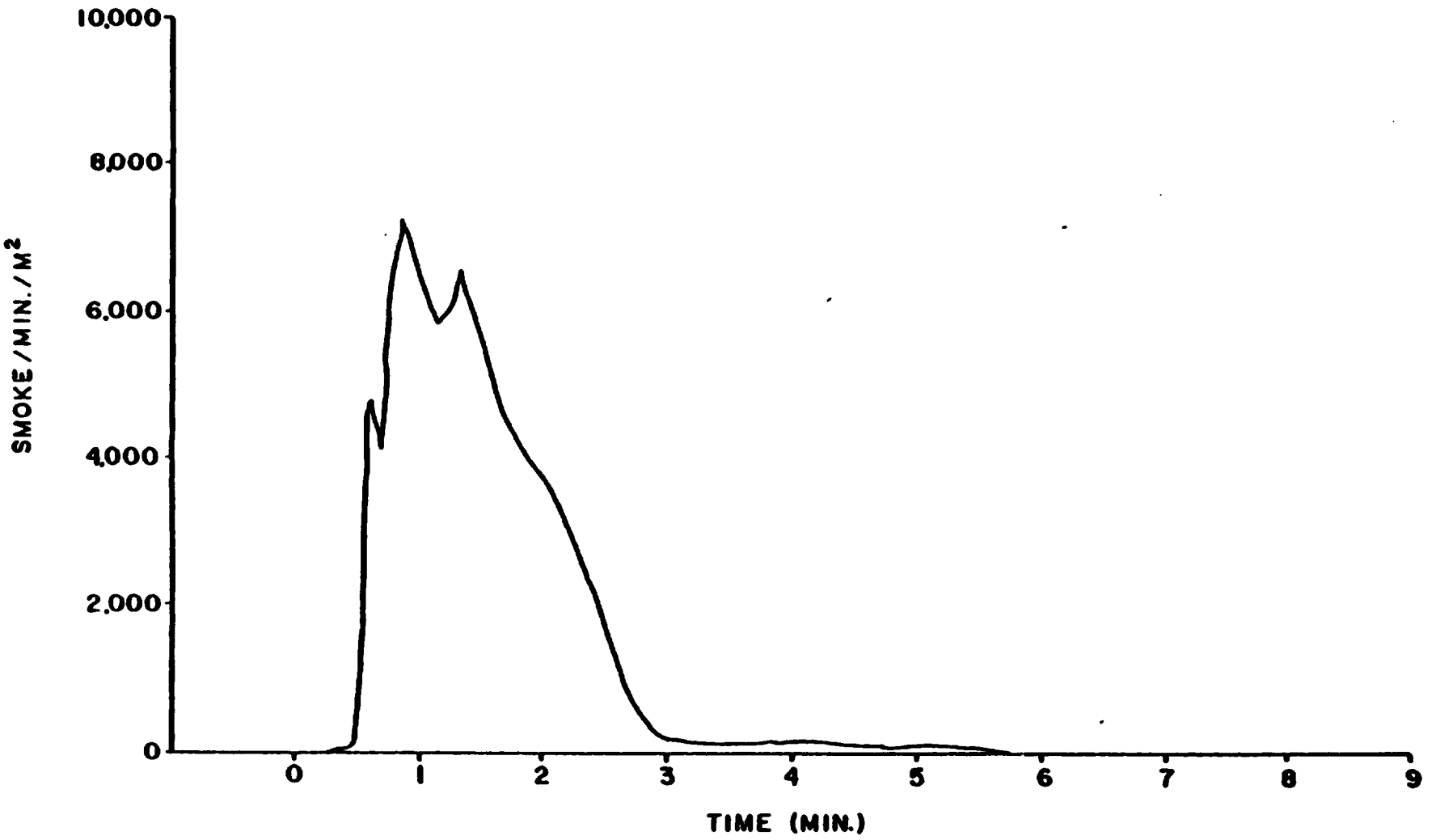

Figure 57. Smoke Release Rate of Graphite/Epoxy (1008A) at 10.0 W/cm² With Piloted Ignition

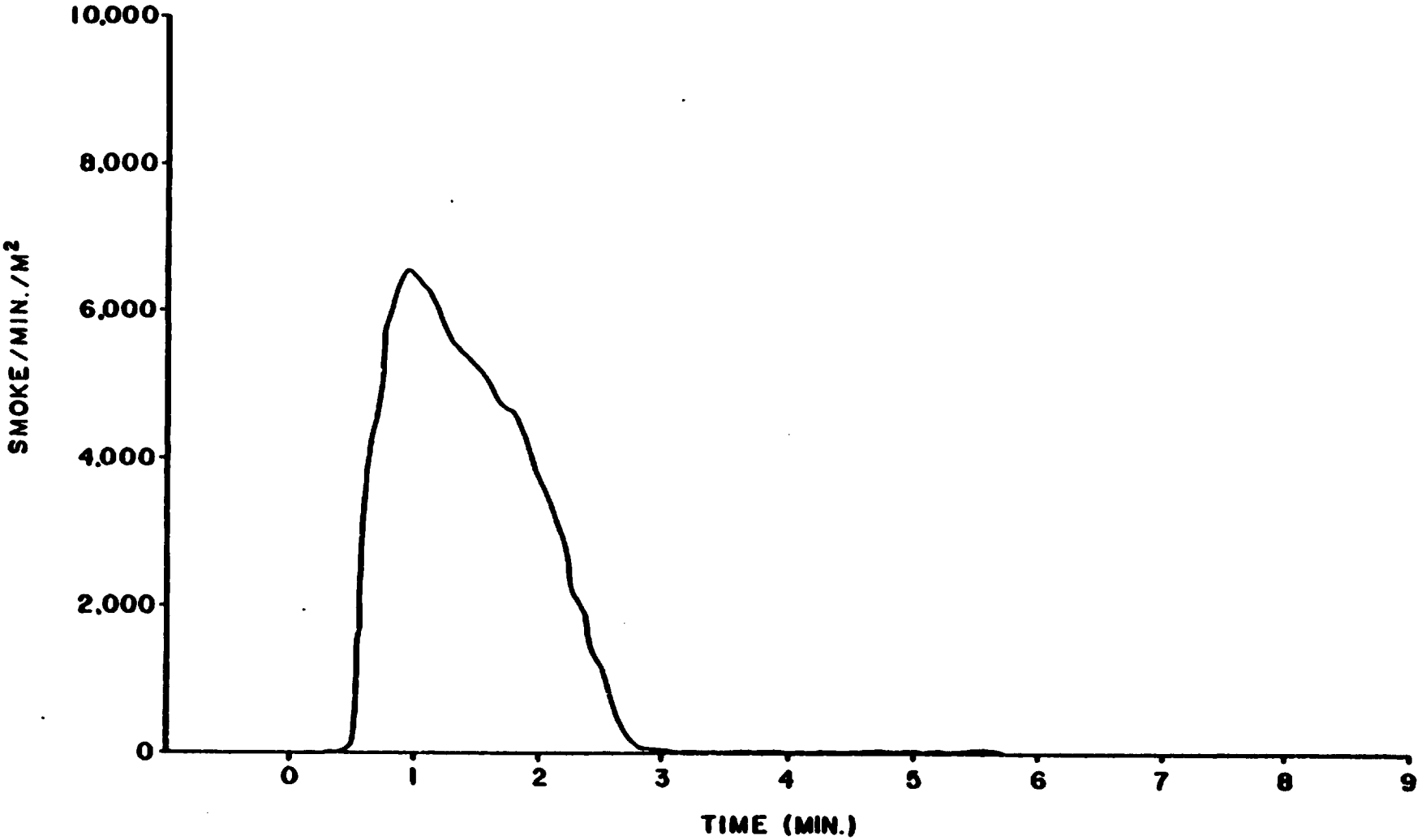

Figure 58. Smoke Release Rate of Graphite/Epoxy (1008A) at 10.0 W/cm² With Non-Piloted Ignition

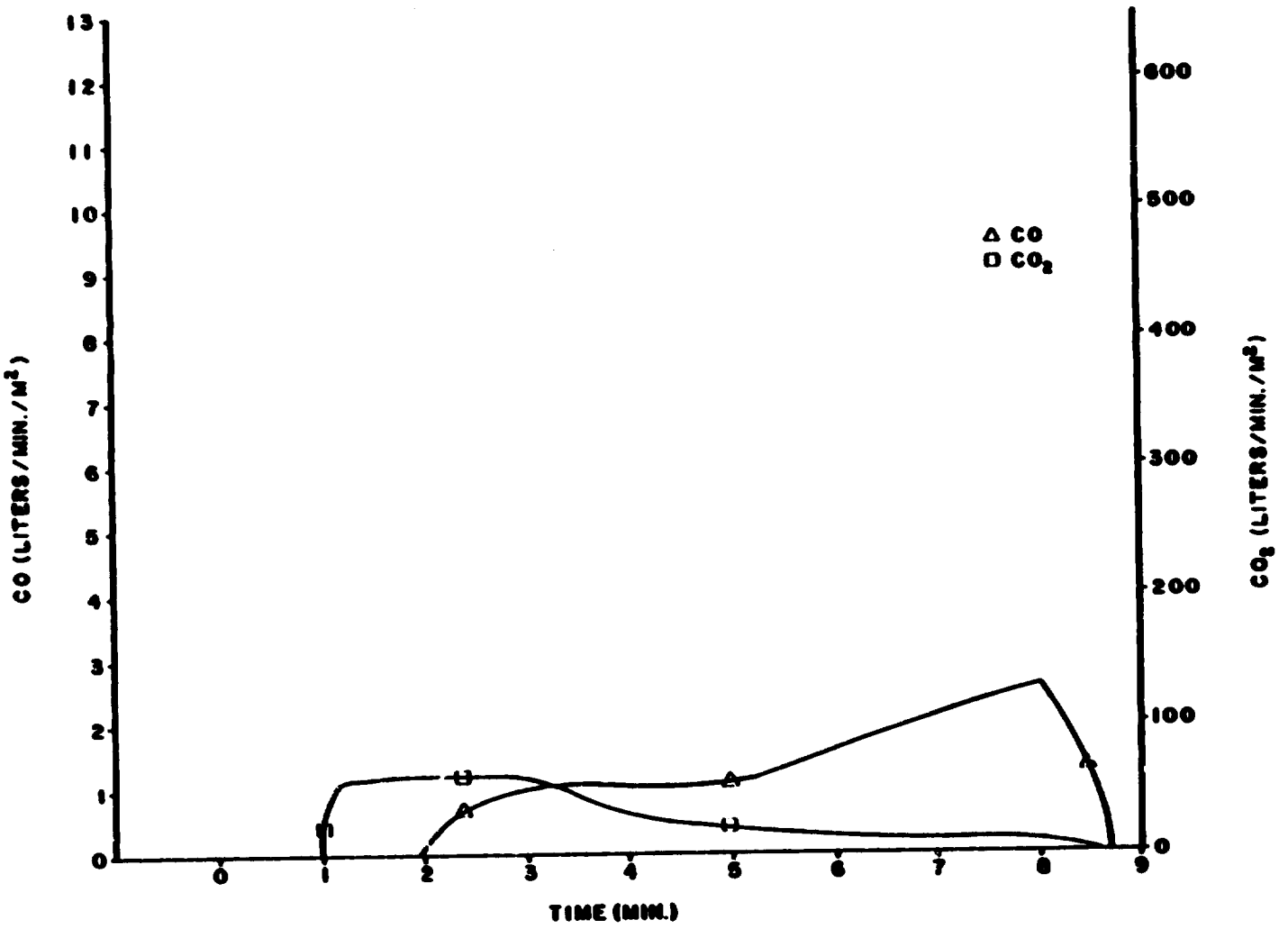

Figure 59. Release Rates of CO and CO_2--Graphite/Bismaleimide (1017) at 5.0 W/cm^2 With Piloted Ignition

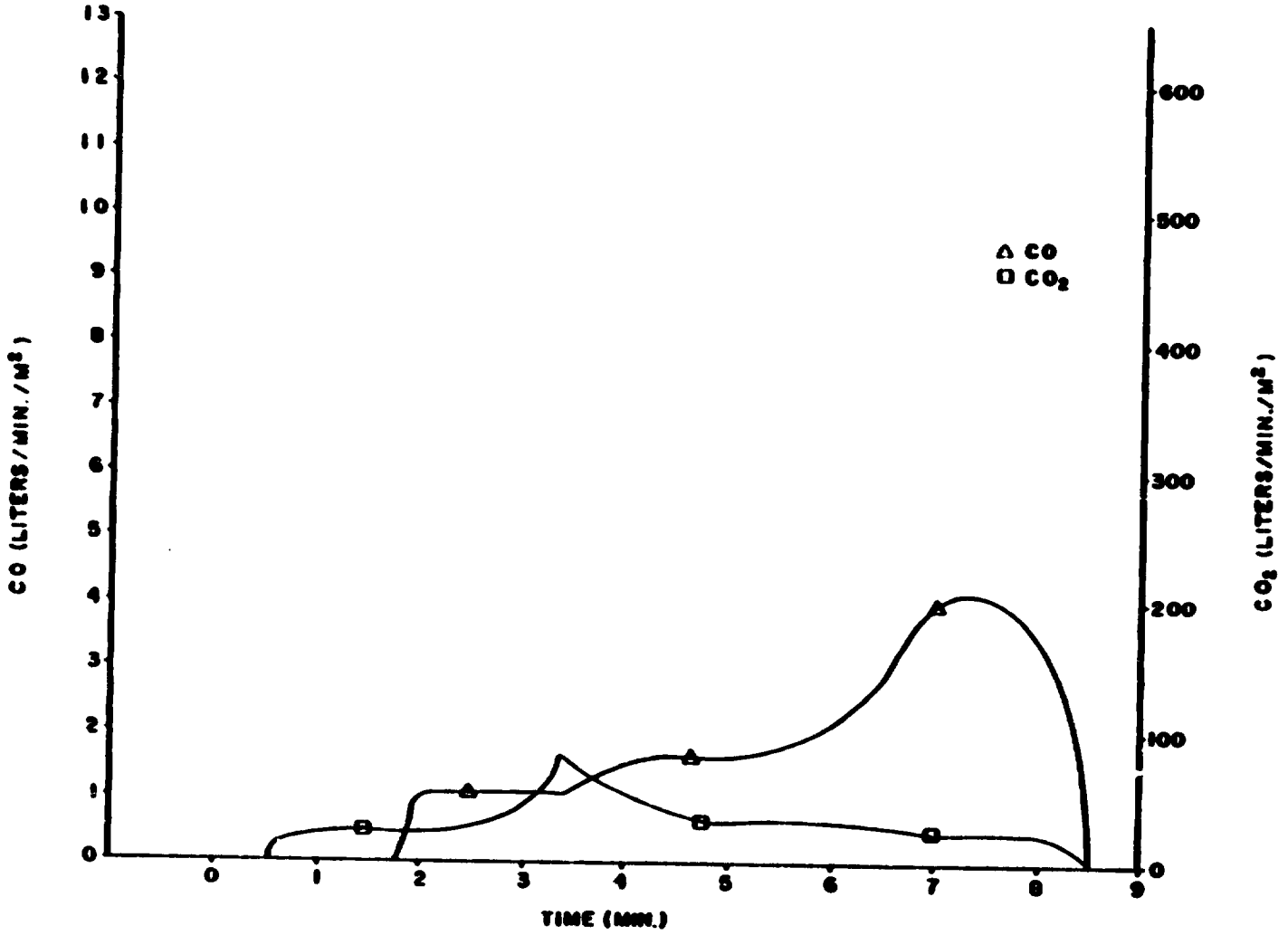

Figure 60. Release Rates of CO and CO_2--Graphite/Bismaleimide (M751) at 6.0 W/cm^2 With Piloted Ignition

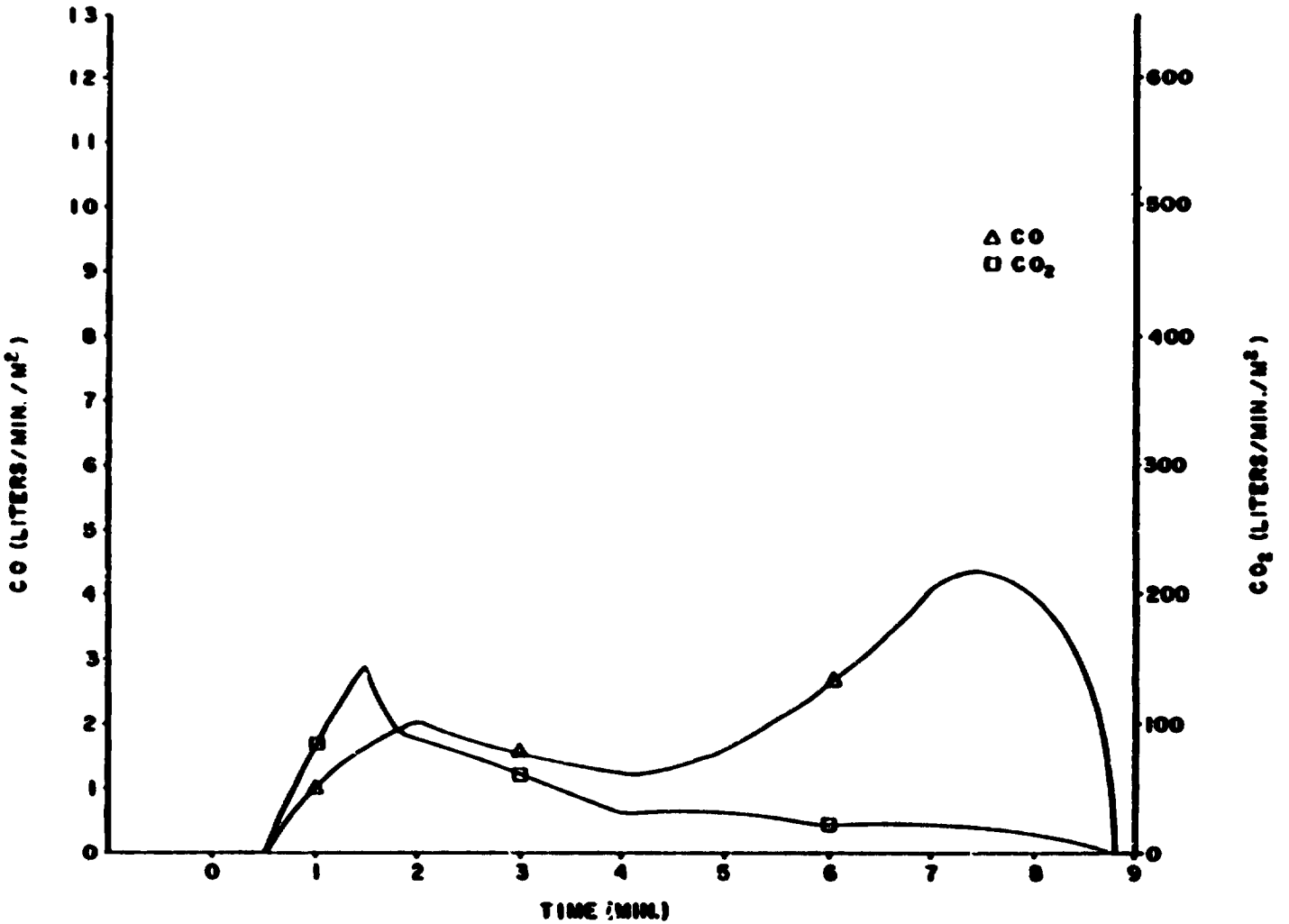

Figure 61. Release Rates of CO and CO_2--Graphite/Bismaleimide (M751) at 7.0 W/cm^2 With Piloted Ignition

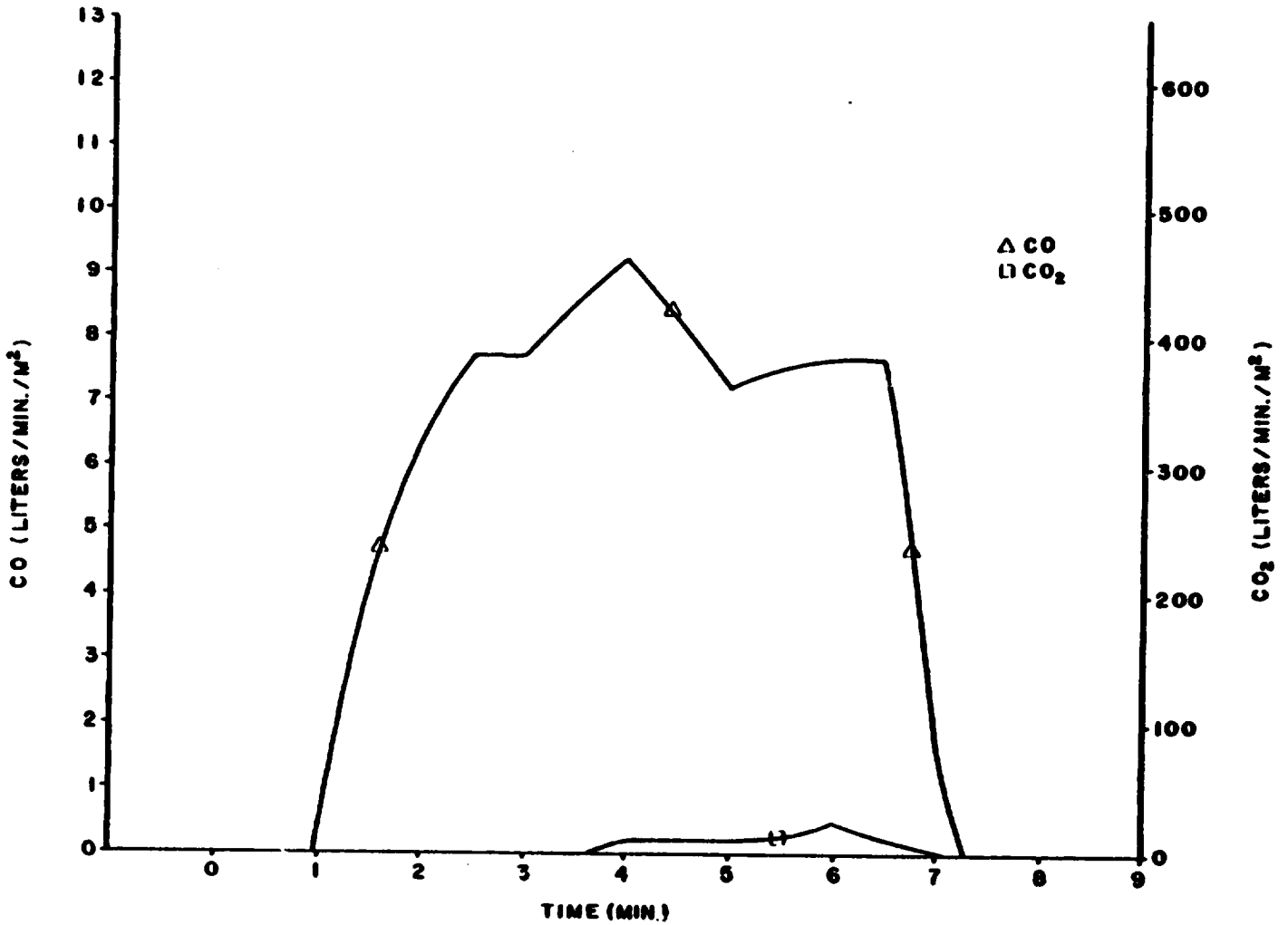

Figure 62. Release Rates of CO and CO_2--Graphite/Bismaleimide (1017) at 7.0 W/cm^2 With Non-Piloted Ignition

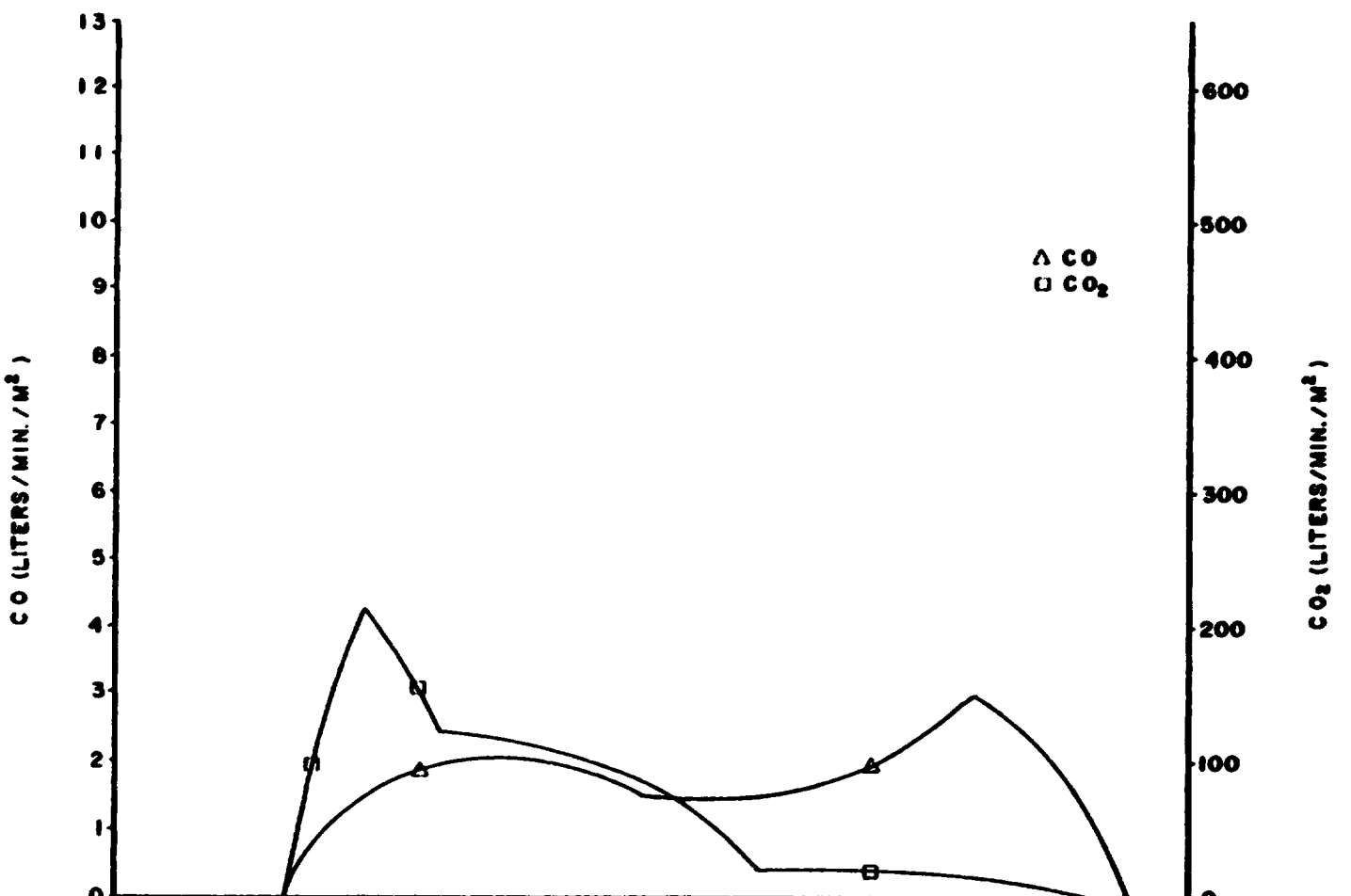

Figure 63. Release Rates of CO and CO_2--Graphite/Bismaleimide (M751) at 8.0 W/cm^2 With Piloted Ignition

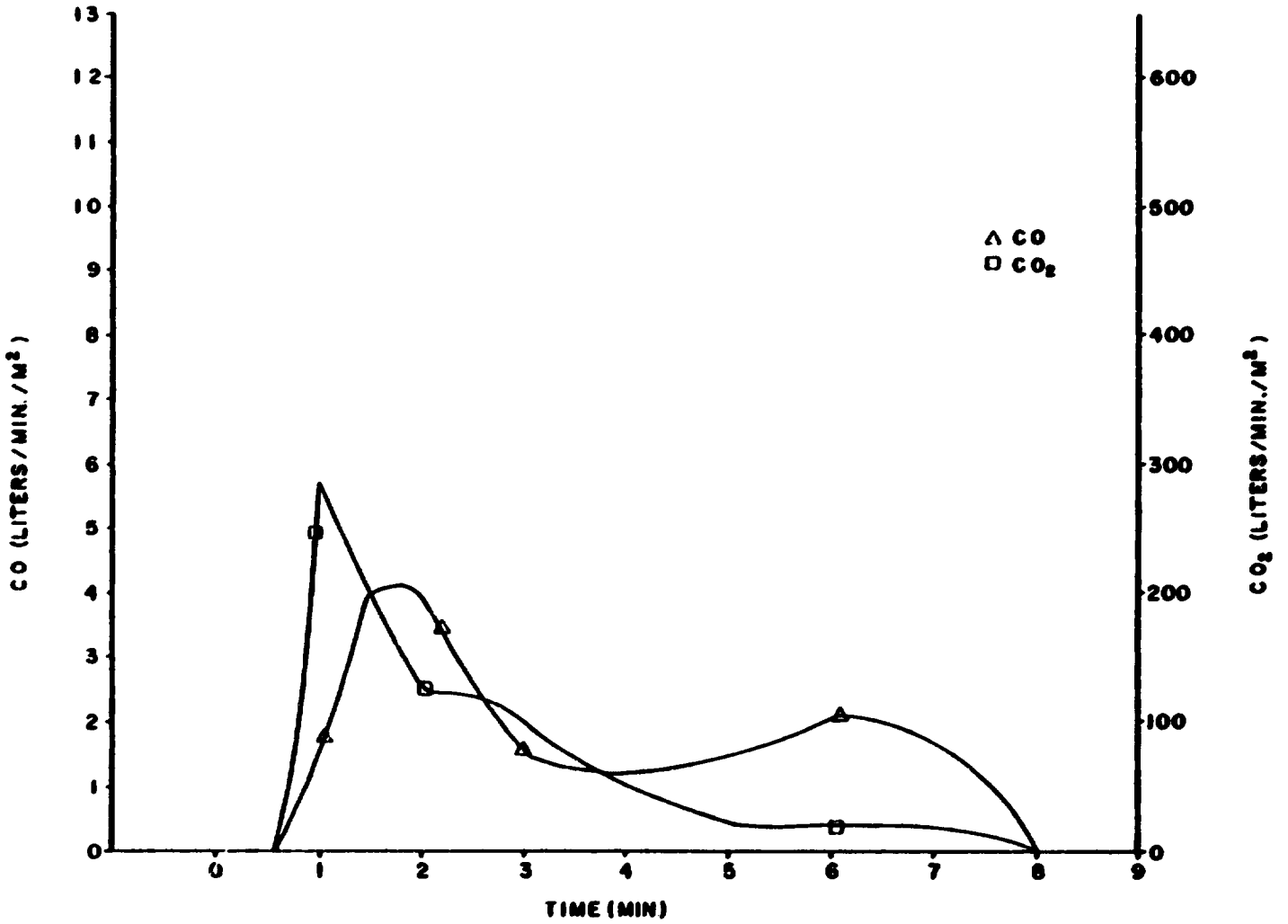

Figure 64. Release Rates of CO and CO_2--Graphite/Bismaleimide (M751) at 9.0 W/cm^2 With Piloted Ignition

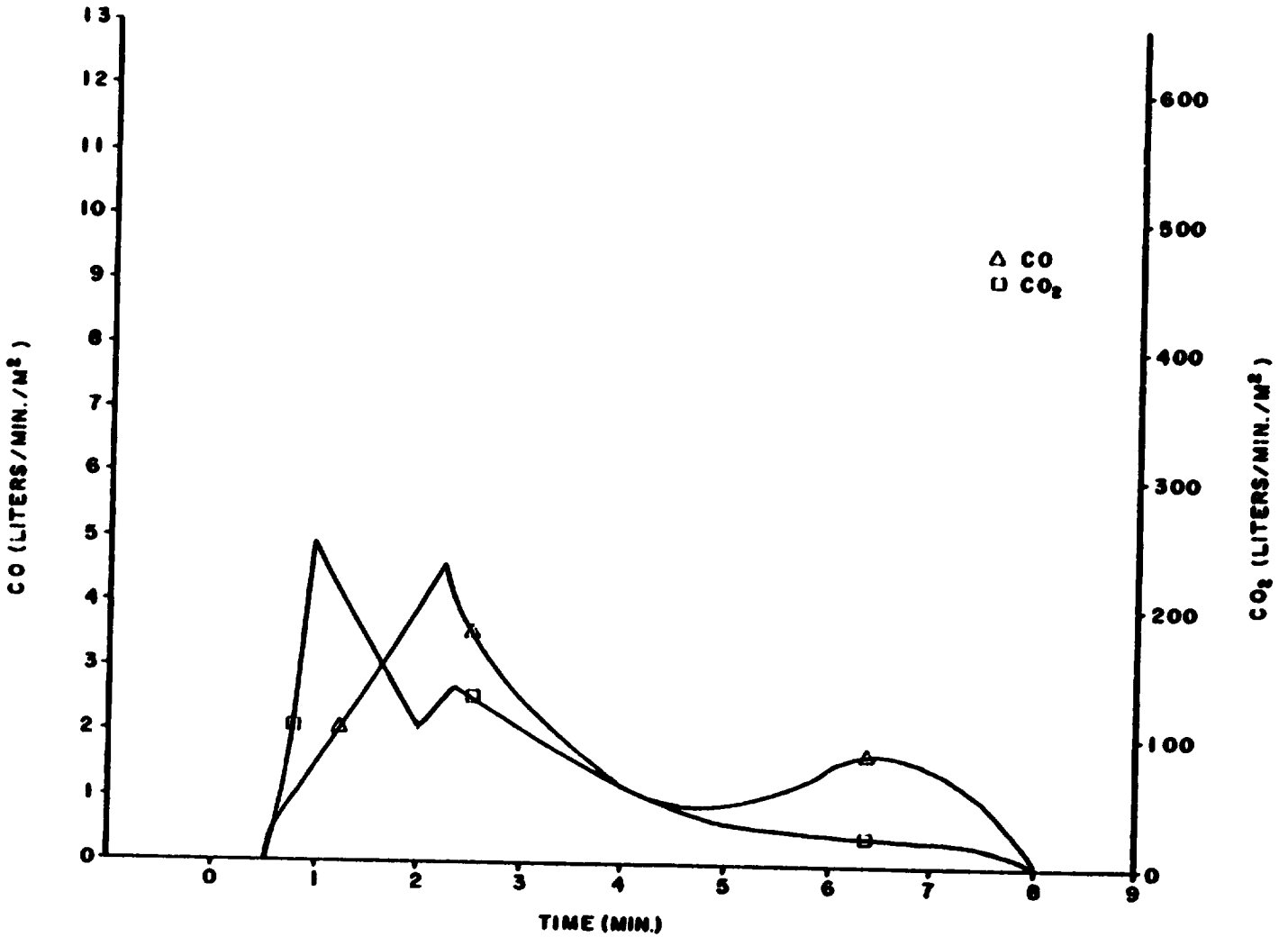

Figure 65. Release Rates of CO and CO_2--Graphite/Bismaleimide (M751) at 10.0 W/cm^2 With Piloted Ignition

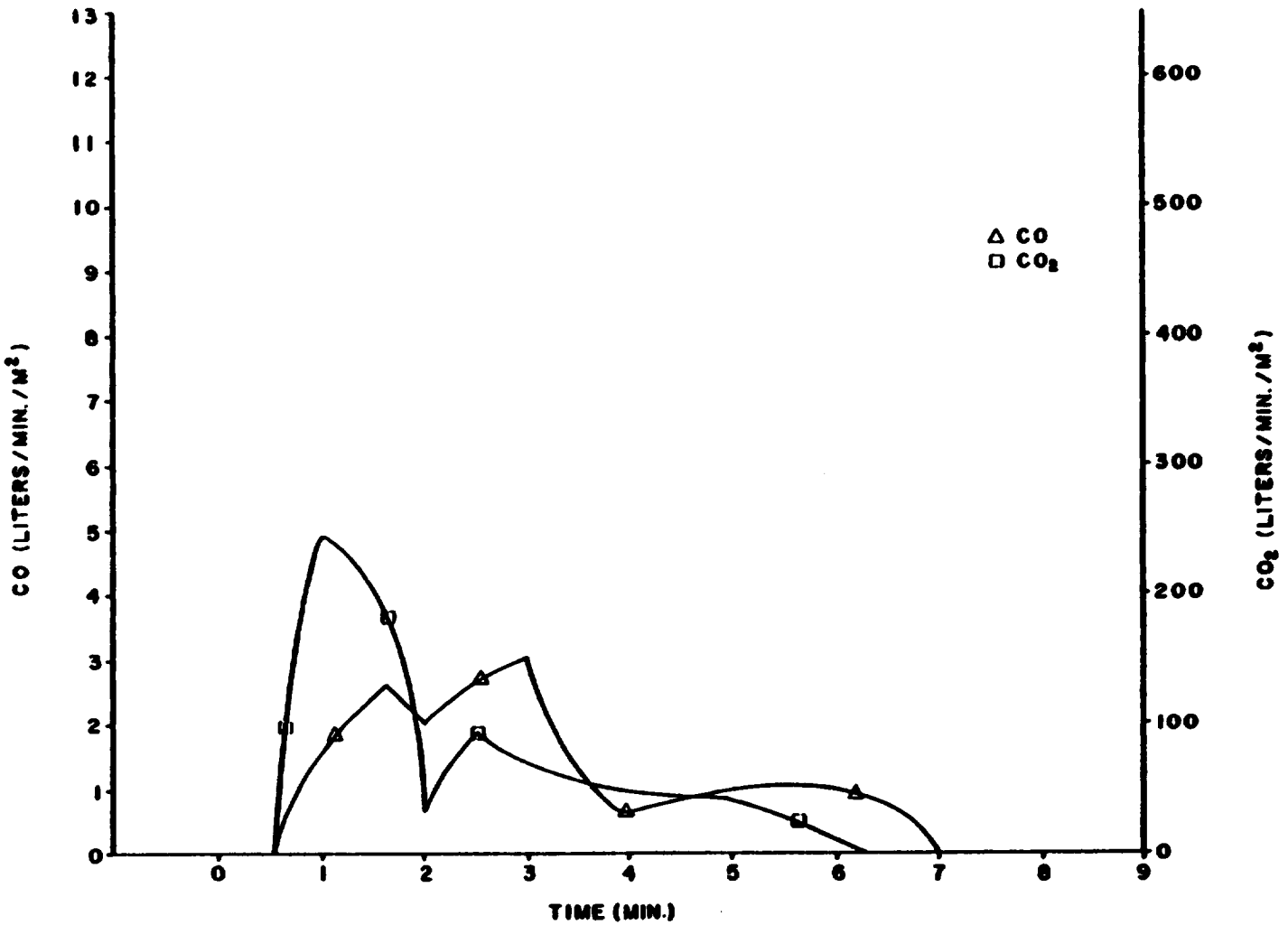

Figure 66. Release Rates of CO and CO_2--Graphite/Bismaleimide (1017) at 10.0 W/cm^2 With Non-Piloted Ignition

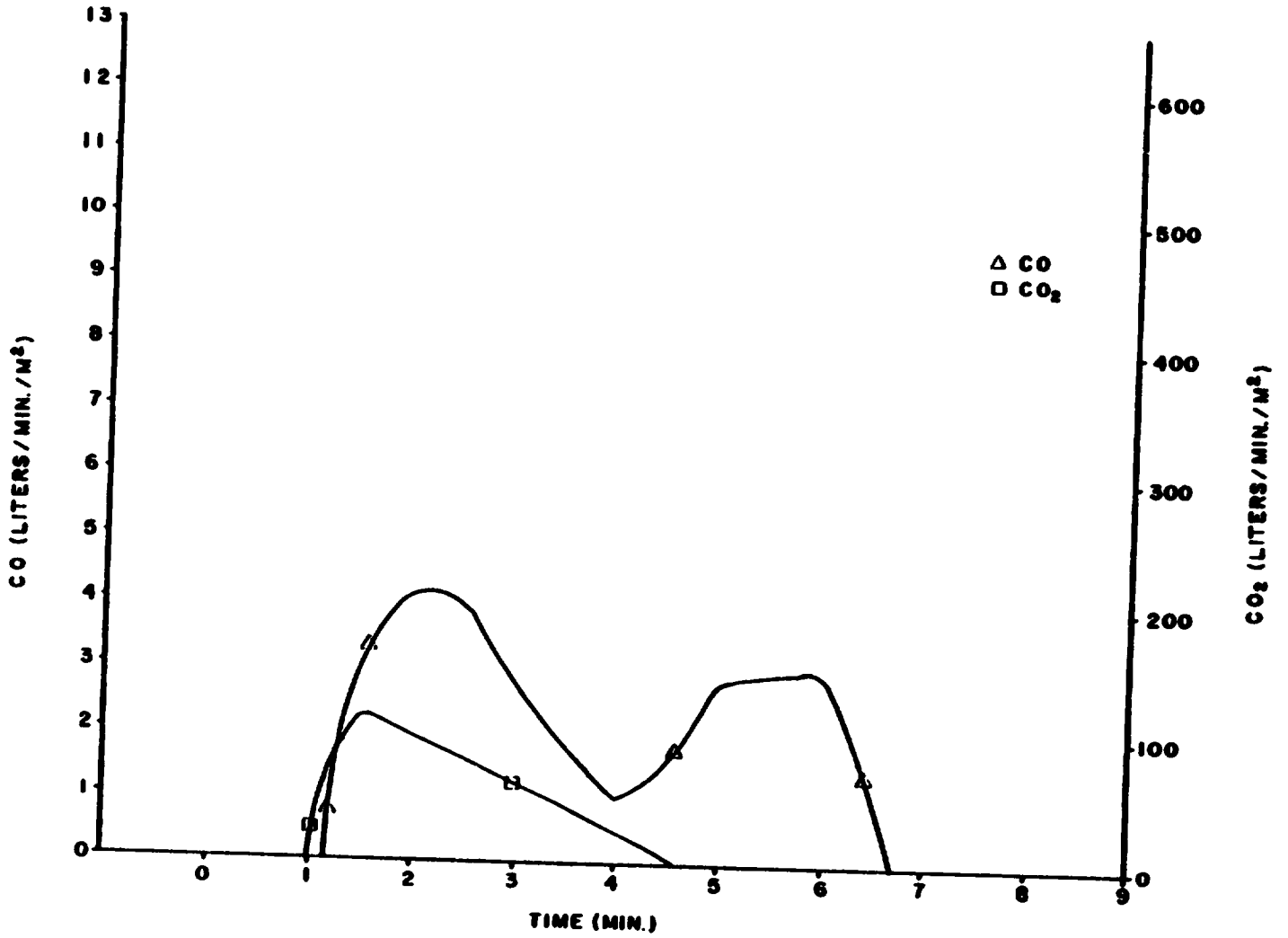

Figure 67. Release Rates of CO and CO_2--Graphite/Epoxy (1008A) at 5.0 W/cm^2 With Piloted Ignition

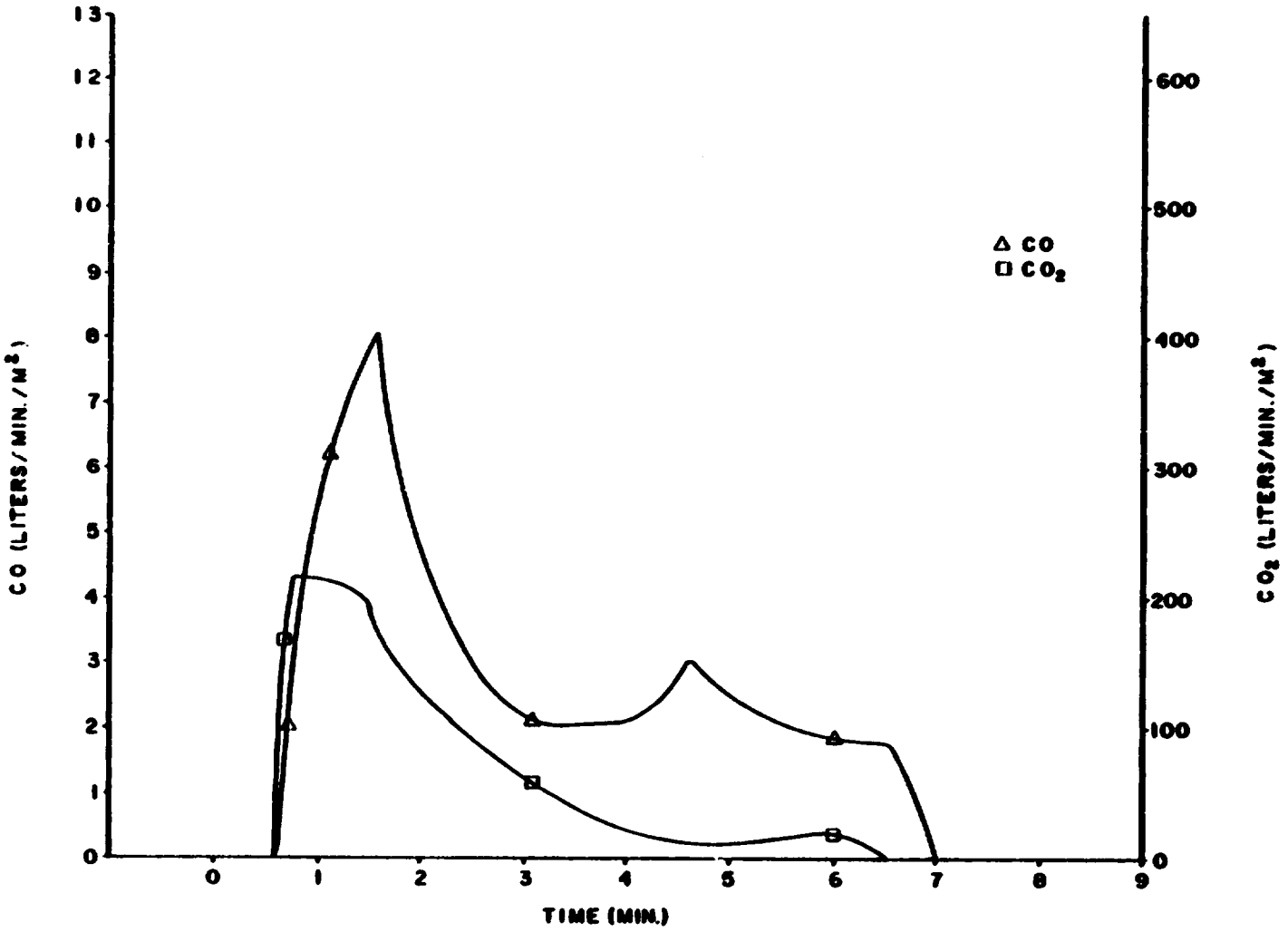

Figure 68. Release Rates of CO and CO_2--Graphite/Epoxy (1012-9) at 6.0 W/cm^2 With Piloted Ignition

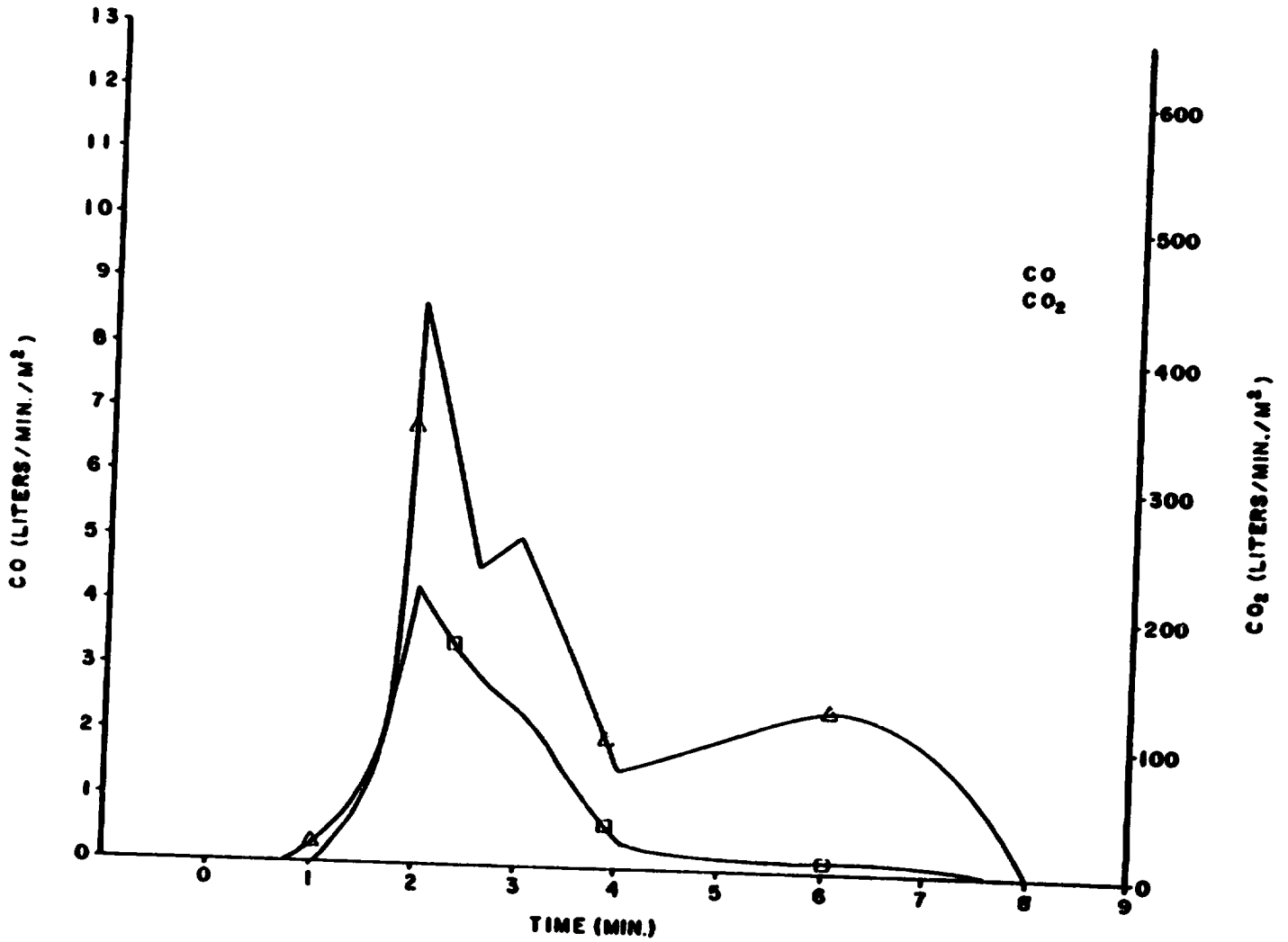

Figure 69. Release Rates of CO and CO_2--Graphite/Epoxy (1012-9) at 7.0 W/cm^2 With Piloted Ignition

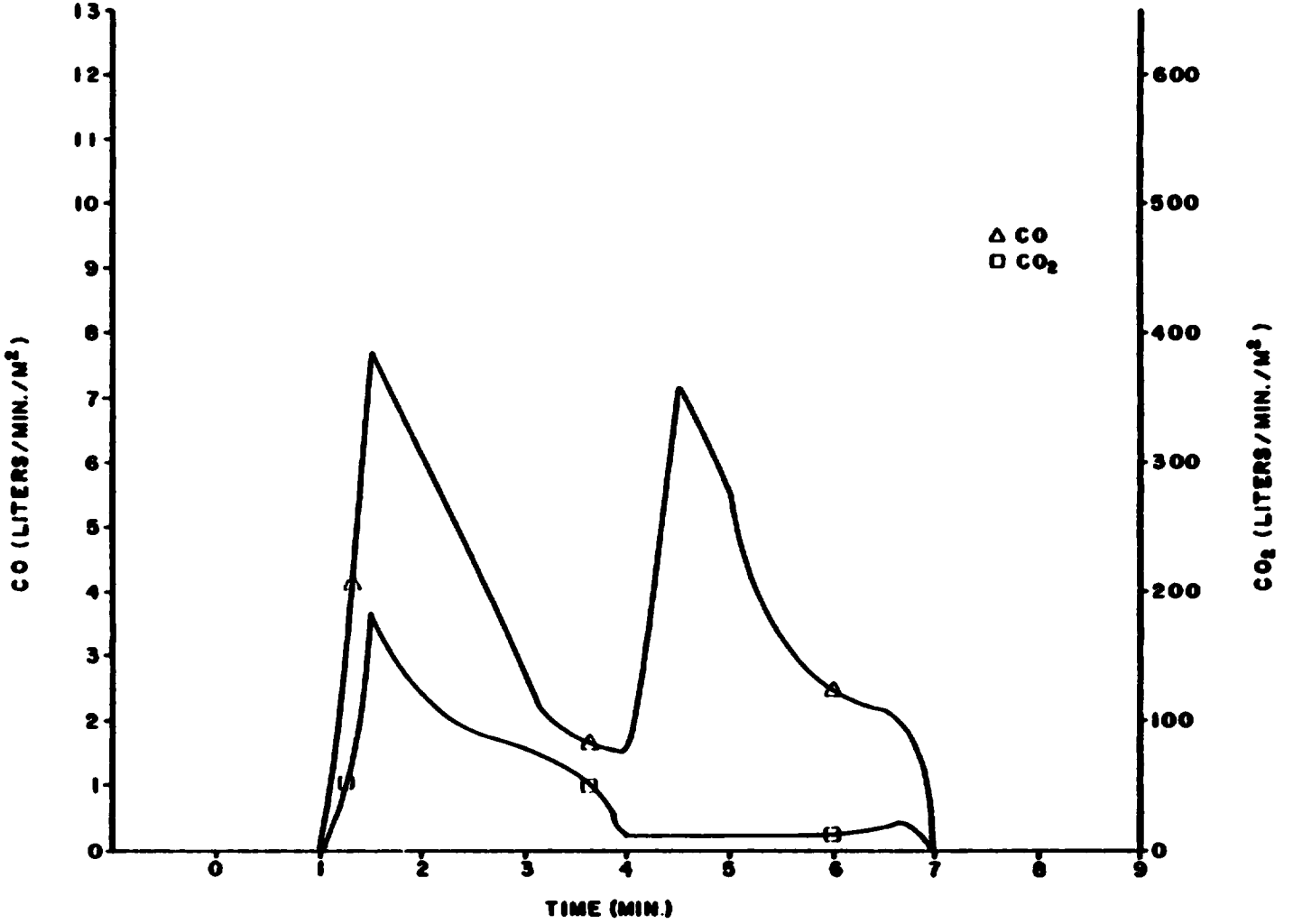

Figure 70. Release Rates of CO and CO_2--Graphite/Epoxy (1008A) at 7.0 W/cm^2 With Non-Piloted Ignition

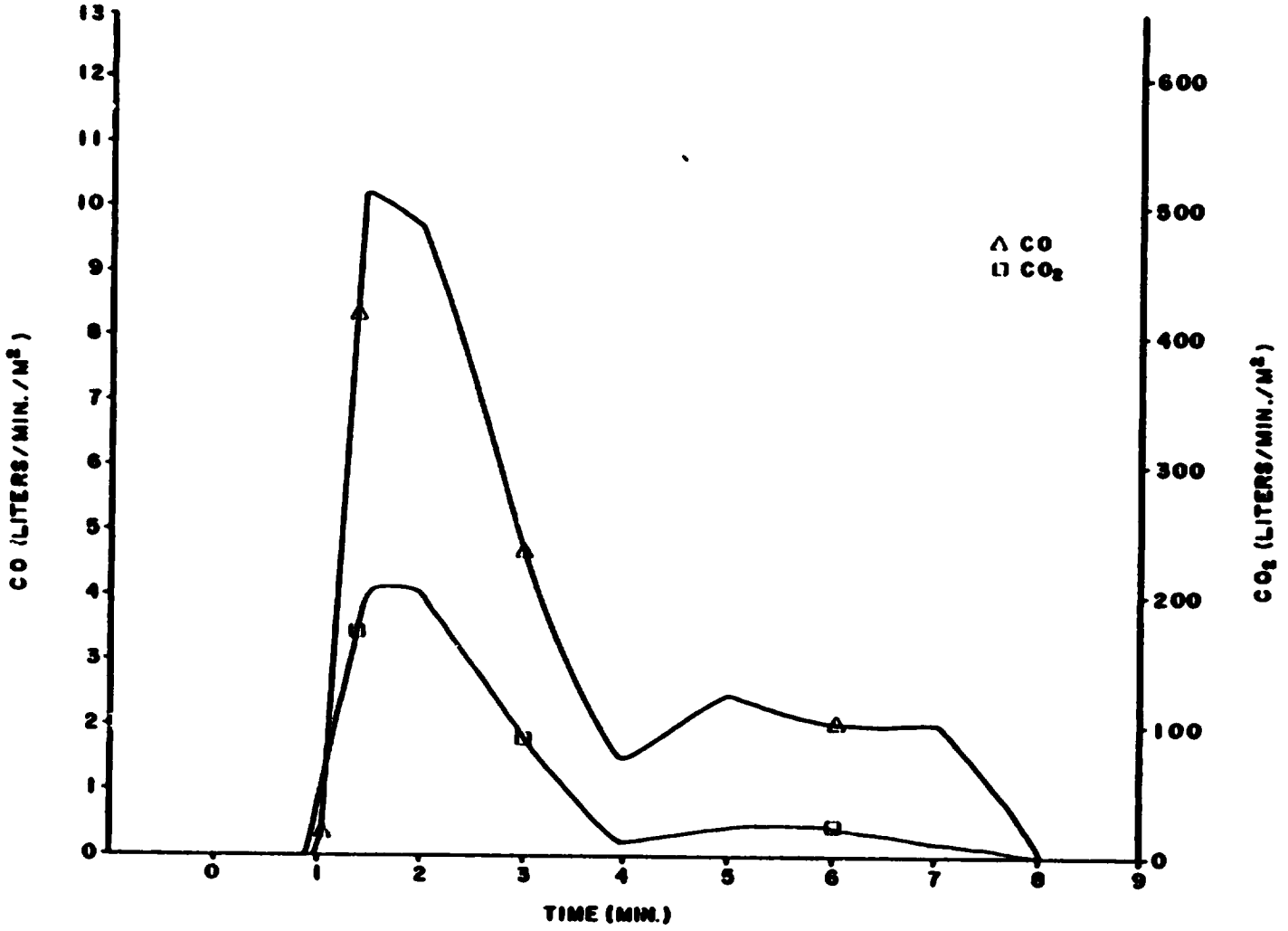

Figure 71. Release Rates of CO and CO_2--Graphite/Epoxy (1012-9) at 8.0 W/cm^2 With Piloted Ignition

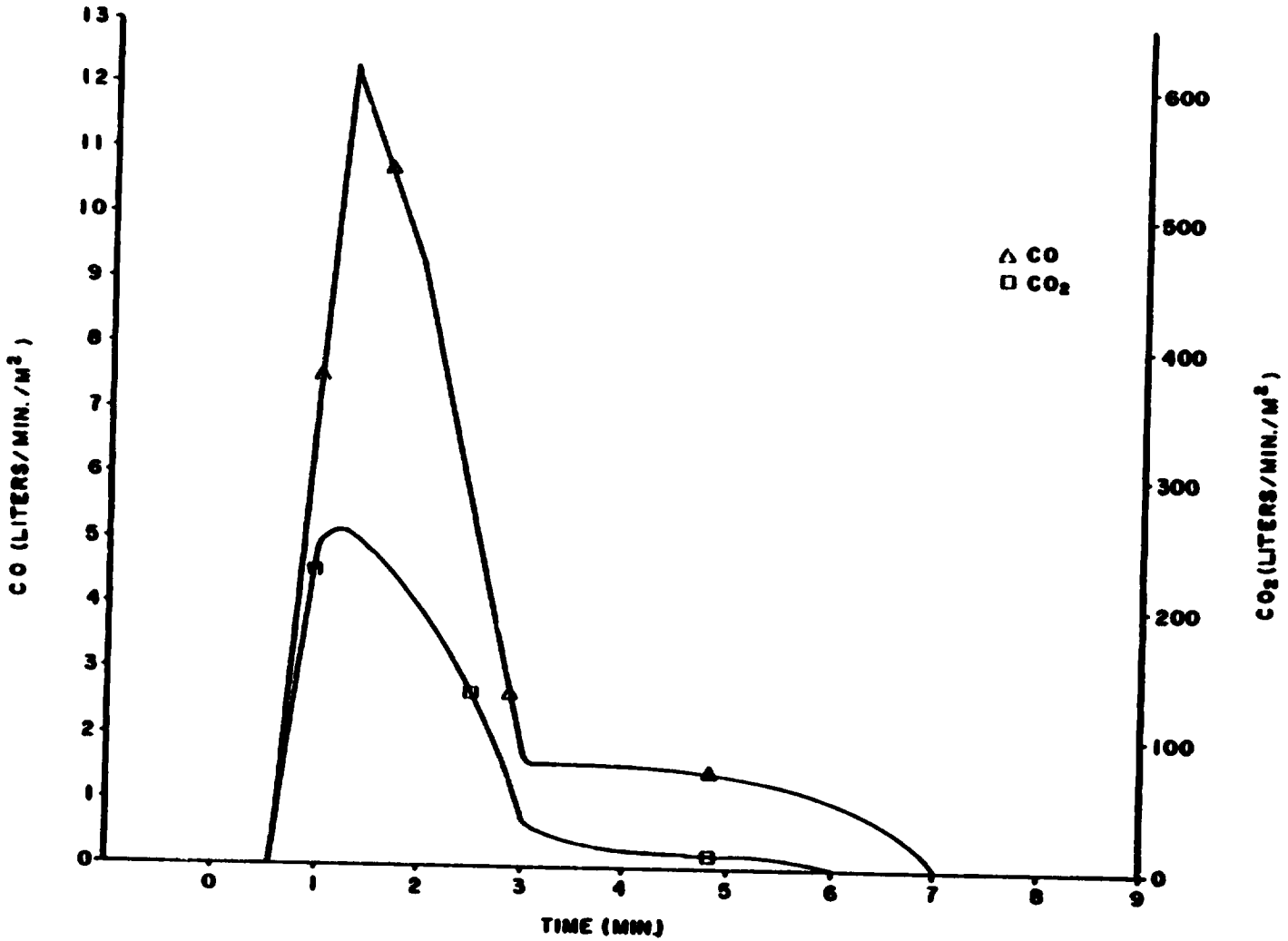

Figure 72. Release Rates of CO and CO_2--Graphite/Epoxy (1012-9) at 9.0 W/cm^2 With Piloted Ignition

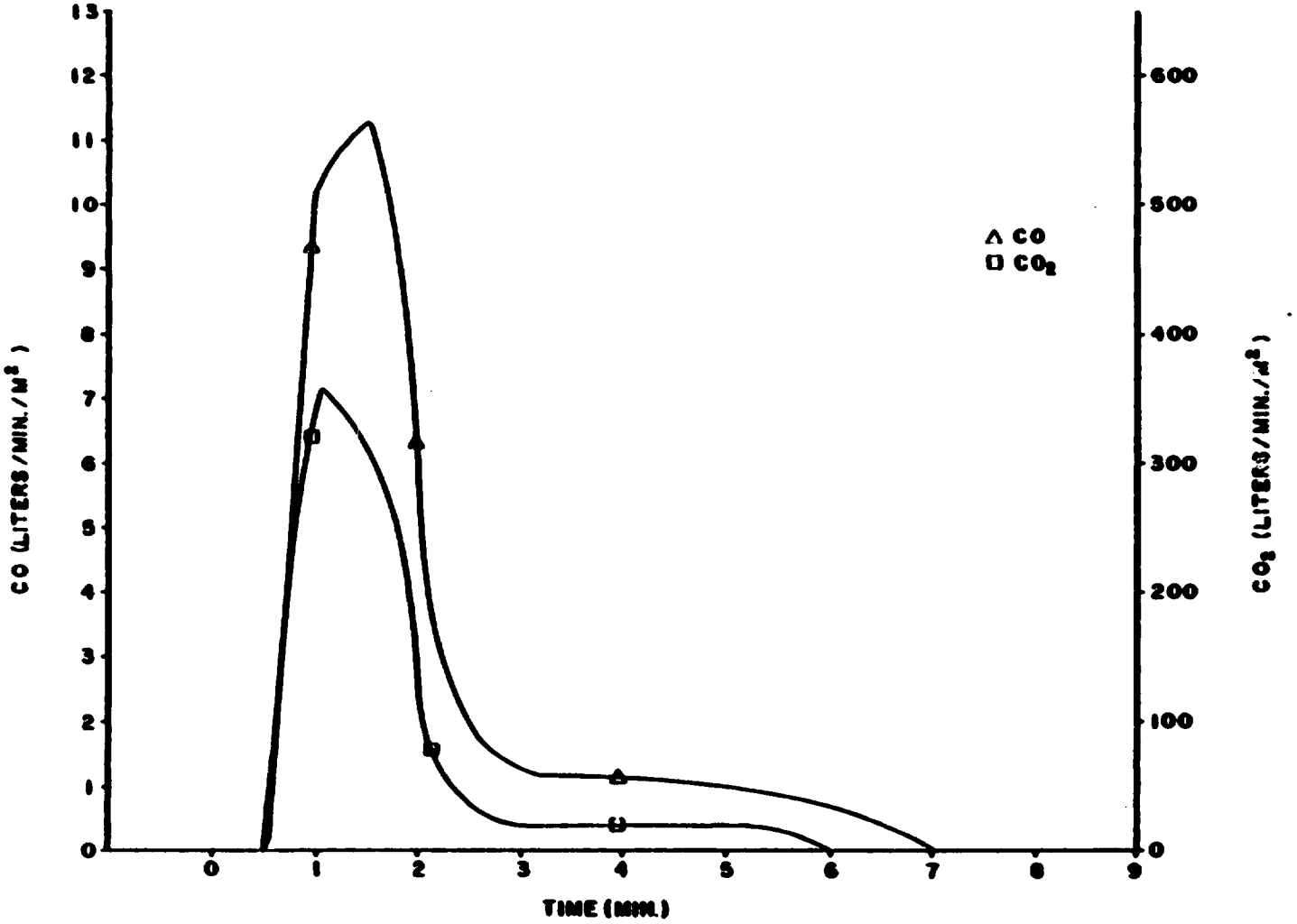

Figure 73. Release Rates of CO and CO_2--Graphite/Epoxy (1012-9) at 10.0 W/cm^2 With Piloted Ignition

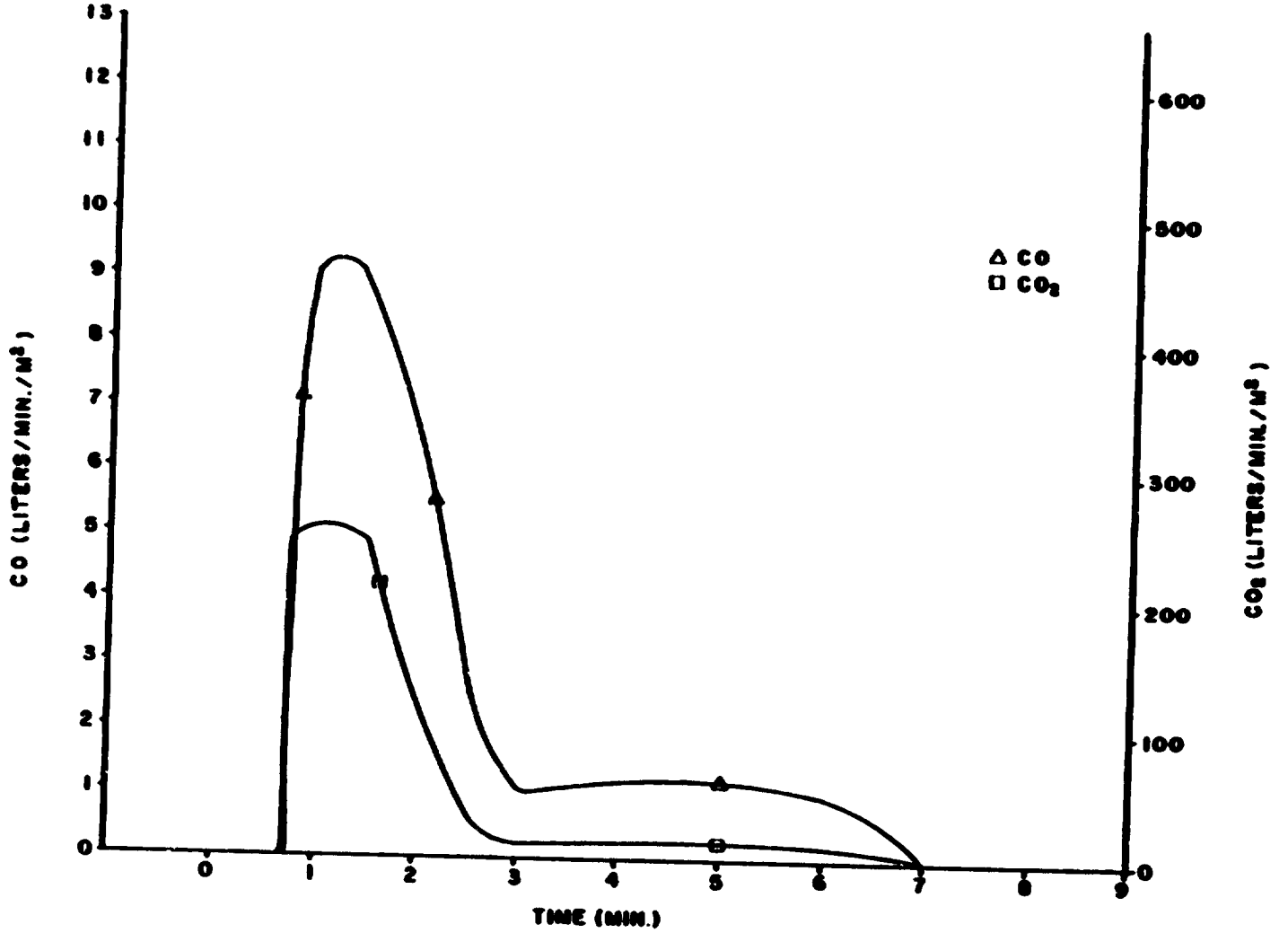

Figure 74. Release Rates of CO and CO_2--Graphite/Epoxy (1008A) at 10.0 W/cm^2 With Non-Piloted Ignition

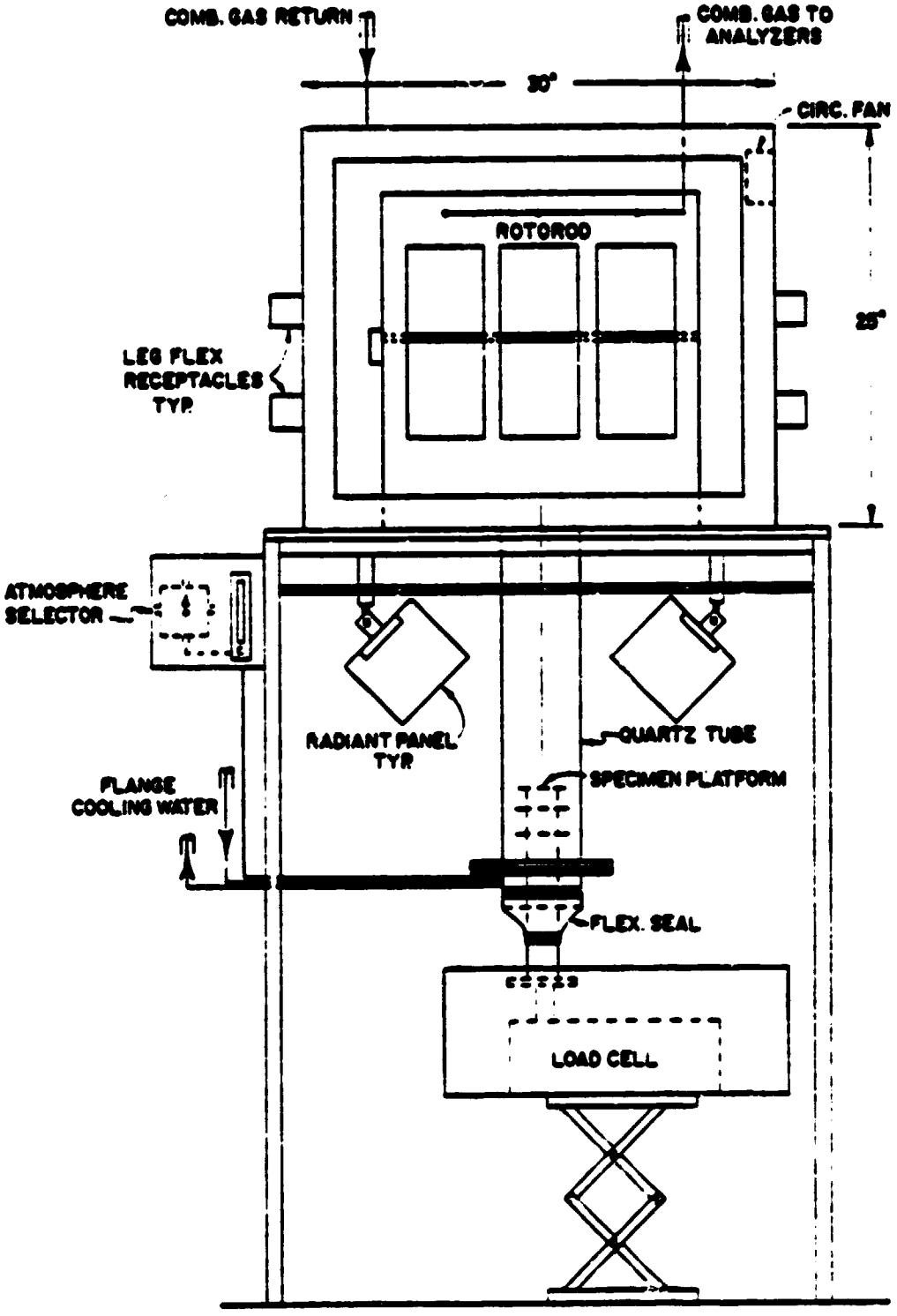

Figure 75. Animal Exposure Chamber